Progress in Polymer Science 90 (2019) 1–34

Contents lists available at ScienceDirect

Progress in Polymer Science

journal homepage: www.elsevier.com/locate/ppolysci

Electrospun polymer biomaterials

Jianxun Ding[a,f,*], Jin Zhang[b,**], Jiannan Li[a,d], Di Li[a], Chunsheng Xiao[a,f], Haihua Xiao[c,**], Huanghao Yang[e], Xiuli Zhuang[a,f], Xuesi Chen[a,f,*]

[a] Key Laboratory of Polymer Ecomaterials, Changchun Institute of Applied Chemistry, Chinese Academy of Sciences, Changchun, 130022, People's Republic of China
[b] College of Chemical Engineering, Fuzhou University, Fuzhou, 350108, People's Republic of China
[c] Beijing National Laboratory for Molecular Sciences, State Key Laboratory of Polymer Physics and Chemistry, Institute of Chemistry, Chinese Academy of Sciences, Beijing, 100190, People's Republic of China
[d] Department of General Surgery, The Second Hospital of Jilin University, Changchun, 130041, People's Republic of China
[e] College of Chemistry, Fuzhou University, Fuzhou, 350116, People's Republic of China
[f] Jilin Biomedical Polymers Engineering Laboratory, Changchun, 130022, People's Republic of China

ARTICLE INFO

Article history:
Received 4 November 2018
Received in revised form
28 December 2018
Accepted 10 January 2019
Available online 14 January 2019

Keywords:
Electrospinning
Polymer
Nanofiber
Microfiber
Functionalization
Biomedical application

ABSTRACT

Electrospinning provides a versatile technique for the preparation of matrices with micro/nanoscopic fibers. The non-woven polymer materials produced by electrospinning have an extremely high surface-to-volume ratio, a complex porous structure with excellent pore-interconnectivity, and diverse fibrous morphologies. These remarkable features impart a wide range of desirable properties to electrospun matrices for meeting the requirements of advanced biomedical applications, such as pharmaceutical repositories, tissue engineering scaffolds, wound healing, sensors, reinforcement, sound absorption, and filtration. This review presents a comprehensive overview of the recent progress and potential developments of electrospun polymer matrices and their application as biomaterials.

Abbreviations: 3D, three-dimensional; AA, acetic acid; ACE, acetone; AGN, aggrecan; APS, ammonium persulfate; AuNP, gold nanoparticle; bFGF, basic fibroblast growth factor; BMP-2, bone morphogenetic protein-2; BMSC, bone marrow stromal cell; BSA, bovine serum albumin; CA, cellulose acetate; CAP, cellulose acetate phthalate; CF, chloroform; CG, cationized gelatin; ChNC, chitin nanocrystal; CLSM, confocal laser scanning microscope; CNC, cellulose nanocrystal; CNF, carbon nanofiber; COL2, collagen type II; CS, chitosan; CS_2, carbon disulfide; CUR, curcumin; DCM, dichloromethane; DGN, dextran glassy nanoparticle; DMAc, *N,N*-dimethylacetamide; DMF, *N,N*-dimethylformamide; DMMP, dimethyl methylphosphonate; DNT, 24-dinitrotoluene; EC, endothelial cell; ECM, extracellular matrix; EGF, epidermal growth factor; ENM, electrospun nanofiber membrane; FM, fluorescence microscopy; GAG, glycosaminoglycan; G-Rg3, Ginsenoside-Rg3; HA, hyaluronic acid; HAP, hydroxyapatite; HAMA, hyaluronic acid–methacrylamide; hDF, human dermal fibroblast; PEUU, polyester urethane urea; PEVA, poly(ethylene-*co*-vinyl acetate); PEVAL, poly(ethylene-*co*-vinyl alcohol); PFDMS, poly(ferrocenyl dimethylsilane); PGA, poly(glycolic acid); PHB, poly(3-hydroxybutyrate); PHEMA, poly(2-hydroxyethyl methacrylate); PLA, poly(lactic acid); PLCL, poly(lactide-*co*-ε-caprolactone); PLGA, poly(lactic acid-*co*-glycolic acid); PLLA, poly(L-lactide); Pluronic, poly(ethylene oxide)-*block*-poly(propylene oxide)-*block*-poly(ethylene oxide); PM, poly(pyrene methanol); PMIA, poly(m-phenylene isophthalamide); PMMA, poly(methyl methacrylate); PP, polypropylene; PPX, poly(p-xylylene); PPy, polypyrrole; PS, polystyrene; PSu, polysulfone; PU, polyurethane; PVC, poly(vinyl chloride); PVCz, poly(vinyl carbazole); HDPE, high-density polyethylene; HFIP, hexafluoroisopropanol; HS, hypertrophic scarring; hSF, human skin fibroblast; IPMC, ionic polymer–metal composite; KGF, keratinocyte growth factor; KGN, kartogenin; LbL, layer-by-layer; LPEI, linear polyethylenimine; MDR, multidrug-resistant; MEW, melt electrospinning writing; MMP, methylphosphonate; MSC, mesenchymal stem cell; Mt, montmorillonite; MWCNT, multiwalled carbon nanotube; MPPA, micro-perforated panel absorber; NSC, neural stem cell; OM, optical microscopy; PA, polyamide; PA-4,6, nylon-4,6; PA-6, nylon-6; PA-6,6, nylon-6,6; PAA, poly(acrylic acid); PAAM, polyacrylamide; PAH, poly(allylamine hydrochloride); PAN, polyacrylonitrile; PANI, polyaniline; PBI, polybenzimidazole; PBz, polybenzoxazine; PC, polycarbonate; PCL, poly(ε-caprolactone); PDA, polydopamine; PDLLA, poly(D,L-lactide); pDNA, plasmid DNA; PEG, poly(ethylene glycol); PEI, polyetherimide; PET, polyethylene terephthalate; PVA, poly(vinyl alcohol); PVDF, poly(vinylidene fluoride); PVP, poly(vinyl pyrrolidone); R6G, rhodamine 6G; RGD, arginine-glycine-aspartic acid; rhBMP-2, recombinant human bone morphogenetic protein-2; rhIGF-I, recombinant human insulin-like growth factor I; rhTGF-β1, recombinant human transforming growth factor-β1; SDF-1α, stromal cell-derived factor-1α; SEM, scanning electron microscopy; siRNA, short interfering RNA; SMCs, smooth muscle cells; TAN, tetrahydroperfluorooctylacrylate; TEM, transmission electron microscopy; TEOS, tetraethyl orthosilicate; TFA, trifluoracetic; THF, tetrahydrofuran; TiO_2, titanium dioxide; TPU, thermoplastic polyurethane; VAN, vancomycin hydrochloride.

* Corresponding authors at: Key Laboratory of Polymer Ecomaterials, Changchun Institute of Applied Chemistry, Chinese Academy of Sciences, Changchun, 130022, People's Republic of China.
** Corresponding authors.
E-mail addresses: jxding@ciac.ac.cn (J. Ding), zhangjin500782@126.com (J. Zhang), hhxiao@iccas.ac.cn (H. Xiao), xschen@ciac.ac.cn (X. Chen).

https://doi.org/10.1016/j.progpolymsci.2019.01.002
0079-6700/

Contents

1. Introduction

Electrospinning provides a facile and straightforward approach to generate micro/nanofiber mats in a continuous process, where the fiber diameter is adjusted from nanometers to microns [1]. More than 75 different types of synthetic and natural organic polymers have already been electrospun to fibers successfully (Table 1) [2–4], while morphologies of these electrospun fibers can be well-regulated by the parameters listed in Table 2. Numerous experimental studies were reported including the electrospinning mechanism [5,6], electrospinning conditions [7], and characteristics of micro/nanofiber membranes [8,9], as shown in Fig. 1. Meantime, these timely publications inspired various fibrous morphologies through modification of the setup for electrospinning, including core–shell [10,11], hollow [12,13], side-by-side [14], multilayer [15], twisted [16,17], and porous-surface structures [18,19], resulting in the electrospun mats with desirable physicochemical properties for diverse applications.

Compared with other morphologies, electrospun matrices comprised of micro/nanofibers have an extremely high specific surface area that can interact with cells [20,21], being ideal for cell adhesion and proliferation. Additionally, depending on the entanglement of these micro/nanofibers, the electrospun membranes possess a highly porous three-dimensional (3D) network with excellent pore interconnection [22,23]. These mats can imitate the diversified extracellular matrix (ECM) well with regard to texture and compositions (dependent on the choice of materials taken), to be excellent candidates for use in tissue engineering. Last but not least, the electrospun polymer chains are always aligned along the fiber axis due to experiencing a rapid stretching force. As a result, some distinct performance differences are present among the various chain orientations of the electrospun fibers, especially the thermal behavior and physical-mechanical properties [24]. As the unique features of electrospinning have already been reviewed in many publications, the primary objective of this review will concentrate on the most recent progress of the electrospun polymer biomaterials, including different structures, remarkable characterizations, standard applications, and potential developments. Fig. 2 displays the major biomedical applications of electrospun fibers.

2. Biomedical applications of electrospun matrices

2.1. Pharmaceutical repositories

Various genes and proteins have been loaded into the electrospun scaffolds mainly through the following four techniques as summarized. The easiest method to load therapeutic agents is dipping the electrospun scaffolds into a biomolecules aqueous phase, where the biomolecules can be closely attached to the scaffolds through electrostatic forces [26]. The second method involves mixing the biomolecules with the polymer solution. Different from the superficial physical adsorption, this blend electrospinning can localize biomolecules within the fibers to guarantee a more sustained release profile [27]. However, the agents locate entirely inside the fibers or randomly on/near the fiber surface. Coaxial electrospinning and emulsion electrospinning are other promising ways to produce core – shell fibers for preserving the activities of proteins well [27]. Through these methods, most of the biomolecules can be fully encapsulated within the inner core of the fibers. More importantly, the core–shell nanofibers were reported to afford a typical biphasic drug release profile, which was consisted of an immediate and a sustained release [28,29]. By adjusting the shell flowing rate, amount of the drug released in the first phase could be precisely tailored, while the remaining drug was released based on a diffusion mechanism [30]. The fourth fabrication method is to realize the immobilization of biomolecules within the fibers, where the corresponding release rate is generally determined by external enzymes [31]. Due to the complexity of immobilizing agents on the fiber surface, this approach is not a typical technique employed for drug delivery.

Electrospun matrices exhibit many advantages as a potential delivery vector of drugs, DNA, and bioactive proteins [33]. First, the mild electrospinning process dependent on the applied voltage has little influence on the activity of therapeutic agents. Moreover, the release performance can be finely-tuned by modulating fiber porosity, morphology, and composition. Last but not least, the high specific surface area, as well as the highly porous structure, makes the carrier system more efficient in medical therapy [34].

Table 1
Electrospun polymers in solution form.

No.	Polymer	Solvent	Concentration	Perspective applications	References
	Polyamide (PA)	HFIP:*N,N*-dimethylformamide (DMF)	10 wt%	Fibers	[259–261]
1	nylon-4,6 (PA-4,6)	HFIP	10 wt%	Transparent composite	[216,262]
	PA-6,6	Formic acid	15 wt%	Nanocomposite bundle	[263]
	PA-6,6/Chitosan	HFIP:Acetic acid (AA)	20 wt%	Tissue engineering	[264]
	PA-6/Poly(m-phenylene isophthalamide) (PMIA)	Formic acid	7.5 wt%	Glass fiber, Filter media	[265]
2	PAA/PM	DMF	26 wt%	Optical sensor	[266]
	PAA/Poly(allylamine hydrochloride) (PAH)	Ethanol:Water	10.3 wt%	Tissue engineering membrane	[267]
3	Polyacrylamide (PAAM)	Water	0.5–1 mg/mL	Mass spectroscope, Modification of surface, Surface coating	[268]
	PAAM/Chitosan	AA	14 wt%	Air and water filtration	[269]
	Polyacrylonitrile (PAN)		12 wt%	Adsorbent	[270,271]
4	PAN/Gold	DMF	10 wt%	Biofuel cell	[272]
	PAN/MWCNTs		8 wt%	Electronic packaging	[273]
	PANI/PEG	Chloroform (CF)	2 wt%	NH_3 sensor	[274]
	PANI/Polystyrene (PS)	Azobenzene sulfonic acid:DMF	3.72 wt%	Antistatic coating	[274]
5	PANI/CNT/PEG	CF	0.67 wt%	Supercapacitor electrode	[275]
	PANI/Poly(3-hydroxybutirrate) (PHB)	2,2,2-trifluoroethanol (TFE)	5 wt%	Conductive sensor	[276]
	PANI/PLA/Silica	CF	50 wt%	Stem cell-based tissue engineering	[277]
6	Polybenzimidazole (PBI)	*N,N*-dimethylacetamide (DMAc)	12–14% (*W*/*V*)	Protective clothing nanofiber reinforced composite	[278]
	PBI/Polybenzoxazine (PBz)		25 wt%	Proton exchange membranes for high-temperature fuel cell	[279,280]
	PBI/MWCNTs		15–20 wt%	Heat dissipation	[281]
7	Polycarbonate (PC)	DMF:Tetrahydrofuran (THF), DMF	10 wt%, 20 wt%	Sensor, Electret filter	[282,283]
	PCL	DMF, THF:DMF	15 wt%	Biomimetic composite scaffold	[284,285]
8	PCL/Gelatin	THF	6 wt%	Anti-infective tissue regeneration membrane	[35]
	PCL/PVP-*b*-PCL	THF:DMF	11–15 wt%	Nanofiber scaffold	[286]
	Poly(ethylene gricol) (PEG)	DMF:Acetone (ACE)	50% (*W*/*V*)	Wound healing, Tissue engineering	[287–289]
9	PEG	CF, Distilled water:CF:ACE	9 wt%	Flexible light-emitting sheet	[290–292]
	PEG/Silk	Silk aqueous solutions, Hydrochloric acid (pH 2.0)	6–8% (*W*/*V*)	Sutureless dural substitute	[293]
	PEG/Cellulose	CF:Methanol	9–11 wt%	Food-packaging material	[287,291]
10	Poly(ether imide) (PEI)	HFIP, DMAc:NMP, Ethanol:Formic acid, Trichloroethylene (TCE)	10 wt%, 25 wt%, 14 wt%	Flat ribbon	[294,295]
11	Poly(ethylene terephthalate) (PET)	DCM:Trifluoracetic (TFA)	4 wt%, 12–18 wt%	Separator in lithium ion battery	[296]
	Poly(ethylene-*co*-vinyl acetate) (PEVA)	CF	14% (*W*/*V*)	Delivery matrix	[297,298]
12	PEVA/PLA	CF	14% (*W*/*V*)	Delivery matrix	[299]
	PEVA/PCL	CF:Methanol	12% (*W*/*V*)	Drug delivery system	[300]
			30 wt%	Nanofiber	[301]
13	Poly(ferrocenyl dimethylsilane) (PFDMS)	THF:DMF	30 wt%	Nanofiber	[301]
	PLA	CF, CF:DMF	14% (*W*/*V*)	Drug delivery system	[302–304]
	PLA/PHB	CF:DMF	8 wt%	Agricultural mulch films, Films for food packaging	[305]
14	PLA/MWCNTs	DCM:DMF, CF	10% (*W*/*V*), 6 wt%	Bone tissue engineering, Chemo- and photothermal therapy	[306,307]
	PLA/Cellulose nanocrystals (CNCs)	CF:DMF	15 wt%	Biomedical	[308]
	PLA-PCL-Collagen	HFIP	6% (*W*/*V*)	Tissue engineering	[309]
			15 wt%	Scaffold for tissue engineering	[310,311]
15	PLGA	THF:DMF	15 wt%	Scaffold for tissue engineering	[310,311]
	PLGA/Chitosan (CS)	THF	24% (*W*/*V*)	Scaffold for tissue engineering	[312]
16	Poly(methyl methacrylate) (PMMA)	DMAc:ACE, DMAc, DMF:THF	12 wt%, 3 wt%	HIV diagnosis, Biochemical separation	[313–315]
	PMMA/Tetrahydroperf-luorooctylacrylate (TAN)	DMF:Toluene	10 wt%	Scaffold for tissue engineering, Semi-permeable membrane, Filter	[316]
	PMMA/PEG	DMF, DMF:BC	25 wt%	Biomedical	[317]
17	Poly(*meta*-phenylene isophthalamide) (PMIA)	DMAc	12.6 wt%	Thermal storage and release	[318,319]

Table 1 (*Continued*)

No.	Polymer	Solvent	Concentration	Perspective applications	References
18	Poly(2-hydroxyethyl methacrylate) (PHEMA)	CF:DMF, DMF	10 wt%	Non-invasive biomedical study, Tissue engineering scaffold	[320,321]
	PHEMA/HA	DMF	4 wt%	Drug delivery, Tissue engineering	[322]
19	PS	ACE:DMF, CF, THF	10 wt%, 8–15% (*W*/*V*), 25 wt%	Tissue engineering, Filtration, Sensor, Storage	[323–326]
	PS/Dopants	DMF	3 wt% Dopants	Catalysis, Fluidic gas storage, Sensing	[326]
20	PU	THF:DMF	13 wt%	Outdoor sportswear fabric	[327]
	PU/Cellulose acetate phthalate (CAP)	THF:DMF	14% (*W*/*V*)	Electret filter, Drug delivery	[328]
21	PVA	Distilled water	4–10 wt%	Toughened structural material	[329,330]
	PVA/Silica	Distilled water	10 wt%	Onlinear optical material, Contact lenses	[331]
	PVA/Chitosan	Distilled water	9 wt%	Nanofiber membrane	[332]
	PVA/Cyclodextrin	Distilled water	7.5% (*W*/*V*)	Filtration, Tissue engineering, Drug delivery	[333]
22	Poly(vinyl carbazole) (PVCz)	DCM, CF	7.5 wt%	Sensor, Filter, Photoconductor, Charge transfer complex, Electroluminescent device, Photorefractive application	[334]
23	Polyvinylchloride (PVC)	DMF: DMAc, THF:DMF	10–15 wt%	Self-cleaning and anti-icing material, Textiles and composite reinforcement	[335,336]
	PVC/Fe_3O_4	THF:DMF	0.17 g/mL	Microwave absorption	[337]
24	PVP	THF	20% (*W*/*V*), 60% (*W*/*V*)	Antimicrobial agent	[338]
	PVP/Tetraethyl orthosixicate (TEOS)	DMF, Ethanol	0.5 g/mL, 0.82 g/mL	Bone repairing, Biomedical material	[339,340]
	PVP/Nafion	1-propanol:Water	8 wt%	CO_2 transport membrane	[341]
	PVP/Curcumin (CUR)	Acetic ether	0.1 g/mL	Drug release, Anticancer	[342]
	PVP/Au	Water:Ethanol	13 wt%	Stretchable conductor	[130]
	PVP/Ag	Ethanol	18% (*W*/*V*)	Organic optoelectronic application, Fluorescent clothing, Counterfeiting label	[343]
25	Poly(vinylidene fluoride) (PVDF), PVDF/CNTs	DMF:DMAc	20 wt%, 18 wt%	Flat ribbons, Sound absorber, Water filtration membrane	[234,344,345]
26	CA	CF:Methanol	55 wt%, 30 wt%	Membrane	[346]
	CA/Chitin nanocrystals (ChNC)	ACE	5 wt%	Water filtration membrane	[245]
	CA/Ag	Dimethylsulfoxide (DMSO):CP	12 wt%	Membrane	[347]
27	Collagen	HFIP	8% (*W*/*V*)	Scaffold for bone tissue engineering	[70,348]
	Collagen/SDF1α	HFIP	20% (*W*/*V*)	Guided nerve regeneration	[349]
28	Silk/PVA	Silk solution	5% (*W*/*V*)	Cosmetic, Fragrance utility	[350]
	Silk/Gold	Formic acid	31 wt%	Bone tissue engineering, Nerve conduit	[351,352]
	Tussah silk fibroin/Silk/Hydroxyapatite (HAP)	Aqueous lithium thiocyanate	10 wt%	Bone tissue engineering	[352]
29	Poly(ethylene-*co*-vinyl alcohol) (PEVAL)	2-propanol, Alcohol:Water	10% (*W*/*V*)	Tissue engineering, Wound healing	[353–355]
	PEVAL/Polypropylene (PP)/CNCs	DMF	5 wt% CNCs	Compatibilizer	[356]

2.1.1. Drug-loaded carriers for medical therapy

Drug-containing electrospun fiber mat has gained widespread interests in diverse biomedical applications, including the wound dressing, tissue remolding, and prevention of the anaerobic bacteria colonization [35]. Compared with the low efficiency of drug delivery *via* microspheres, hydrogels, and micelle systems, fibrous carriers are more promising because of their relative ease of use and adaptability. However, there are still some challenges that researchers must face, especially for the burst release of drugs from the sample surface during the first 10–12 h. In order to avoid this phenomenon, researchers should study the reason of such burst release and how try to achieve a constant drug release profile.

If the drug could not dissolve entirely in the polymer solution, it would only be dispersed or located near the fiber surfaces. As a result, a rapid diffusion into the media was exhibited. By this typical diffusion-controlled release mechanism, the burst release effect can be weakened by using drugs that are compatible with the polymer matrix, in which the drug release with nearly zero-order kinetics occurs due to the degradation of the polymer fibers under the effect of proteinase K [36,37]. In addition, the variation of fiber characteristics is another approach to realize an adjustable drug release behavior and a stable degradation profile. For example, fibers with relatively larger diameters always exhibit a longer period of nearly zero-order release, while a higher drug concentration results in a more pronounced burst release after

Table 2
Electrospinning parameters (solution, processing, and ambient) and their effects on fiber morphology.

Parameters	Effects on fiber morphology	References
Solution parameters		
Viscosity	Low-bead generation, high-increase in fiber diameter, disappearance of beads	[357]
Polymer concentration	Increase in fiber diameter with increase in concentration	[292]
Molecular weight of polymer	Reduction in the number of beads and droplets with increase in molecular weight	[358]
Conductivity	Decrease in fiber diameter with an increase in conductivity	[359]
Surface tension	No conclusive link with fiber morphology, high surface tension results in instability of jets	[360]
Processing parameters		
Applied voltage	Decrease in fiber diameter with increase in voltage	[361]
Distance between tip and collector	Generation of beads with too small and too large distance, minimum distance required for uniform fibers	[362]
Feed rate/Flow rate	Decrease in fiber diameter with decrease in flow rate, generation of beads with too high flow rate	[363]
Collector type	Influence structural morphology of electrospun fibers. A non-conductive collector creates a porous structure with circular pores on the fiber surfaces	[364]
Ambient parameters		
Humidity	High humidity results in circular pores on the fibers	[365]
Temperature	Increase in temperature results in decrease in fiber diameter	[366]

incubation [38,39]. Fluorescent intensity revealed from the fluorescence microscopy (FM) and optical microscopy (OM) images increase with increasing pH values, demonstrating that the loading and release kinetics of drugs (rhodamine 6 G, R6 G) from electrospun polymer fibers could be finely tailored by regulating different pH values at specific times. Such pH-responsive drug delivery system has potential applications *as per* the pathophysiological and specific needs of the disease [40].

Rather than merely varying the technological parameters of electrospinning, core – shell structured nanofibers using coaxial electrospinning have also been proposed recently for controlled drug release. In this technique, the biomacromolecule solution formed the inner jet and then a polymer solution was co-electrospun to form the outer jet [41]. Compared with the commonly-used electrospinning method, fibers fabricated from this modified device are originated from two separate solutions. It minimizes the interaction between the organic polymer solution and the aqueous-based biological molecules, to preserve the bioactivity of unstable biological molecules well [42]. As shown in Fig. 3, a coaxial electrospinning approach is employed to fabricate the core – shell poly(vinyl phenol)/poly(ε-caprolactone) (PVP/PCL) nanofiber mats, where vancomycin hydrochloride (VAN) is utilized as a model drug, a mixture of graphene oxide (GO) sheets and PVP is regarded as the core matrix and PCL as the shell [32]. A typical biphasic drug-release profile is exhibited in such a system, and which is controlled by adjusting the GO sheet content due to the molecular interactions between GO and VAN molecules. Interestingly, the core – shell nanofiber mats possess different antimicrobial activities as revealed by an antimicrobial test, depending on the GO content.

Up until now, integrating various antitumor drugs with different hydrophobic/hydrophilic properties into one platform to achieve sustained or sequential release behaviors and synergistically inhibit cancer progression remains challenging [43]. In our recent work, a local drug delivery system was proposed, which was mainly made of an emulsion electrospun polymer patch. Especially, the hydrophilic tea polyphenols (TP) and the hydrophobic 10-hydroxycamptothecin (HCPT) formed the core and shell of the nanofibers, respectively. This class of core – shell structured nanofiber membranes exhibited a sustained and sequential release. HCPT suppressed the malignant transformation and proliferation of hepatoma, whereas TP decreased the oxygen free radical levels and further prevented the metastasis and invasion of tumor cells [44]. Collectively, the core – shell nanofiber mats provided a promising approach to generate a drug delivery system with biphasic and a time-programmed release behavior.

2.1.2. Nucleic acid delivery for gene therapy

Nanofiber scaffolds have always been regarded as ideal tissue constructs because their fibrous topography closely resembles the natural ECM, which offers a 3D microenvironment to induce physiologically-relevant cellular phenotypes. Within the past five years, exponentially-increasing popularity toward the combination of biomolecules and scaffolds has been observed, *e.g.,* growth factors [45], cytokines [46], and therapeutic genes [47,48]. About the construction of scaffolds, the structural stability as well as the biochemical activity should meet some specific requirements. In detail, the scaffolds should be able to offer a controllable and sustainable manner for the site-specific delivery of genes. Then, biomacromolecules within the scaffold should be adequately protected in a biological system until they are entirely released [49]. The scaffolds with controlled biomolecule release not only express biological signals but can also provide physical support to enhance physiological response or modulate tissue regeneration.

During gene delivery, the most challenging part lies in the protection of nucleic acids from extracellular or intracellular enzymes, to successfully pass through the cell membranes and reach the nucleus. Non-viral or viral vectors are good candidates for targeted and continuous delivery of genes, where the nucleic acids are always incorporated in the vectors and then integrated with the electrospun fibers. For example, scaffolds loaded with keratinocyte growth factor (KGF) were once implanted into a full-thickness wound in mice. Improvement in the histological maturity of the wound suggested that a functionalized electrospun construct with highly-controlled DNA delivery was a promising bioactive substrate for treating cutaneous wounds [50]. In addition, some diabetic patients express higher levels of methylphosphonate (MMP). Thus an attenuated wound recovery is inevitably exhibited. Fig. 4 shows a schematic diagram of MMP-cleavable nanofibers for local gene delivery. A heptapeptide responsive to MMP protease attack is chemically conjugated on the nanofibrous meshes through the surface-exposed amine groups. Upon exposure to a high MMP level like diabetic ulcers, MMP-labile linkages are readily cleaved, and then a complex of DNA and linear polyethylenimine (LPEI) are gradually released. It has great potential for treating the diabetic ulcers as a local gene delivery system [26].

To achieve successful delivery of genes, it is necessary to overcome several challenges of existing electrospinning methods, such as the bioactivity preservation of biomolecules, high efficiency of gene transfection, and well-defined release kinetics to fit the time frame of tissue regeneration. Compared to a single nanofiber construct, a sustained delivery of short interfering RNA (siRNA) and an enhanced gene-knockdown efficiency are exhib-

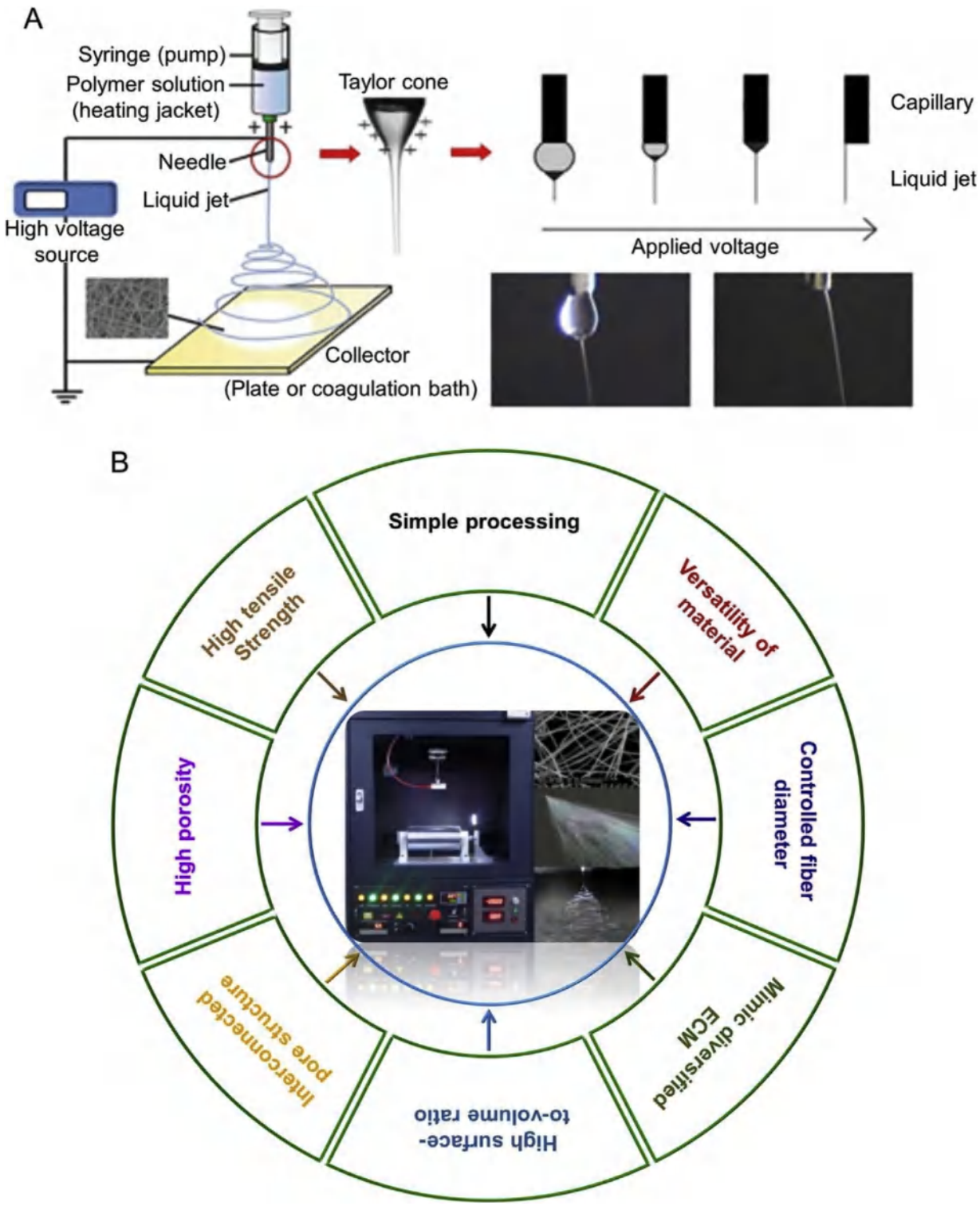

Fig. 1. Basic electrospinning setup and properties of electrospun fibers. (A) Schematic illustration of electrospinning setup (left) and Taylor cone formation (right). (B) Distinct characteristics of electrospun matrices. [25], Copyright 2017. Reproduced with permission from Elsevier Ltd.

ited in the co-encapsulating siRNA-transfection reagent complexes, which can be utilized in the long-term gene silencing applications [51]. The effect of various processing parameters, including molecular weight, polymer concentration, and plasmid DNA (pDNA) concentration, on the release kinetics and transfection efficiency, has been systematically investigated [42]. It is determined that the increase of these parameters can upregulate the average fiber diameter and at the meantime results in variable transfection properties and release kinetics. Additionally, with regard to the electrospun scaffold composed predominantly of poly(D,L-lactide)–poly(ethylene glycol) (PDLA – PEG) block copolymer and poly(lactic acid-*co*-glycolic acid) (PLGA) random copolymer, variations in the ratio of PDLA – PEG block copolymer to PLGA vastly affect the overall structural morphology, as well as both the site-specific delivery and sustainable manner of the pDNA [52].

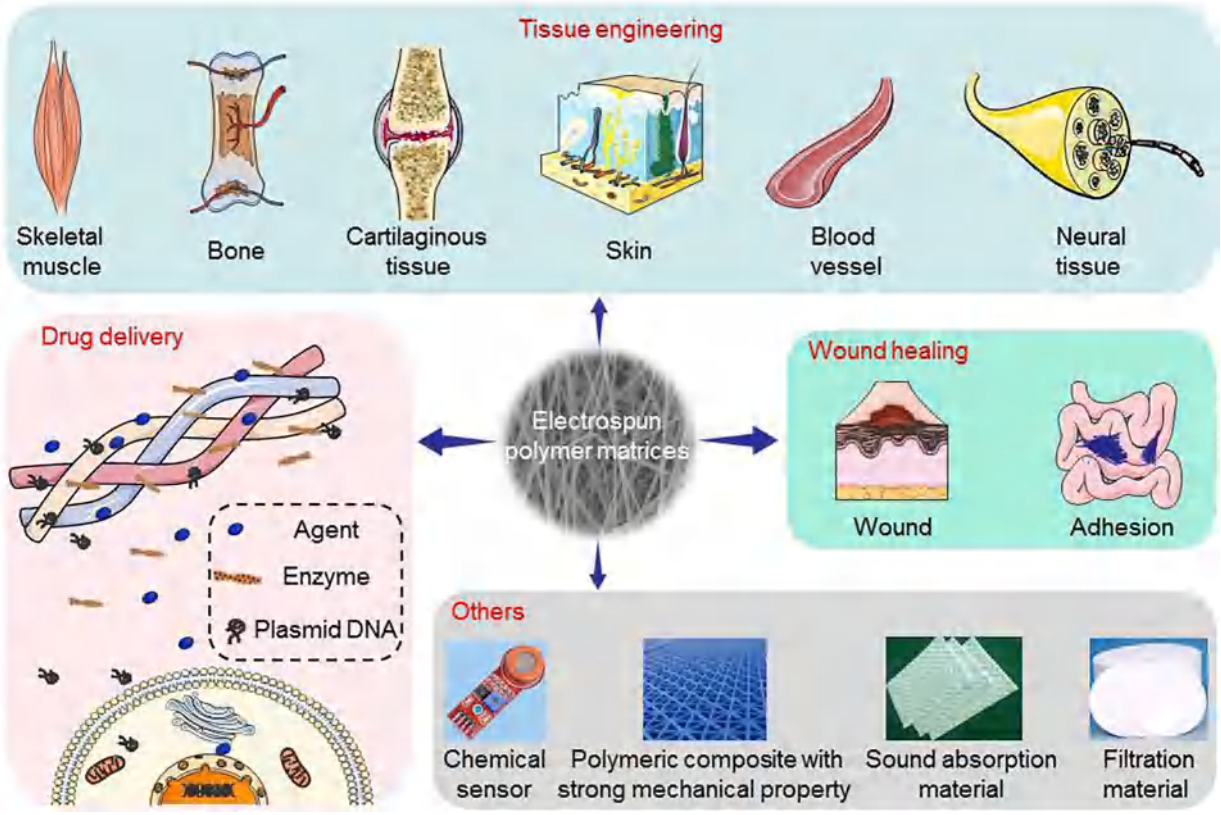

Fig. 2. Possible biomedical applications of electrospun fibers.

2.1.3. Enzyme carriers for biomedical application

Enzyme-encapsulation systems have great potential to be utilized for enzyme-catalyzed reactions, *e.g.,* sensing [53], active packaging [54], and bioprocessing [55]. By increasing the surface area-to-volume ratio of the polymer matrix, it is possible to improve the storage efficiency of enzymes and reduce diffusional limitations [56]. Electrospinning natural proteins, such as enzymes and casein into fibrous membranes, have also been widely investigated, where natural proteins can become the electrospun micro/nanofibers after adding another polymer like PVA or PEG. In comparison with the cast films from the same solution, the lipase encapsulated within the electrospun fibers exhibits higher catalytic activity toward hydrolyzing olive oil [57].

It is of great interest to systematically study how to recognize a sustained and efficient enzyme release. As we mentioned before, the coaxial electrospinning can acquire a different hollow nanofiber-based artificial cell that performs multi-step reactions involving highly-efficient coenzyme regeneration [58]. Similarly, the chemical vapor deposition can also realize the formation of core–shell structure to prevent the burst release of enzymes, where poly(p-xylylene) (PPX) is employed as a coating layer of PVA/bovine serum albumin (BSA) nanofibers. Differing from the uncoated PVA/BSA nanofibers, unique polymer-coated nanofibers, exhibit a significantly-delayed release of the intact enzyme and preserve the enzyme activity well, and such behavior is primarily dependent on the coating thickness of PPX [59]. In addition, composite nanofibers consisted of surfactant-treated enzyme and polymer significantly stabilize the enzyme activity, as a result of the improved mass-transfer rate of the substrate to an enzyme active site. Specifically, the encapsulated enzyme is stable in a buffer for more than two weeks under shaking conditions. These nanofiber mats are ideal candidates for constant usage because they are highly durable and can be easily recovered from a reaction solution [60]. An original inverse-miniemulsion electrospinning method has been proposed recently to make the enzymes and fluorophores distributed as nano-reservoirs into the fibers [61]. As shown in Fig. 5, the remaining activity and release rate of the loaded-enzymes are mainly dependent on the position and type of the enzymes. A near-complete release of the loaded-fluorophore is achieved before the complete degradation of the fibers, suggesting that the nanofibers with sustained mechanical integrity are suitable as a self-triggered enzyme-release system.

Among various electrospun porous membranes, a kind of stimuli-sensitive porous polymer materials with the ability to trap and release biomacromolecules on demand has promising biomedical applications. Such a smart structure by responding to an externally-applied stimulus can seal their pores in a controlled manner, such as temperature, pH, or local light absorption [62]. In our recent work, a generally applicable electrospinning/leaching strategy is described to fabricate the poly(lactic acid) (PLA)/CNT composite fibers with controllable surface pores, where the carboxyl-functionalized CNTs are utilized to realize the pore self-closure through the photothermal-conversion ability. FITC-Dex, fluorescein-labeled DNA (FLU-DNA), and tetramethylrhodamine (TMR)-BSA are chosen as the model agents to determine the encapsulation capability of biomacromolecules into the porous electrospun fibers. Interestingly, such smart carrier is able to capture free molecules from the FITC-Dex, FLU-DNA, or TMR-BSA aqueous solutions upon UV light irradiation, meantime providing a sustained release along with a gradual degradation of the polymer matrix as well as a reversible surface pore reopening. Such novel porous electrospun fibers with self-sealing capability can prevent some inflammatory diseases by scavenging cytokines from interstitial body fluids [63].

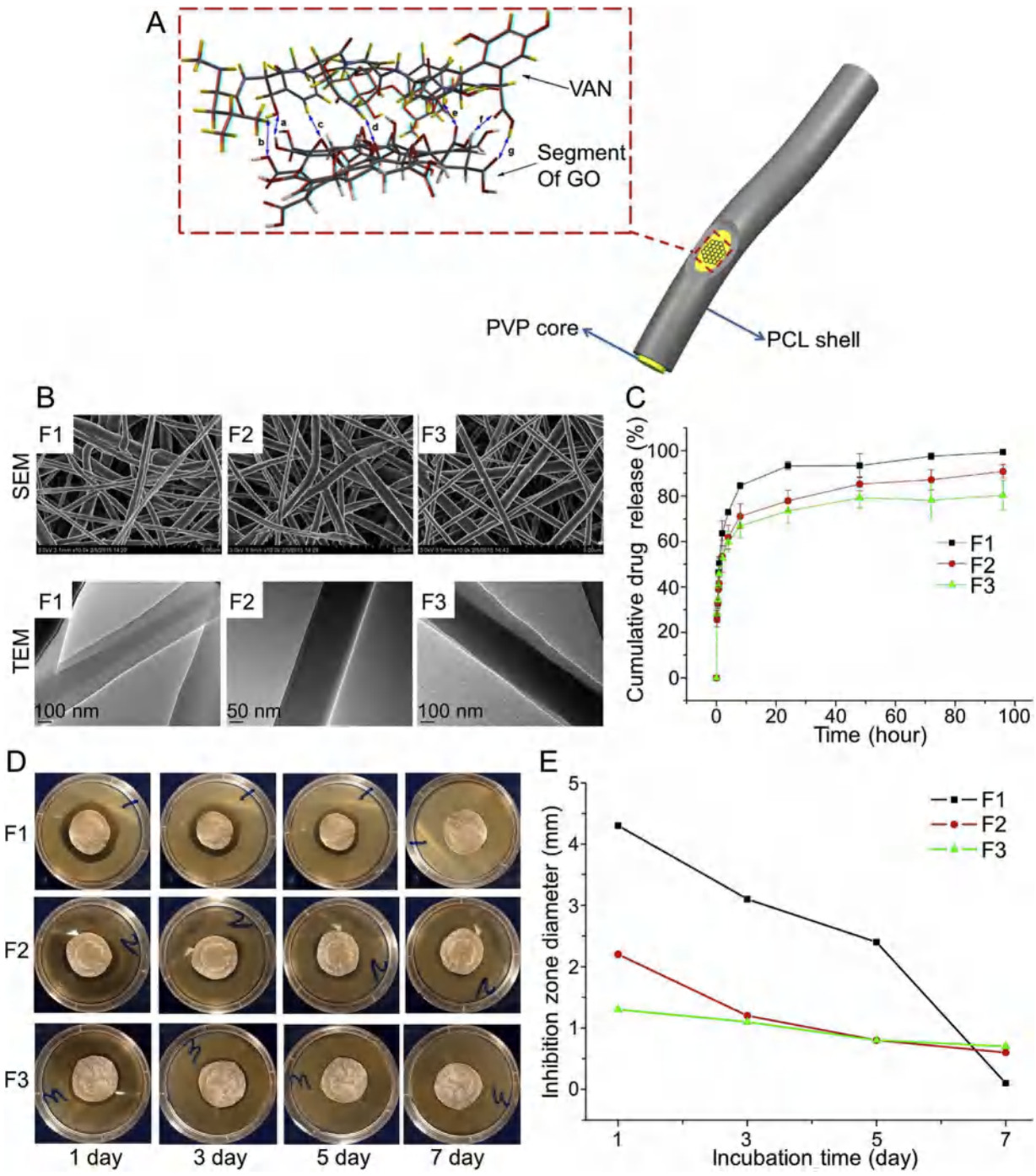

Fig. 3. Characterizations and antimicrobial activity of PVP/PCL core – shell nanofiber mats. (A) Schematic illustration of PVP/PCL core – shell nanofiber. (B) SEM (scanning electron microscopy) and transmission electron microscopy (TEM) images of the nanofibers. To study the effect of the GO content on the VAN release behavior, different volumes of the 10 mg/mL GO solution (0, 2, and 4 mL) were mixed with PVP and VAN as the core solution, and the resultant PVP/PCL core – shell nanofibers were denoted as F1, F2, and F3, respectively. (C) VAN release profiles over time. (D and E) Antimicrobial activity of PVP/PCL core – shell nanofiber mats against S. aureus. [32], Copyright 2016. Reproduced with permission from Elsevier Ltd.

2.2. Tissue engineering scaffolds

Tissue engineering is one of the most interesting interdisciplinary fields of research that applies the principles of life sciences and engineering. It mainly involves the use of living cells and the development of biological substitutes to be implanted into a defect site for tissue reparation. From the basic principle of tissue engineering, a vital point of this technology lies in the construction of polymer scaffolds for providing a good connection between seeding cells and regenerated organs. For a scaffold to function effectively as a temporary ECM, it must possess a few basic requirements [64–66]. First and foremost, the scaffold should be biocompatible and positively promote cell proliferation, without eliciting an immune response. Secondly, an interconnected 3D microenvironment with high porosity is essential for the transportation of nutrients, cellular ingrowth, and vascularization. Thirdly, the scaffolds are typically composed of biodegradable polymers, and the degradation rate should be designed to coincide or at least be controllable to match the regeneration rate of tissue. Finally, sufficient mechanical properties are required in order to maintain the structural integrity

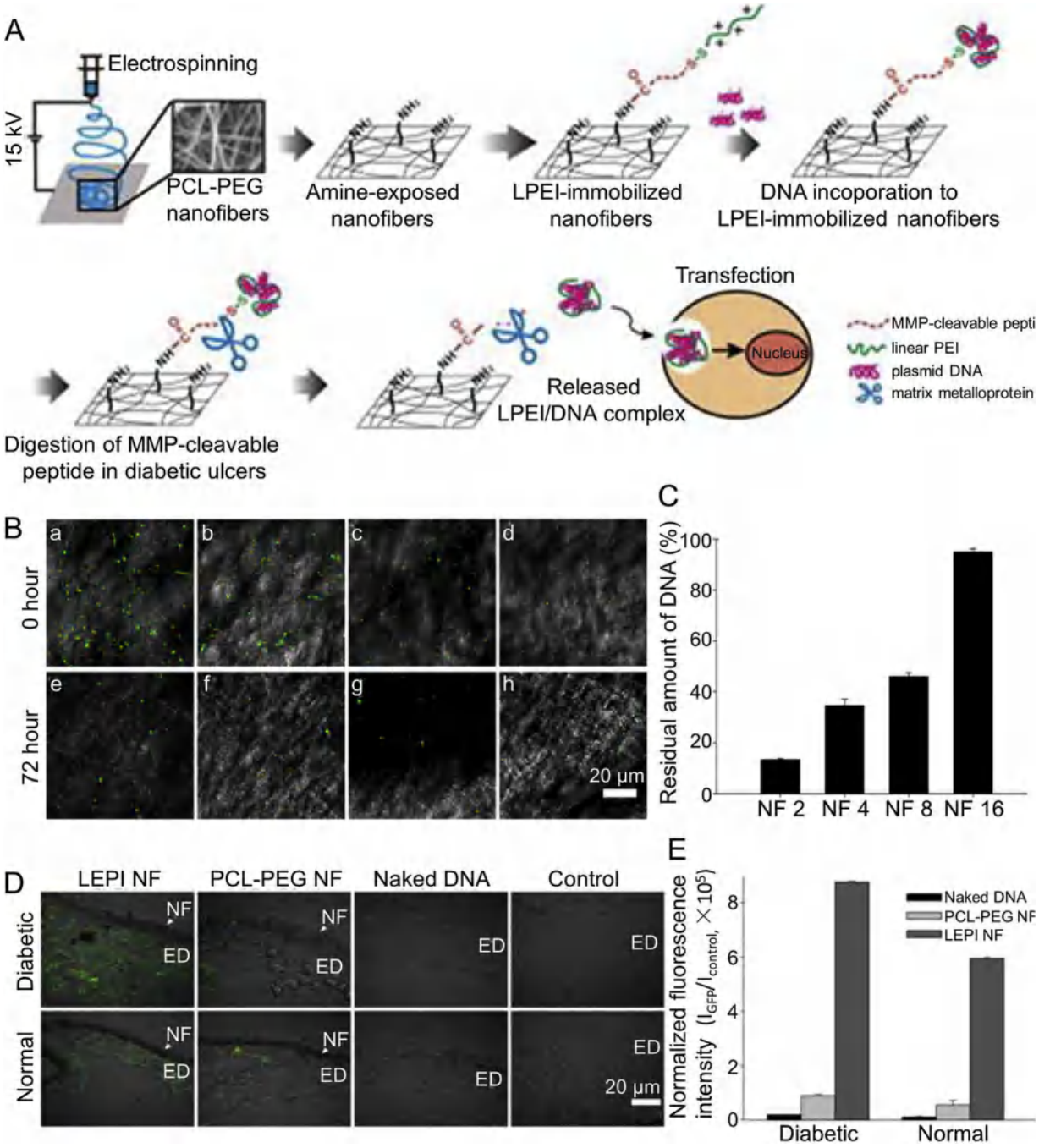

Fig. 4. Preparation, characterizations, and diabetic ulcer treatment effects of MMP-responsive nanofibrous matrix (NF). (A) Schematic diagram of MMP-responsive electrospun nanofibrous matrix for gene delivery. (B) Confocal laser scanning microscope (CLSM) of DNA (green) incorporated LPEI-immobilized NFs at various nitrogen/phosphate (N/P) ratios. DNA in the N/P ratios ranging from 2 to 16 was defined as NF 2 (a, b), NF 4 (c, d), NF 8 (e, f), and NF 16 (g, h), respectively. Release of DNA from LPEI-immobilized NFs at 72 h after MMP-2 treatment (b, d, f, h). (C) Fluorescence intensity ratios of the residual amount of DNA were evaluated by comparing fluorescence intensities at 0 and 72 h. (D) Cross-sectional images of diabetic and normal wound tissue administered with DNA-incorporated NFs on day 3. (E) Image-analysis methods based on intensity was employed to quantify each image, and average values and standard deviation were obtained ($n = 3$). [26], Copyright 2010. Reproduced with permission from Elsevier Ltd (For interpretation of the references to colour in this figure legend, the reader is referred to the web version of this article).

and prevent the collapse of the porous scaffold. Extensive research has been conducted on tissue engineering scaffolds over the past few decades, and as a result a variety of approaches have been proposed to facilitate tissue regeneration, including solvent casting – particulate leaching technique [67], molecular self-assembly [68], thermally-induced phase separation [69], and electrospinning [70], and so forth. Among them, the electrospinning has gained popularity with the tissue engineering community for providing a versatile and cost-effective mean to produce scaffolds with a complex biomimetic structure. Furthermore, fabrication of electrospun fibers can be originated from a broad range of polymers, including synthetic, purely natural, composite mixtures, and even organ-specific extracts [71]. More interestingly, mechanical and biological properties of the electrospun scaffolds can be easily-regulated by varying the processing parameters or the polymer compositions. Due to these advantages, electrospun techniques have been employed for engineering various tissues of skeletal

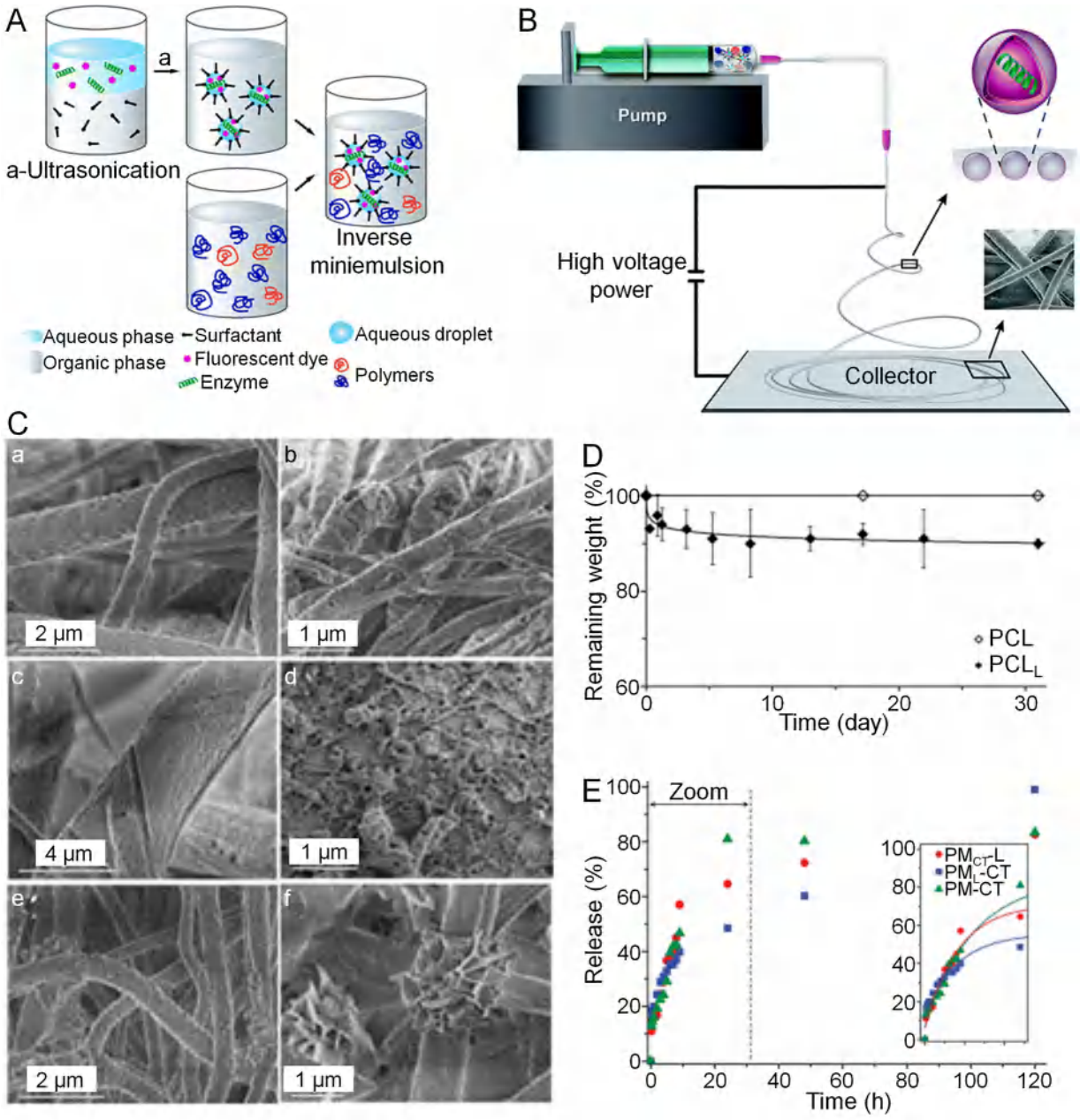

Fig. 5. Inverse-miniemulsion preparation, colloid-electrospinning setup, and properties of enzyme-loaded scaffolds. (A) Scheme of inverse-miniemulsion preparation and (B) colloid-electrospinning setup to obtain fibers loaded with enzymes and fluorophores. (C) SEM micrographs of (a) PCL scaffold after 412 h of immersion in PBS medium, (b) PCL_L (PCL loaded with lipase dissolved in PBS) enzyme-loaded scaffold after 198 h of immersion in PBS medium. (c) Sample PM-CT (PCL/coPEA dissolved in PBS and α-chymotrypsin complex solution) after immersion in α-chymotrypsin medium for 16 h and (d) 88 h. (e) Sample PM_L-CT (PCL/coPEA loaded with lipase dissolved in PBS and α-chymotrypsin complex solution) after immersion in α-chymotrypsin medium for 48 h. (f) Sample PM_{CT}-L (PCL/coPEA loaded with α-chymotrypsin dissolved in PBS and lipase complex solution) after immersion in lipase medium for 48 h. (D) Weight loss of the nanofibers by enzymatic degradation *versus* time for PCL and PCL_L scaffolds. (E) R6 G (an encapsulated fluorescent dye) release percentage determined by fluorescent detection *versus* time for the different scaffolds (PM) in enzymatic media (L: lipase and CT: α-chymotrypsin). [61], Copyright 2015. Reproduced with permission from the Royal Society of Chemistry.

muscle [72], bone [73], cartilage [74], skin [75], blood vessel [76], and nerve [77].

It is worthy to notice that almost all electrospun scaffolds are either non-degradable or degraded hydrolytically, different from the proteolytical degradation way of natural ECM through matrix metalloproteinases. Recently, a kind of reactive macromer containing protease-cleavable and fluorescent peptides has been synthesized, which is able to form an electrospun fibrous hydrogel through photo-initiated polymerization. Such biomimetic scaffold is susceptible to protease-mediated cleavage *in vitro* and can monitor degradation *in vivo* using transdermal fluorescent imaging in a subcutaneous mouse model, representing a unique biomimetic approach to generate protease-sensitive fibrous scaffolds [78]. To determine the degradation rate of an implant *in vivo* and show its role in tissue regeneration, noninvasive tracking of biomaterials is vital. Current biomaterials always require labeling with fluorescent dyes or nanoparticles to enable tracing. A fully-conjugated electrospun scaffold is fabricated, which can be visualized *in situ* after implantation based on a semiconducting luminescent polymer of (poly[2,3-bis-(3-octyloxyphenyl)quinoxaline-5,8 -diyl-*alt*-thiophene-2,5-diyl] (TQ1)), using fluorescence imaging in the near-infrared region. Fluorescent properties of the TQ1 fibers retain

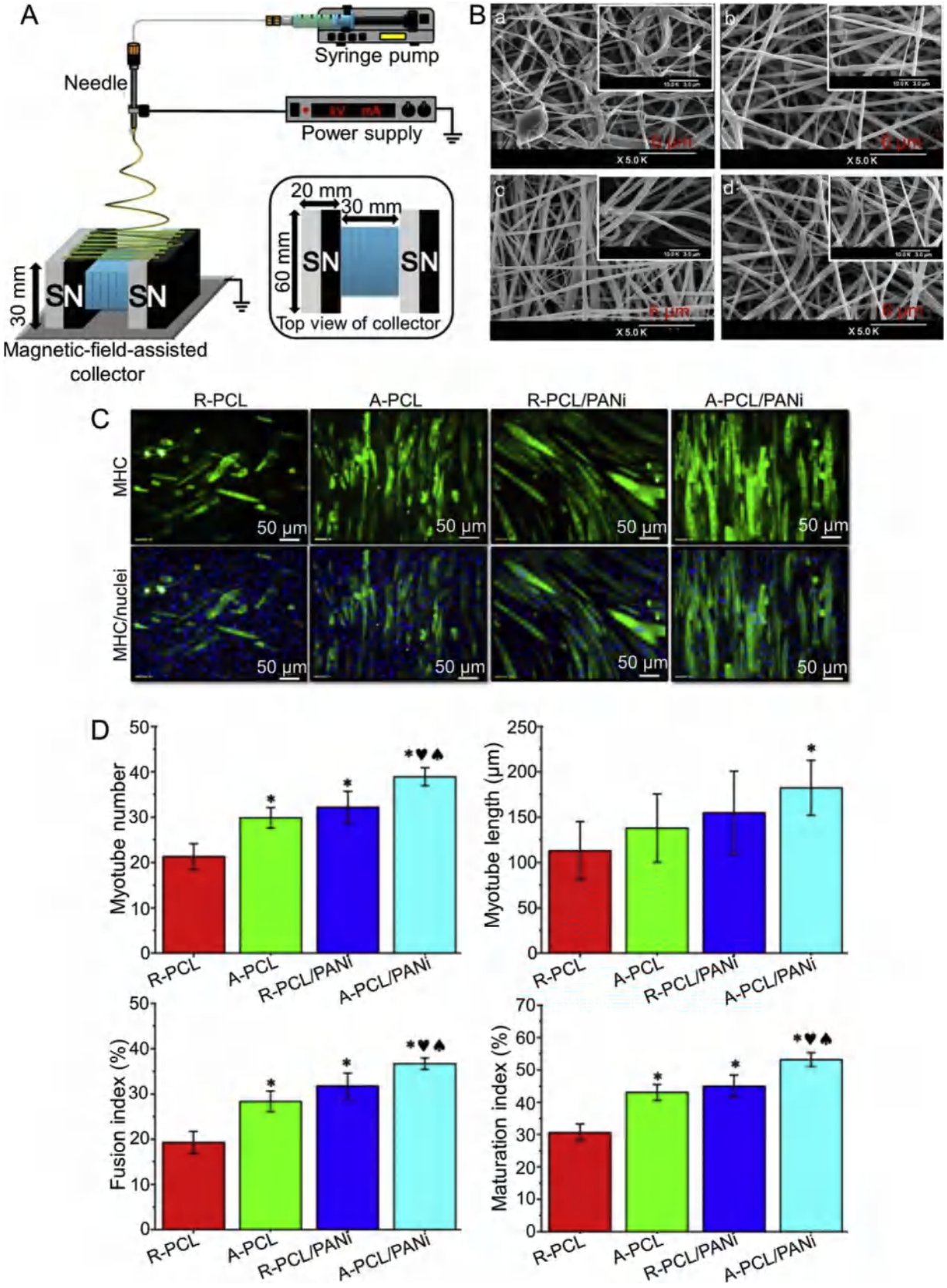

Fig. 6. Basic setup used in magnetic field-assisted electrospinning, properties of obtained fibers, and their effects in myotubes. (A) Schematic illustrations of set-up used in magnetic field-assisted electrospinning (MFAES) method for preparing aligned nanofibers. (Insets) Specifications of magnetic field-assisted collector. (B) SEM images of electrospun nanofibers: (a) containing 0 wt% (PCL), (b) 1 wt% (PCL/polyaniline (PANI-1)), (c) 2 wt% (PCL/PANI-2), and (d) 3 wt% (PCL/PANI-3) PANI. (Insets) A higher magnification image of each sample. (C) Representative immunofluorescent images of myotubes differentiated for five days on random PCL (R-PCL), aligned PCL (A-PCL), random PCL/PANI-3 (R-PCL/PANI), and aligned PCL/PANI-3 (A-PCL/PANI) nanofibers and immunostained for myosin heavy chain (MHC) (green) and nucleus (blue). (D) Quantification of the myotube number, myotube length, fusion index, and maturation index of the myotubes formed in (a). *Significantly different in comparison with the

up to 90 days following implantation, of great potential to be a candidate for pro-angiogenic and traceable biomaterial [79].

2.2.1. Skeletal muscle tissue engineering

Skeletal muscle makes up approximately 48% of the body mass and is mainly responsible for protecting abdominal viscera, controlling voluntary movement, and maintaining the process of respiration, which may be injured by exposure to myotoxic agents, excessively hot or cold temperatures, sharp or blunt trauma, and ischemia [80]. Mature skeletal muscle predominantly consists of multinucleated post-mitotic fibers that cannot regenerate [81]. When muscle structure has been irreversibly-ablated by significant injuries or surgical procedures, engineering new muscle fibers *via* satellite cells becomes exceptionally challenging. In this situation, constructing muscle scaffolds becomes a readily-available method for the treatment of large tissue defect and enhancement of muscle regeneration. More importantly, it can effectively avoid the lack of autologous transfer and maintain the functional integrity of the donor site [82,83].

Many attempts have been tried so far to reconstruct the skeletal muscle tissue *in vitro,* and all these studies suggest that tissue engineering is indeed feasible to regenerate bioartificial muscles [84]. Through successfully transplanting isolated myoblasts within the biological substitutes of electrospun poly(glycolic acid) (PGA) fibers, the myoblasts can organize well along the polymer matrix because of different geometric structure and the large specific surface area, and even can regenerate neo-muscle-like strands in a short period of six weeks [85]. Nevertheless, the majority of these scaffolds composed by classic degradable polyesters (*e.g.,* PGA, PLA, and copolymers) suffer from some disadvantages, mainly concerning the low yield elongation rate of 3% – 4%. In order to overcome the drawback of inflexibility, a concept of electrospun DegraPol® (a known biodegradable block copolymer) has been proposed [86]. Such gel exhibits promising prospective for utilizing as a scaffold in the field of skeletal muscle tissue reparation. In addition, the composition of the most scaffold materials cannot be visualized by methods available to clinicians (*e.g.*, radiography), and therefore it is not possible to assess their performance *in situ*. To this end, a kind of nanofibrous scaffold including radiopaque nanoparticles is developed. The inclusion of such biocompatible radiopaque particles can not only increase the tensile modulus of the scaffold but also provides sufficient radiopacity for *in vivo* visualization *via* fluoroscopy and microcomputed tomography, facilitating non-invasive long-term evaluation and image-guided implantation of scaffold performance [87].

Structure and organization of muscle fibers are well-known to dictate the tissue function. In engineering functional skeletal muscle, an essential step is to mimic the structure of native tissue that is comprised of highly-oriented myofibers with multinucleated cells derived from myoblasts. By the established c̈ontact guidancëtheory [89,90], a critical factor in designing appropriate scaffolds is to realize the formation of continuous muscle fibers, which is also essential to support cell fusion, proliferation, and differentiation in a preferential direction. In comparison to the randomly-oriented nanofibers, unidirectionally-oriented nanofibers significantly induced the muscle cell alignment and promoted the functional myotube formation [91]. Except for the topographical cues, other essential stimuli to influence the adhesion and differentiation of specific cell types are electrical signals. Up to now, various conductive materials, such as polypyrrole (PPy) [92], PANI [93], and carbon nanotubes (CNTs) [94], have been added into the polymer matrices to generate the electrically-active fibers. As shown in Fig. 6, the highly-ordered electrospun nanofibers composed by PANI and PCL along with the introduction of an external magnetic field significantly increased the electrical conductivity [95]. Consequently, these highly-oriented and electrically-conductive scaffolds provide topographical and electrical characteristics for cell attachment simultaneously, serving as a promising scaffold for electrically-stimulated muscle regeneration.

Nonetheless, tissue-engineered skeletal muscle analogs are still far from being a clinical reality. More recently, it was claimed that a possible approach to solve the problem of lacking tissue utility was to use an ionic polymer – metal composite (IPMC) for the regeneration of skeletal muscle tissue [96]. IPMC is always composed of a conductive polymer or carbon/graphite, a noble metal, as well as a charged polyelectrolyte membrane [97]. Considering the attractive mechanical and sensing properties involved with these composites, it is reasonable to believe that these artificial muscles can be produced with viable strength. A unique reverse IPMC scaffold has been successfully created recently using coaxial electrospinning, where acid-functionalized multiwalled carbon nanotubes (MWCNTs) and PCL were regarded as the inner core, and the exterior sheath was composed by the poly(acrylic acid)/poly(vinyl alcohol) (PAA/PVA) hydrogel [98]. The results showed that such a composite scaffold induced a significant amount of actin interaction of multinucleated cells.

2.2.2. Bone tissue engineering

An increasing number of tissue transplant surgeries have expanded the demand for tissue grafts, especially for the bone substitutes [99]. Natural bone is always composed of approximately 70 wt% inorganic nanocrystals like HAP and 30 wt% organic matrices like collagen nanofibers. Additionally, it is hierarchically organized from nano-, micro-, to macro- scale about the structure [100]. Among a variety of fabrication methods, electrospinning is particularly efficient for producing continuous fibers with tunable fiber size as well as a morphological similarity to natural ECM. Electrostatic fiber spinning as an alternative scaffold fabrication technique for treating bone defects has already been comprehensively assessed, through seeding mesenchymal stem cells (MSCs) on the highly-porous nonwoven PCL fabrics consisting of ultrafine fibers for up to four weeks [22]. Their morphological, histological, and immunohistochemical results fully demonstrate that such cell–polymer constructs provide a platform to support the regeneration of mineralized tissue and might be a suitable candidate for engineering bones *in vitro*. Similarly, other biodegradable polyesters, such as PLA [101] and PLGA [102], have also been intensively investigated for bone tissue engineering due to their controllable degradation rate and excellent mechanical properties, especially after annealing post-treatment these electrospun polyester scaffolds exhibit improved mechanical behavior [103]. With hierarchically-compositional and -structured pores close to the natural mineralized nanofibril counterparts, scaffolds based on these electrospun polyester membranes are demonstrated with great potential for bone tissue engineering applications [104].

Although polymer materials alone have already displayed some positive results for bone reparation, surface chemistry of these scaffolds that directly interact with the host cells is still the critical issue to be considered. To improve the osteoconductivity of polymer scaffolds, a layer-by-layer (LbL) method [105], an

R-PCL nanofibers (n = 5; P < 0.05), ♥significantly different compared with the A-PCL nanofibers (n = 5; P < 0.05), ♠ significantly different compared with the R-PCL/PANI nanofibers (n = 5; P < 0.05). [88], Copyright 2013. Reproduced with permission from Elsevier Ltd (For interpretation of the references to colour in this figure legend, the reader is referred to the web version of this article).

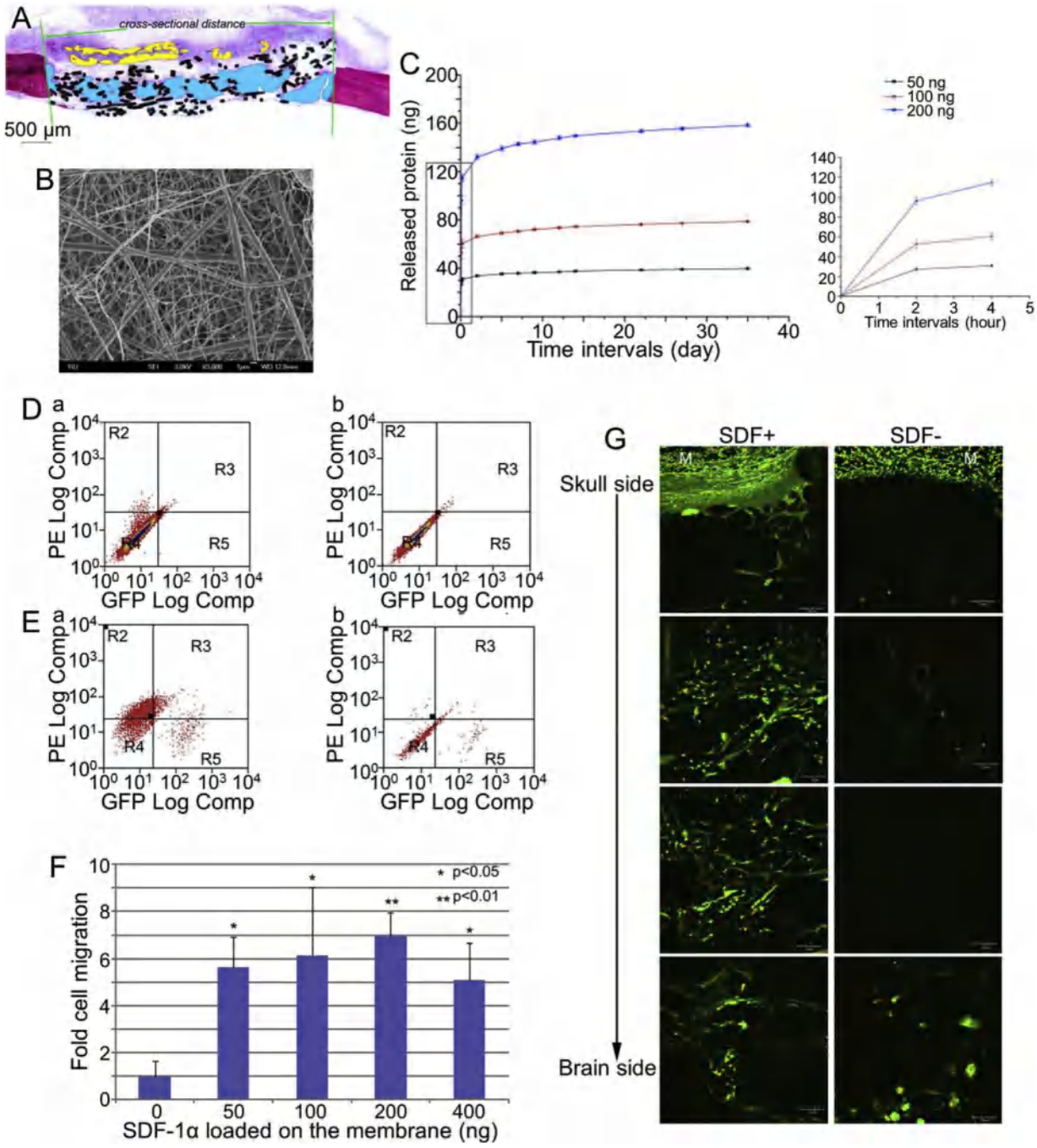

Fig. 7. Schematic overview of histomorphometric evaluation of bone repair, properties of stromal cell-derived factor-1α (SDF-1α) loaded electrospun fibers and bone repair effects of the membranes. (A) Schematic overview of histomorphometric evaluation. The bone formation area (μm^2) was determined as a newly-developed bone in two regions: (i) inside titanium fiber mesh (blue area) and (ii) outside titanium fiber mesh (yellow area). (B) SEM image of SDF-1α-loaded electrospun fibers. (C) *In vitro* SDF-1α release profiles. A volume of 20 μL ^{125}I-labeled/unlabeled mixture of an SDF-1α solution containing 50, 100, or 200 ng was absorbed onto disc-shaped PCL/gelatin electrospun membrane. (D and E) A representative example of extracellular and intracellular expression of SDF-1α receptor (CXCR4) in rat bone marrow stromal cells (BMSCs) by (a) antibody staining and (b) isotype control, respectively, which indicated a negative extracellular expression and a positive intracellular expression of CXCR4. (F) Five different amounts of SDF-1α (0–400 ng) were loaded on the electrospun membrane and tested *in vitro* chemotactic effect on rat BMSCs using transwell migration system. (G) CLSM images of samples retrieved from rats. M indicates the polymer membrane. Scale bar = 30 μm. [113], Copyright 2013. Reproduced with permission from Elsevier Ltd (For interpretation of the references to colour in this figure legend, the reader is referred to the web version of this article).

in situ co-precipitation synthesis approach, and [100] a direct deposition of gelatin [106], type II collagen [107], HAP [108], or biomimetic calcium phosphate [109] have been proposed for the surface modification of scaffolds. Among them, electrospun nanofibers that surface-modified with calcium phosphate showed strongly-promoted proliferation and osteoblastic differentiation for a prolonged cell culture period, and collagen was employed for enhancing stem cell attachment and proliferation [110]. Taken all together, these bioactive substances rendered innate biological guidance to cells, support the differentiation of progenitor cells toward osteoblastic lineages, and finally calcify the surrounding matrix [111]. Recently, the effects of HAP particle size and thermoplastic polyurethane (TPU) properties on scaffold physical properties and osteoblast-like cell behavior were also studied in detail [112]. It was found that soft TPU was highly hydrophilic, but hard TPU was hydrophobic. Addition of both micro-HAP and

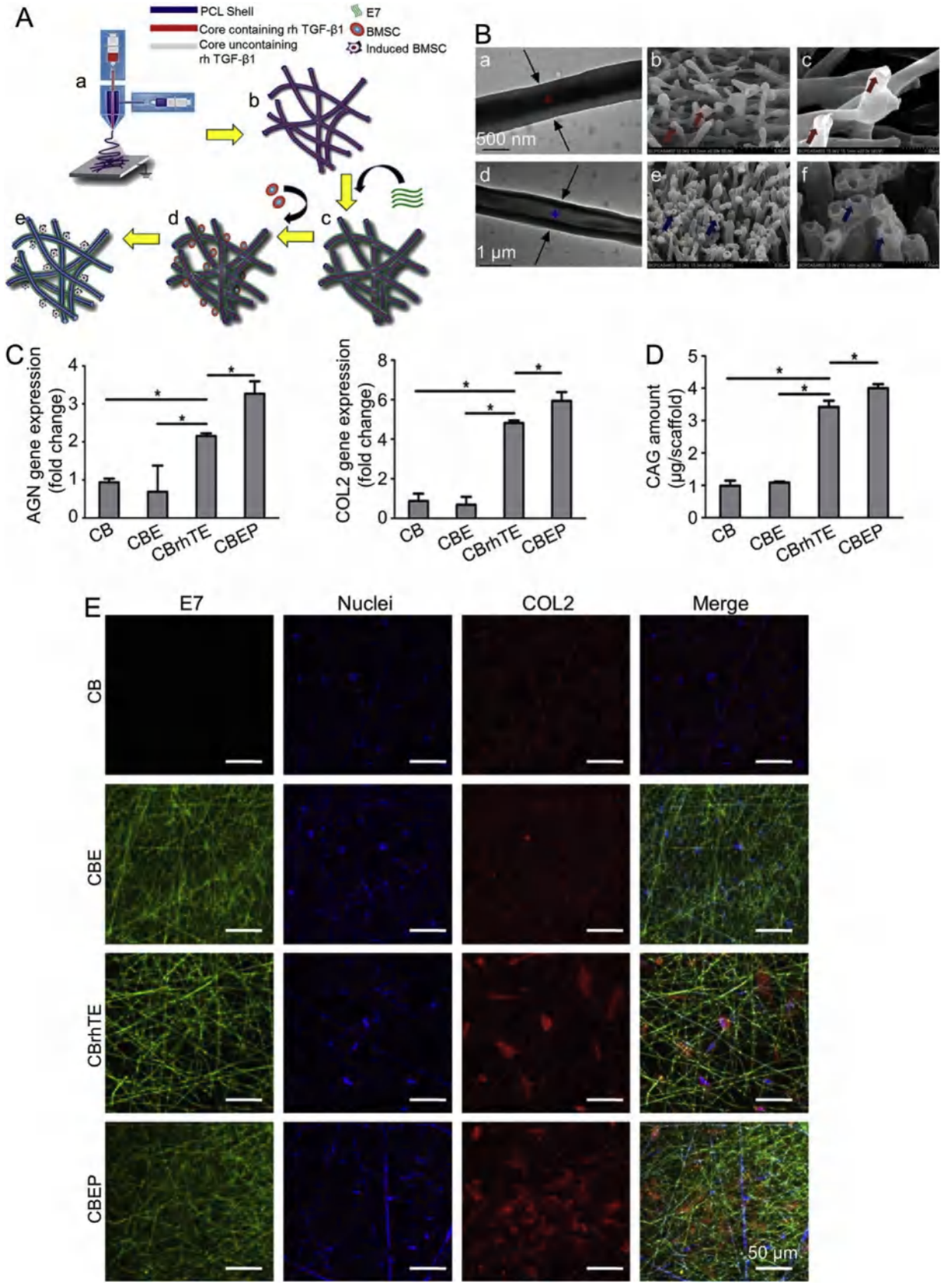

Fig. 8. Preparation and characterizations of rhTGF-β1- and E7-loaded coaxial electrospun fibers and their effects on BMSCs differentiation. (A) Schematic illustration of preparation process and working hypothesis for coaxial electrospun fiber scaffolds. (a) Setup of coaxial electrospinning. (b) Scaffold composed of electrospun coaxial fibers. (c) Scaffold conjugated with the BMSC-specific affinity peptide (E7) (green). (d) E7-modified scaffold promoting adhesion of BMSCs onto the scaffold. (e) The rhTGF-β1 encapsulated in the core of the coaxial fibers was released sustainably to promote chondrogenic differentiation of BMSCs adhered on the scaffolds. (B) Core-shell structure of CBrhT fibers (rhTGF-β1 loaded PCL/PVP/BSA fibers). (a–c) Images of fibers before rhTGF-β1 release: (a) TEM image showed the core with rhTGF-β1 (red asterisk) that was evenly encapsulated by the PCL shell (arrow); (b) Cross-sectional SEM image displaying rhTGF-β1 in the core section (red arrow); (c) Cross-sectional SEM image with

nano-HAP weakened the tensile properties, with a more significant decrease for micro-HAP. Overall, the soft nano-HAP scaffold outperformed the rest regarding hMSCs differentiation, which might be ascribed to the hydrophilicity of the material and high aspect ratio of nano-HAP. Interestingly, the calcium phosphate layers on the nanofibers owned similar characteristics to human bones, indicating potential applications in bone tissue engineering.

Another excellent example of applying surface-modified nanofibers to tissue engineering was immobilizing cell adhesive molecules, including the fibronectin and arginine-glycine-aspartic acid (RGD) peptides [114,115]. Morphologies of the surface-modified nanofibers were the same with the unmodified ones. High surface areas enabled a significant amount of cell adhesive molecules to be deposited onto the surface, which consequently increased cell adhesion and promoted proliferation of cultivated cells compared to other conventional tissue engineering scaffolds. Cell adhesion proteins were conjugated to electrospun micro/nanofibers for cultivating epithelial cells [116]. To further optimize electrospun scaffolds for bone tissue engineering applications, sensitive growth factors of HAP and bone morphogenetic protein-2 (BMP-2) were also incorporated onto the scaffolds [117]. It was found that the silk fibroin-based scaffolds promoted hMSCs differentiation toward osteogenic outcomes. Significantly, the coexistence of HAP and BMP-2 resulted in an enhanced BMP-2 transcription level of bone-specific markers and the highest calcium deposition, indicating that these electrospun scaffolds offered substantial benefits for controlling the delivery of growth factors during specific tissue formation. Among the various choices of osteogenic factors, SDF-1α also plays a particularly important role in the migration of BMSCs to a defect site (as shown in Fig. 7). One kind of guided bone regeneration membranes acquired by electrospinning PCL/type B-gelatin blends and functionalizing with SDF-1α *via* physical adsorption was once reported. The results showed that compared with the bare membranes, SDF-1α loaded membranes stimulated BMSCs recruitment and yielded a 6-fold increase in the bone reconstruction amount, thus being beneficial for optimizing the clinical reparation of large bone defects [118].

2.2.3. Cartilage tissue engineering

Degenerative diseases, such as traumatic injuries and osteoarthritis, are both prominent causes of cartilage defects. Due to the avascular nature and the low mitotic ability of chondrocytes, adult human cartilage has a limited self-repair capacity *in vivo* [119]. Tissue engineering scaffolds with predesigned properties provide a promising alternative therapy for serving as a carrier for MSCs or chondrocytes, which could simulate the native cartilage structure and then improve the cartilage formation and functionalities [74]. Electrospinning is a simple economic mean to produce scaffolds of ultrafine fibers derived from various polymers. The 3D electrospun fibrous scaffolds are well-known for their morphological similarity to natural collagen fibrils, high porosity, and large surface area to volume ratio. These physical characteristics afford favorable biological responses for seeding cells *in vitro*, such as enhanced cell adhesion, proliferation, and maintaining the chondrocyte phenotype [120]. For instance, a multilayered electrospun scaffold consisted of collagen type I and II was demonstrated with the high potency to induce chondrogenic differentiation of hMSCs *in vitro* [74]. Of note, the healthy articular cartilage is primarily composed of some specifically-oriented chondrocytes and extracellular matrices. Previous studies have reported that the oriented scaffolds have great potential to repair cartilage through improving cell affinity and alignment [121]. In detail, after culturing articular chondrocytes on the longitudinal-oriented PLGA scaffolds for 12 weeks, the cell migration toward the inner region of the constructs has been efficiently promoted in the oriented scaffold group [122]. More importantly, after 12 weeks of *in vivo* implantation, the oriented constructs formed thicker cartilage tissue with stronger mechanical property, a more homogeneous structure, and more abundant cartilage-specific ECM deposition compared to that of the nonoriented group.

Polymer-derived scaffolds always lack cell recognition signals, and their hydrophobic nature hinders cell attachment. To create cell – biomaterial interfaces, a variety of surface modification agents may potentially be immobilized onto the plasma-treated substrates, including collagen [120], fibronectin [124], chitosan (CS) [125,126], and gelatin [127]. For instance, poly(L-lactide) (PLLA) nanofibers can be treated with oxygen plasma to introduce —COOH groups on the surface, followed by covalently-grafting cationized gelatin (CG) onto the fiber surface with water-soluble carbodiimide as the coupling agent [128]. Both *in vitro* and *in vivo* experiments demonstrate a superior ability of CG-grafted PLLA nanofibrous membranes, which act as a kind of promising cartilage tissue engineering scaffolds to support the proliferation, differentiation, and cartilaginous matrix biosynthesis of chondrocytes.

Growth factors are another type of polypeptides that can stimulate the differentiation of hMSCs into specific tissue-forming cell lineages, such as myocytes, chondrocytes, adipocytes, and osteoblasts [129]. However, slow tissue penetration has hindered their applications. For maintaining stability and enhancing the *in vivo* efficacy, the spatially-controlled release of growth factors (*e.g.,* kartogenin (KGN), recombinant human insulin-like growth factor-I (rhIGF-I), and recombinant human bone morphogenetic protein-2 (rhBMP-2)) in polymeric biomaterials is crucial for engineering a complex osteochondral construct [120,130]. Two kinds of growth factors, *i.e.*, rhIGF-I and rhBMP-2, were once functionally microencapsulated into the silk microsphere/scaffold system. Through evaluating their impact on the osteochondral differentiation of hMSCs, it was found that rhIGF-I enhanced the rhBMP-2 effect, but did not solely induce hMSCs differentiation, which was likely due to its fast release and limited loading. This finding offers a new option for spatial controlled delivery of multiple growth factors in a polymer scaffold for bone repair applications [131]. Another approach to guarantee a sustained release of incorporated growth factors is employing the core – shell electrospinning technique. Transforming growth factor-β (TGF-β) plays a critical role in chondrogenesis during bone defect reparation and embryonic skeletal development. It is especially applicable for TGF-β1, TGF-β2, and TGF-β3, which have been verified to stimulate the chondrogenesis of MSCs and enhance the synthesis of cartilaginous ECM in chondrocytes [132,133]. As shown in Fig. 8, the coaxial electrospun fibers were formed with PVP/BSA/recombinant human transforming growth factor-β1 (rhTGF-β1) composite solution as a

higher magnification showed the presence of PVP/BSA/rhTGF-β1 compound in the core section (red arrow). (d–f) Images of fibers after rhTGF-β1 release (immersed for 21 days in PBS): (d) TEM image showed that the core (blue asterisk) became hollow following rhTGF-β1 release; (e) Cross-sectional SEM image displayed the uniform morphology of fibers and homogeneous hollow structure (blue arrow) owing to the release of core content; (f) Cross-sectional SEM image with higher magnification showed the hollow core (blue arrow). (C–E) Analyses of chondrogenic differentiation for BMSCs on different scaffolds after incubation for 14 days. (C) Real time-qPCR analyses of aggrecan (AGN) and collagen type II (COL2) gene expression (n = 3; *P < 0.05). (D) The glycosaminoglycan (GAG) content (n = 3; *P < 0.05). (E) Immunofluorescence analysis of COL2. CB: pure PCL/PVP/BSA fibers. CBE: PCL/PVP/BSA fibers loaded with E7. CBrhT: PCL/PVP/BSA fibers loaded with rhTGF-β1. CBEP: BMSCs were seeded on CBE scaffold and cultured with assay medium supplemented with 10.0 ng/ml rhTGF-β1. [123], Copyright 2014. Reproduced with permission from Elsevier Ltd (For interpretation of the references to colour in this figure legend, the reader is referred to the web version of this article).

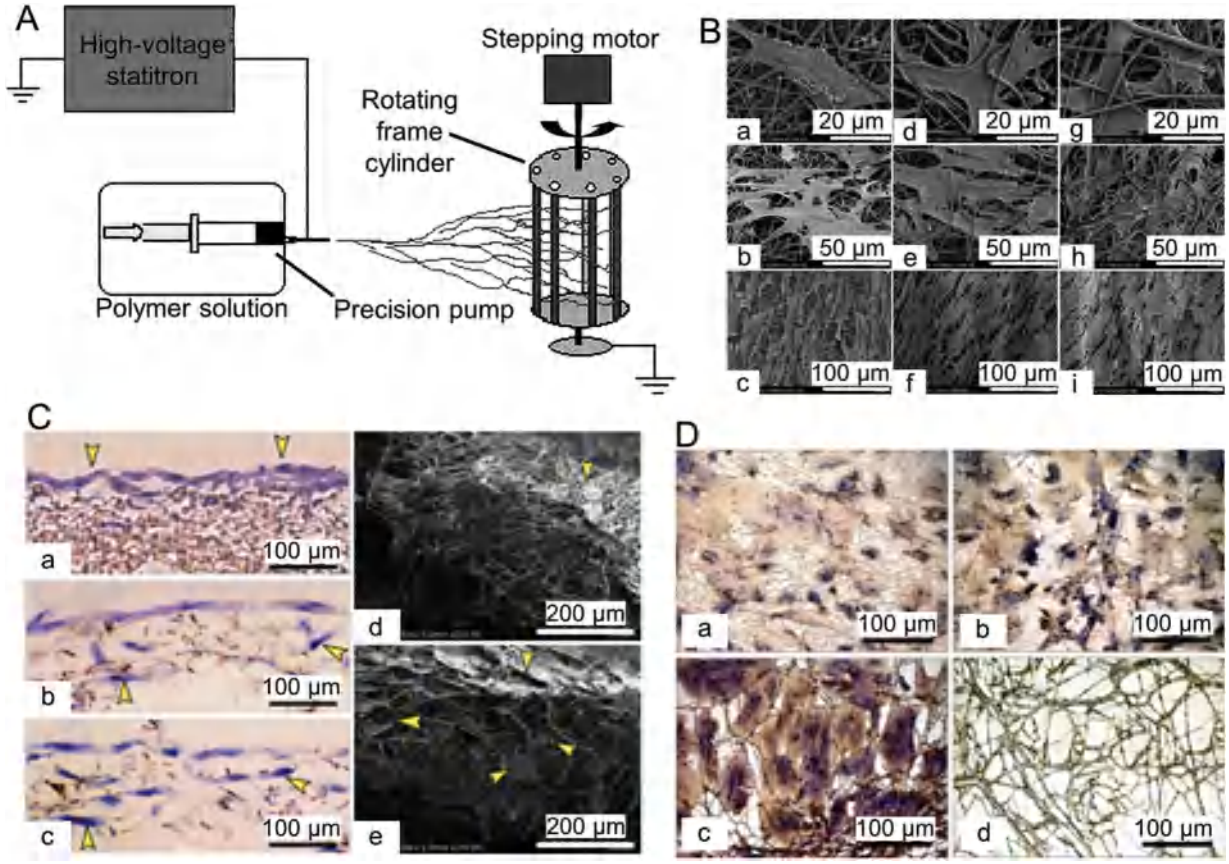

Fig. 9. Illustration of electrospinning setup with rotating collector, properties of electrospun mats which deposited on different collectors, and their effects on hDFs. Three types of fibrous mats were harvested from these collectors: deposited on the plate (FM-P), acquired on the frame cylinder at the rotation speed of 28 rpm (FM-LR) and 60 rpm (FM-HR). (A) Electrospinning apparatus with the collector of rotating frame cylinder. (B) SEM images of cell-grown fibrous mats collected on plate (FM-P, a–c), the frame cylinder with rotating speed of 60 rpm (FM-HR, d–f) and 28 rpm (FM-LR, g–i) on day 1 (a, d, g), 3 (b, e, h), and 5 (c, f, i) after incubation. (C) Cross-sections of hematoxylin and eosin (H&E)-stained cell-grown fibrous mats collected on plate (FM-P, a), the frame cylinder with rotation speed of 60 rpm (FM-HR, b) and 28 rpm (FM-LR, c). SEM images of cross-sections of cell-grown fibrous mats of FM-P (d) and FM-LR (e) after a 5-day incubation. Arrows indicate cells residing at the surface and inner part of the scaffold. (D) Immunohistochemical analyses of collagen type I of cell-grown fibrous mats of FM-P (a), FM-HR (b), and FM-LR (c) after a 5-day incubation. FM-LR without cell loading was used as control (d). [142], Copyright 2008. Reproduced with permission from the American Chemical Society.

core fluid and PCL solution as sheath fluid. Subsequently, the BMSCs specific affinity peptide (E7) was covalently conjugated to the coaxial electrospun fibers. Cell culture tests indicated that E7 enhanced the initial adhesion and growth of BMSCs, while the rhTGF-β1 synchronously promoted the chondrogenic differentiation ability of BMSCs. Overall, scaffolds containing both rhTGF-β1 and E7 were the most favorable for BMSCs survival and cartilage repair [123].

2.2.4. Skin tissue engineering

Skin acts as a protecting barrier against chemical damage, mechanical impairment, or microbial invasion. In general situations, skin defects often result from severe tissue trauma and burns. Wounds with large-scale skin loss require essential coverage with a dressing to protect the wound against infection. Traditionally, autografts, allografts, and xenografts have been frequently used to treat full-thickness skin defects or burns. However, these approaches are limited in supply and may cause an immunological rejection or disease transmissions, such as primary graft contraction and failure [134]. Tissue engineering substitutes have emerged as a practical, convenient, and inexpensive alternative to treat skin defects or injuries [135]. Ideal tissue engineering substitutes should protect the injury from protein loss, improve the aesthetic appearance of the wound site, inhibit exogenous microorganism invasion, and mimic the natural skin functions [136]. In an attempt to fabricate an excellent scaffold imitating the structural properties of ECM of natural skin, different kinds of electrospun matrices have been investigated.

Collagen type I has been widely applied for skin tissue regeneration, but it typically increases the production costs of tissue-engineered skin substitutes. To address this problem, electrospun PCL/gelatin scaffold modified with a small amount of collagen type I has been fabricated for use in skin tissue engineering field [137]. This method was proved to be successful in accelerating the cell proliferation rate and maintaining the characteristic shape of fibroblasts. Except for some ingredients, such as gelatin, chitosan, and collagen, new material has also been developed to improve the biological and mechanical properties of the scaffolds. Poly(ethylene oxide)-*block*-poly(propylene oxide)-*block*-poly(ethylene oxide) (Pluronic), a non-ionic surface-active agent, improves the hydrophilic performance of the polymer scaffolds without the use of any harmful chemicals after being added into the electrospun fibers [138]. As a broad-spectrum surfactant molecule, Pluronic not only possesses high hydrophilicity or enhanced mechanical property but can also increases the protein solubility and metabolic stability. Compared to poly(lactide-*co*-ε-caprolactone) (PLCL) scaffold, the blended elastic PLCL/Pluronic scaffold always exhibited better cell attachment and proliferation potential of adipose-derived stem cells [138]. Epidermal growth factor (EGF) has been widely accepted as one of the most common factors for treating wounds, which improved cell motility, as well as epidermal and mesenchymal regeneration. The EGF-encapsulated

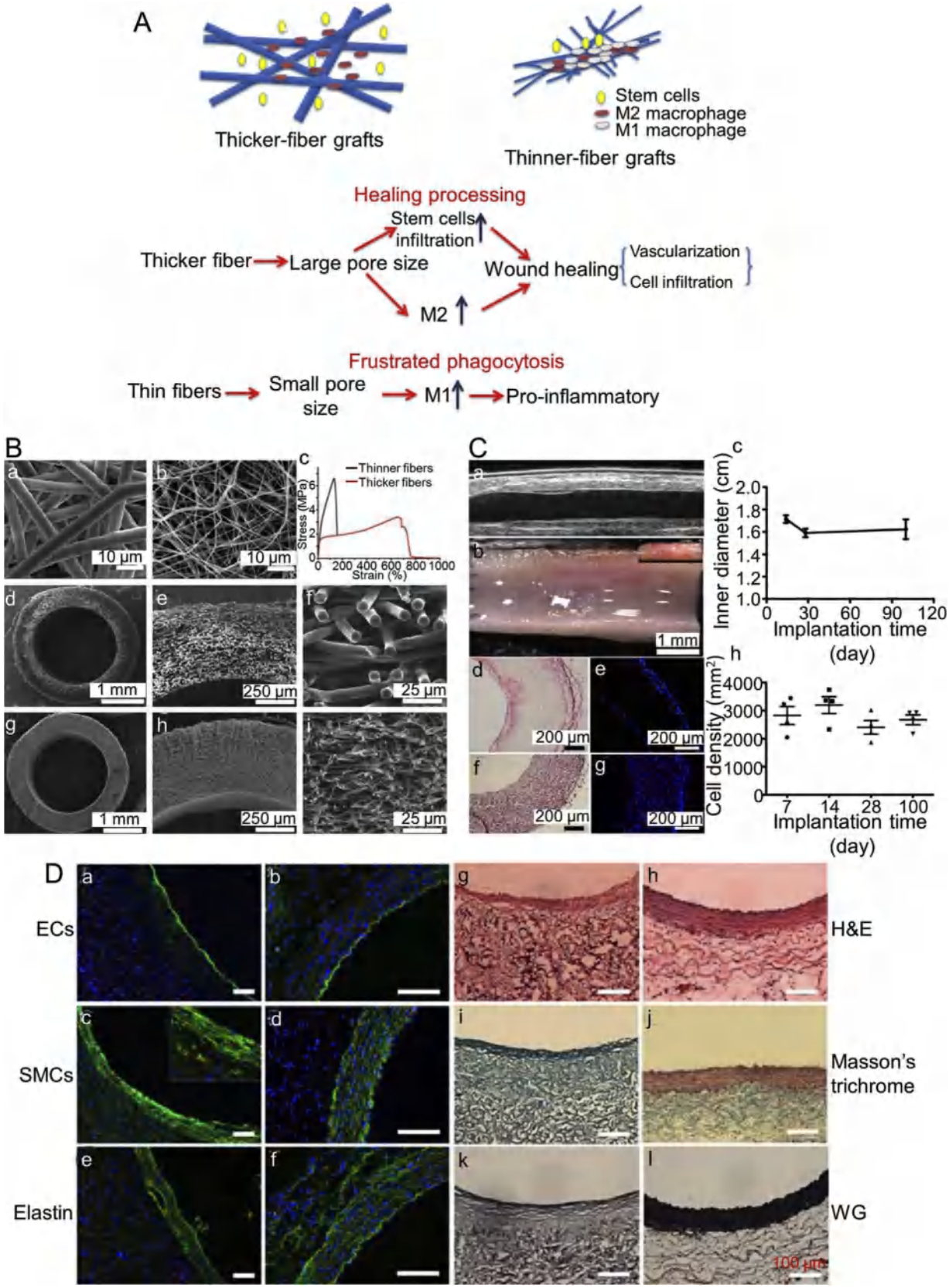

Fig. 10. Mechanisms of scaffold fiber diameter on regulating the macrophage phenotype, properties of thicker and thinner PCL fibers, and their effects on vascular tissue engineering. (A) Effects of fiber diameters on the macrophage phenotype. (B) Structure and mechanical property of electrospun PCL. SEM images of electrospun PCL mats with (a) thicker fibers and (b) thinner fibers. Cross-sections of (d–f) tubular thicker-fiber grafts and (g–i) thinner-fiber grafts. The characteristic tensile strain–stress curve was shown in (c). (C) Evaluation of tubular PCL grafts *in vivo*. (a) The ultrasound image of the thicker-fiber graft on day 100, (b) the luminal morphology of the thicker-fiber graft on day 100 was observed under a stereomicroscope, (c) the inner diameters of the grafts were calculated based on ultrasound measurement (n = 4). H&E staining show cellularization of the (d) thinner-fiber and (f) thicker-fiber grafts on day 28, and cellularization of the (e) thinner-fiber and (g) thicker-fiber grafts were also confirmed by

PLGA nanofibers through the emulsion electrospinning technique induced the expression of high-affinity receptors in both keratinocytes and fibroblasts, meanwhile accelerating the wound healing [139]. In conclusion, highly-porous biocompatible scaffolds with the capability of encapsulating and controlling growth factor release hold great potential to be utilized in skin tissue engineering applications [140].

In addition to the studies related to composition exploration, the personalized design of scaffold structure is another crucial point with considerable attention in skin tissue engineering field. The effect of varied fiber diameter of electrospun matrices on skin regeneration has been investigated through fabricating porous PLGA matrices with different fiber diameters of 3250–6000, 2500–3000, 600–1200, 500–900, 250–467, 200–300, and 150–225 nm, meanwhile evaluating their reparation efficacy by seeding them with human skin fibroblasts (hSFs) [141]. It was found that the hSFs exhibited a well-spreading morphology, showed a significant progressive growth, and acquired a high collagen type III expression in the diameter range of 350–1100 nm. In addition to the fiber diameter, porosity and pore size are also crucial parameters influencing cell infiltration, especially when the relatively large-sized pores are needed. To appropriately increase the porosity of electrospun mesh and extend the pore size, a slow-rotating metal frame cylinder has been proposed to deposit fibers, as shown in Fig. 9 [142]. When the metal struts are used as the collector, the electrostatic forces drive the fibers to move toward the metal struts, while the fibers of less density are deposited between them. Ultimately, fibrous mats with an average pore size of 132.7 μm and a porosity of 92.4% were obtained. The viability test further indicated that large amounts of human dermal fibroblasts (hDFs) generated well on such highly-porous fibrous mats and own great potential in skin tissue engineering field.

2.2.5. Blood vessel tissue engineering

In many developed countries, a vast majority of deaths are attributed to cardiovascular diseases and half of these deaths are the result of vascular system failure [143]. Tissue engineering has great potential in providing some effective therapeutic strategies to replace degenerated or damaged vessels with functional ones. However, these engineered vessels should meet several strict standards regarding the performance, such as possessing a highly porous structure, a vessel-like tubular shape, and sufficient mechanical properties, to provide a suitable environment for cell adhesion, growth, and colonization [144]. Generally, vascular grafts are fabricated by electrospinning, because it is a versatile processing technique to generate non-woven fibrous structures [145]. However, one major problem faced by electrospinning lies in the small pores that are generated, which often results in a limited cell infiltration and thus hindering the remodeling of vascular grafts in the long term. For that, macroporous electrospun PCL scaffolds with larger pores (~30 μm) have been fabricated by increasing the fiber diameter of electrospun mats. Interestingly, it was found that the thicker-fiber scaffold structure regulated the phenotype of macrophages as illustrated in Fig. 10 [146]. Specifically, a large number of macrophages cultured on the thinner-fiber scaffolds expressed a proinflammatory phenotype (M1), while those cultured on the thicker-fiber scaffolds tended to polarize into the tissue remodeling phenotype (M2). *In vivo* results further revealed that the macroporous grafts enhanced the cell infiltration, vascular regeneration, and tissue remodeling. However, the thinner-fiber grafts maintained the macrophages in the M1 phenotype, which secreted pro-inflammatory factors and played a negative role in tissue regeneration. Similarly, the pore size in the range of 30–40 μm reduced fibrotic response and increased vascularization due to a shift in macrophage polarization toward the M2 state [116], which consequently mediated the regeneration of cell-free electrospun grafts into neo-arteries *in vivo*.

Early studies of blood vessel tissue engineering are termed "top – down" approaches because they are based on seeding cells on porous scaffolds to form tubular tissue-engineered constructs. However, such an archetypal approach through using biodegradable scaffolds for the newly-constructed vessels generally raises some concerns about inflammation, foreign body reaction, and infection due to bacterial colonization [147]. In this context, "bottom – up" tissue engineering strategies have been developed recently. In this approach, individual sections of the tissue are separated and then are built together to generate a biomimetic tissue-engineered construct with higher fidelity. Additionally, "bottom – up" approaches are always scaffold-free, which promises less inflammation and toxicity as the scaffold degradation [148]. In a recent study, a "bottom – up" and scaffold-free approach (a combination of electrospinning and cell sheet technology) has been introduced to the human blood-vessel tissue engineering, where a tubular construct of circumferentially-aligned smooth muscle cells showed enough mechanical strength and a high expression of contractile genes to enable facile cell-sheet handling within days [76].

To address the increasing demand on vascular grafts for cardiovascular diseases, developing substitutes with bio-functionalities is also necessary, such as rapid endothelialization, anticoagulation, smooth muscle regeneration, and hemocompatibility [149,150]. In detail, to enhance the blood vessel tissue engineering efficacy, hydrophilic surfaces of the vascular grafts have been created by various approaches. Moreover, these grafts are also required to induce *in situ* tissue regeneration for reconstructing blood vessels with complete endothelialization. RGD molecule, a tripeptide derived from the cell-adhesion fibronectin, has always been applied to modify the surface properties of electrospun polyester scaffolds. It was demonstrated that the RGD-modified polymer grafts exhibited an improved revascularization capability, as evidenced by a 3-fold increase of endothelial cell attachment compared to that of the untreated grafts [151,152]. Additionally, a blend of polyester urethane urea (PEUU) and phospholipid polymer was another kind of favorite candidate for fabricating vascular grafts [152]. The elastomer PEUU provideed sufficient mechanical properties, while the incorporation of phospholipids was responsible for improving the implantation patency in rat abdominal aorta. The compositions of the natural ECM, such as collagen [153] and elastin [154], have also been combined with polymers to favor the adhesion of vascular cells. In conclusion, surface modification plays an essential role in the blood-vessel tissue engineering field to obtain the biomimetic and bioactive scaffolds [155].

DAPI staining. (h) The density of cells within the thicker-fiber grafts was calculated based on DAPI staining (n = 4). (D) Histological analysis and deposition of ECM in regenerated grafts on day 100 in comparison with native aorta. Cross-sectional images of the (a, c and e) regenerated grafts and (b, d, and f) native artery were immunochemically stained to identify the endothelial cells (ECs), smooth muscle cells (SMCs), and elastin. H&E staining showed the structure of the (g) explanted grafts and (h) native aorta. Masson's trichrome staining showed the presence of collagen (green) in the (i) explanted grafts and (j) native aorta. Verhoeff's staining showed the presence of elastin (black) in the (k) explanted grafts and (l) native aorta. [146], Copyright 2014. Reproduced with permission from Elsevier Ltd (For interpretation of the references to colour in this figure legend, the reader is referred to the web version of this article).

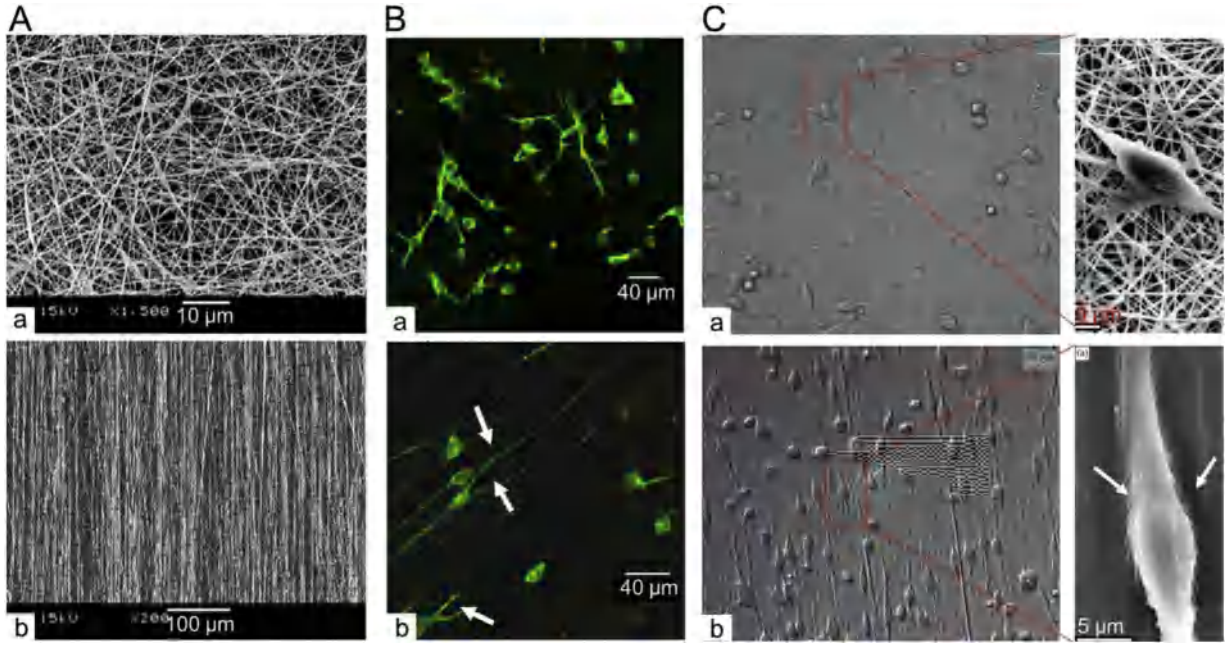

Fig. 11. Properties of random or aligned PLLA electrospun fibers and their effects on NSCs growth. (A) SEM micrographs of PLLA (a) random nanofibers and (b) aligned nanofibers. (B) LSCM micrographs of NSCs seeded on (a) random nanofibers, (b) aligned nanofibers after two days of culture. (C) SEM micrographs of NSCs attached on (a) random nanofibers, (b) aligned nanofibers for two days, the cell – matrix adhesion was exhibited. [158], Copyright 2005. Reproduced with permission from Elsevier Ltd.

2.2.6. Neural tissue engineering

Nerve tissue repair that directly impacts the quality of life is a valuable concept of treatment in human health care. Nerve tissue engineering is one effective therapy for restoring the nervous system, in which the scaffold design plays a pivotal role [156,157]. By comparing the performance of perfectly-aligned PLLA micro/nanofibrous scaffolds with the random samples, better contact guidance on the neurite outgrowth is exhibited on the aligned fibers, demonstrating that the anisotropic fibers are desirable cell carriers in the neural tissue engineering field [158]. The representative SEM images of the single neural stem cells (NSCs) cultured for two days on the PLLA scaffolds were shown in Fig. 11. An apparent bipolar-elongated morphology along the same direction of the aligned nanofibers was observed, and the cell body had the outgrowing neurites. Additionally, some filament-like structures extended out from the NSC cell body, which were suspected to be the focal adhesions, which mediated a robust cell-matrix interaction and transmit information in a bi-directional manner between the cytoplasm and ECM molecules. On the contrary, almost no similar signals were revealed on the random fibers, further implying that the fiber alignment was effective in modulating the interaction between scaffolds and NSCs. No obvious differences were observed in the cell orientation concerning the fiber diameters. However, NSC differentiation rate was higher for PLLA nanofibers than that of the microfibers.

Polymers are typically used to produce a 3D scaffold for mimicking the structure of ECM. However, the synthetic polymer is generally poor in cell affinity due to their low hydrophilic property and lacking surface cell-recognition domains [159,160]. Natural polymers and bioactive proteins are therefore incorporated into the micro/nanofibers to enhance the cell – scaffold adhesions [161]. For example, gelatin is a natural biopolymer derived from collagen by controlled hydrolysis. Due to its commercial availability at a relatively low cost, biocompatibility, and biodegradability, composite nanofibrous scaffolds consisting of PCL and gelatin at differing weight ratios have been widely reported. It is found that the PCL/gelatin 70:30 nanofibers exhibit the optimum comprehensive properties to meet all the required specifications for nerve regeneration. Addition of gelatin is proved to enhance the degradation properties, and act as a positive cue to support nerve differentiation and neurite outgrowth compared to PCL nanofibrous scaffolds [162]. More recently, culturing neural cells on the scaffold surface under electrical stimulation has attracted lots of attentions, because an apparent increase in neurite growth caused by the electrical stimulation is revealed [163]. By this, a conductive polymer of PPy has been synthesized on the electrospun cellulose nanofibers. In comparison with the unmodified cellulose nanofibers, PPy particles located on the cellulose nanofiber surface result in a 10^5-fold increase in conductivity. Additionally, enhanced cell adhesion, viability, and differentiation of human neuroblastoma cells are exhibited on the PPy-coated cellulose material [164]. The nano-scale surface roughness, as well as the passive conductive property induced by the PPy coating, is able to favor cell attachment to the nanofibers and slightly promote the neurite outgrowth.

2.3. Wound healing

Skin is the largest organ covering the entire external surface of the body, occupying about 8% of the total body mass, and forming a self-repairing interface between the environment and the body [166]. Additionally, it is capable of adsorbing and excreting certain chemical substances, while simultaneously withstanding stretch, compression, and friction. Trauma to the skin is classified into several levels [167]. The least level is located at the most superficial layer of the skin, the epidermis layer. More serious damaging trauma is related to partial or complete damage of subdermal or dermal tissues. Wound healing is a natural process to regenerate dermal and epidermal tissues. Unfortunately, there are no remaining cells for the wound regeneration in the cases of a full-thickness burn or a deep dermal injury [168]. As a result, a wound dressing material is necessary to protect the wound as a physical barrier against bacterial penetration, mechanical impairment, and chemical damage, while simultaneously accelerates the re-epithelialization process. Recently, employing the electrospinning apparatus for wound-dressing material has attracted increasing interest, because the morphological, mechanical, and biological fea-

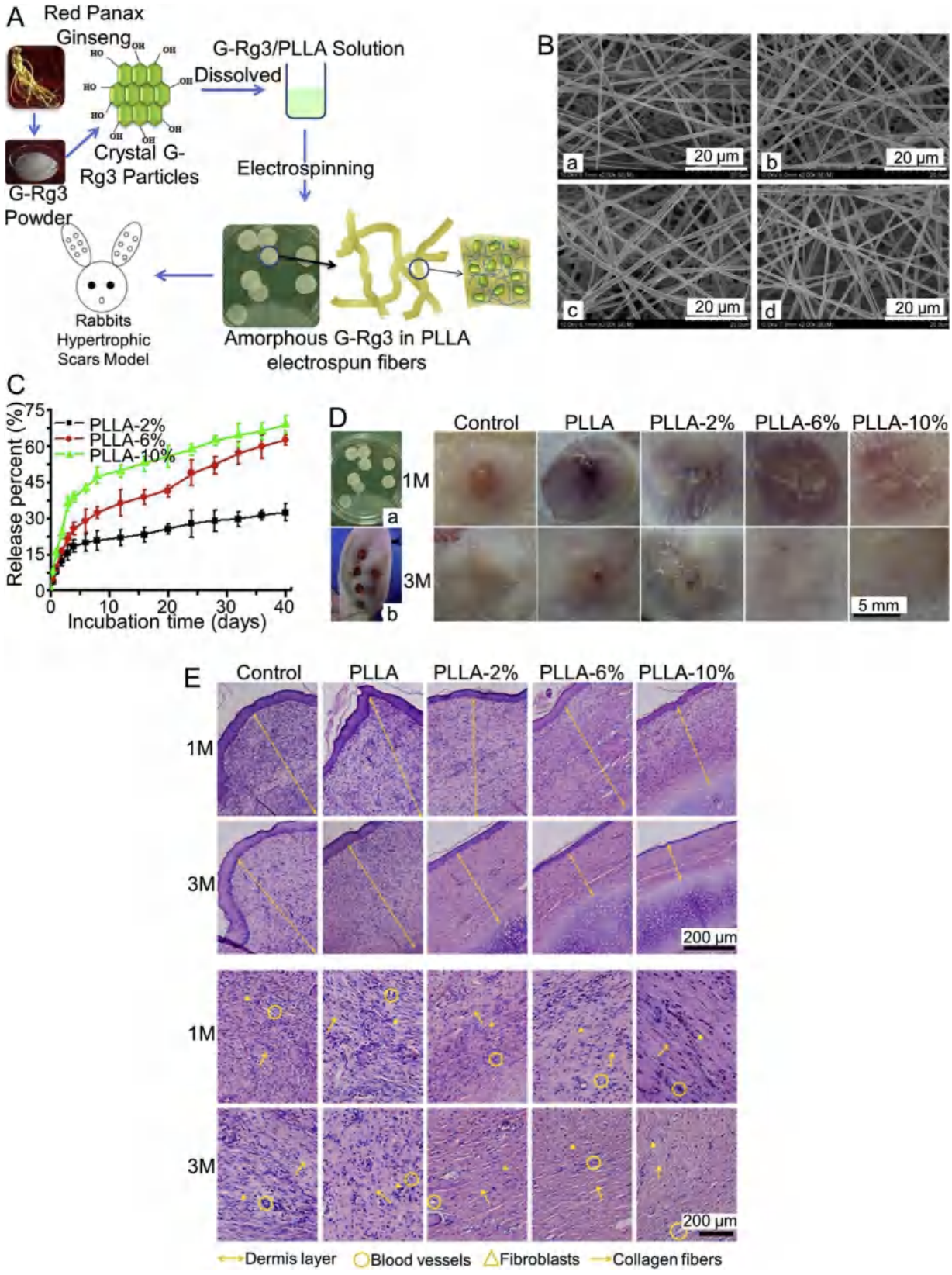

Fig. 12. Preparation, properties, and scar-hypertrophic treatment efficacy of Ginsenoside Rg3 (G-Rg3)-loaded PLLA electrospun scaffolds. (A) Amorphous state G-Rg3 in PLLA electrospun fibrous scaffolds for inhibiting hypertrophic scar formation. (B) SEM images of electrospun fibers. (a) PLLA fibers, (b) PLLA-2%, (c) PLLA-6%, and (d) PLLA-10% with 0%, 2.0%, 6.0%, and 10.0% Rg3, respectively. (C) *In vitro* Rg3 release percent from electrospun fibers after incubating in PBS at 37 °C. (D) Gross observation of scar hyperplasia treated with (a) implanted fibrous scaffolds and (b) blank after operation for one or three months. (E) H&E staining of sections of scar hyperplasia at one or three months after wounding. [165], Copyright 2013. Creative Commons Attribution license.

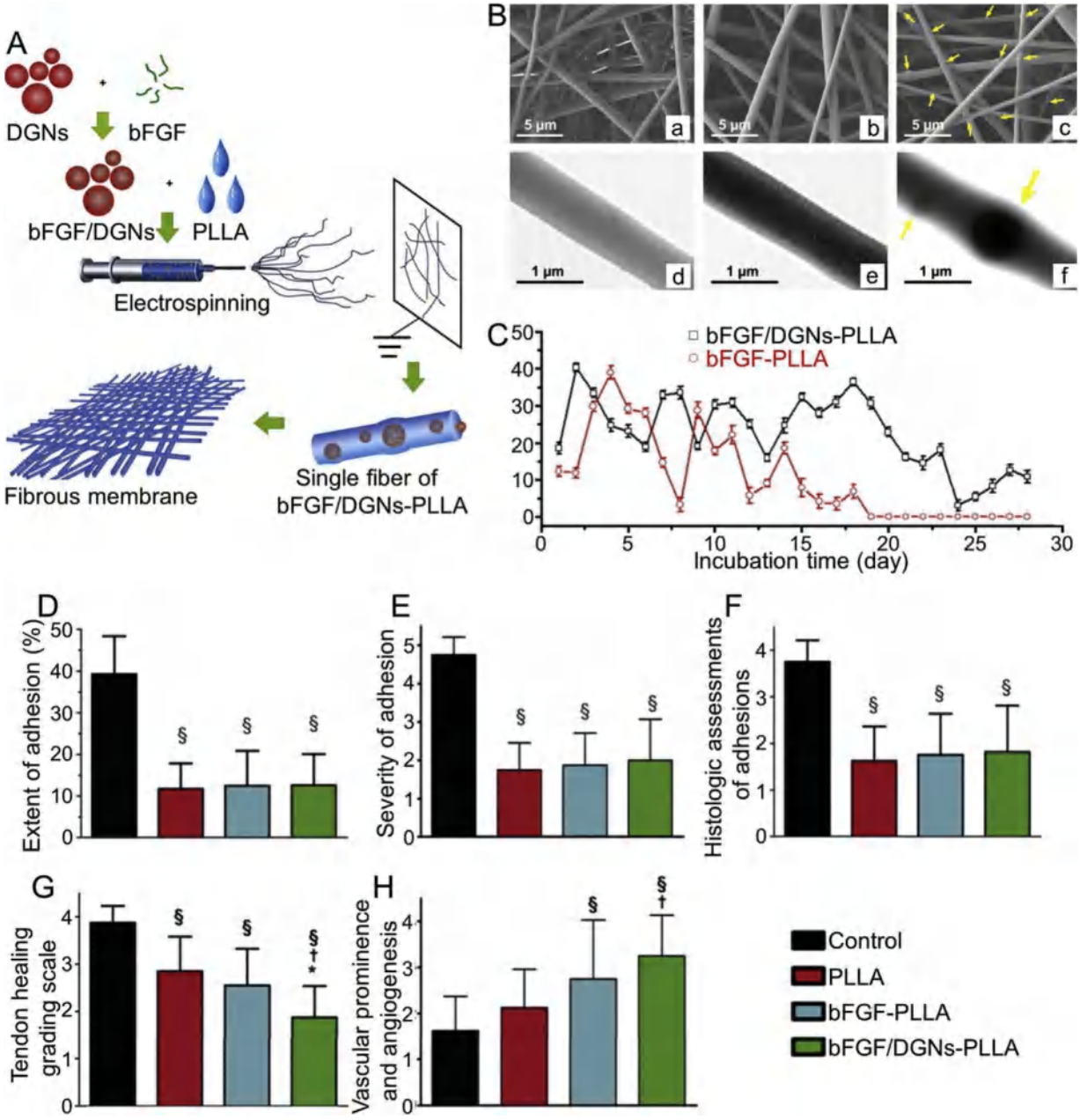

Fig. 13. Preparation, characterizations, and adhesion prevention effects of bFGF/DGNs-PLLA electrospun fibers. (A) Preparation process of bFGF/DGNs-PLLA electrospun fibers. (B) SEM images of electrospun (a) PLLA, (b) bFGF-PLLA and (c) bFGF/DGNs-PLLA fibers. TEM images of electrospun (d) PLLA, (e) bFGF-PLLA and (f) bFGF/DGNs-PLLA fibers. Yellow arrows indicate the DGNs embedded into fibers with thickened regions of PLLA visible around them. (C) Everyday release of bFGF from the electrospun bFGF-PLLA (red circles) and bFGF/DGNs-PLLA (black squares) fibers. (D) Parameters for peritendinous adhesions: extent of adhesion, (E) severity of adhesion, (F) histologic evaluation of tendon adhesions, (G) histologic quality of tendon healing and (H) vascular prominence and angiogenesis, 21 days after surgery. $^{\S}P < 0.05$ compared with control; $^{\dagger}P < 0.05$ compared with group treated with the PLLA membrane; $^{*}P < 0.05$ compared with group treated with the bFGF-PLLA membrane. Data are expressed as mean ± SD for eight tendons/group. [200], Copyright 2013. Reproduced with permission from Elsevier Ltd (For interpretation of the references to colour in this figure legend, the reader is referred to the web version of this article).

tures of the non-woven micro/nanofibrous structure are analogous to the natural ECM in skin [169]. Furthermore, the biocompatible electrospun membrane always produces interconnected pores with a high porosity, which can provide a feasible approach to add antibacterial drugs when utilized as a wound dressing. The electrospun mat could not only eliminate the post-surgery adhesion significantly but also improve the healing of injured skin [170,171].

2.3.1. Wound dressings

It is necessary for an ideal wound dressing material to support an antimicrobial environment, to prevent infections and eliminate invasion of pathogens in the wound. Of note, silver nanoparticles have strong inhibitory and antibacterial activity against a series of microorganisms [172]. Previous reports suggested that silver nanoparticles could be successfully synthesized by using leaf extracts of Piper nigrum and no chemical reagents were introduced during the biosynthesis [173]. Additionally, biosynthesis of the silver nanoparticles belongs to an eco-friendly and cost-effective approach for large-scale production. On this context, silver nanoparticles have been increasingly used in biological or therapeutic applications due to their low toxicity to human cells and antimicrobial activity, such as medical devices, wound dress-

ings, and textile fabrics [174]. Incorporating biosynthesized silver nanoparticles into electrospun PCL membranes for wound dressing applications has been reported recently. The obtained material showed excellent antibacterial activity against both Gram-negative (E. coli) and Gram-positive (S. aureus) bacteria, suggesting superior ability at preventing bacterial colonization in the wounds [175].

Multidrug-resistant (MDR) wound infection is very harmful because few available drugs are against MDR Gram-negative bacteria [176]. Several antibacterial nanomaterials are effective against MDR bacteria-caused wound infection, including zinc oxide, silver, tellurium, titanium dioxide (TiO_2), and copper oxide nanoparticles [177,178]. However, these nanomaterials can be cytotoxic or hemolytic. Thus, exploring wound-dressing materials to protect against MDR bacteria is extremely necessary. A unique kind of wound dressings has been designed recently through doping 6-aminopenicillanic acid-coated gold nanoparticles (Au – APA) into electrospun PCL/gelatin fibers, which was demonstrated with the ability to guard against MDR bacteria-caused wound infection. Taken together, a remarkable antibacterial activity, outstanding biocompatibility, and an *in vivo* bacteria-infected wound-healing capability of such Au – APA/PCL/gelatin scaffold presented great potential in wound-dressing applications, even in the case of MDR bacteria [179].

In addition to an antimicrobial environment, an ideal wound-dressing material should also possess excellent mechanical properties for replacement of the dressing. In general situations, synthetic polymers possess good mechanical strength, but poor cell affinity. The blending of synthetic and natural polymers overcomes these shortcomings and brings together their merits from each form of the polymer. Polyurethane (PU) is widely accepted in the field of wound dressings because of its excellent oxygen permeability and barrier properties, as some clinical wound-dressing materials with the trade-names of Tegaderm™ and Op-Site® that are based on PU [175]. However, the poor hydrophilicity of PU restricts their applications in wound dressings through preventing fluid exuding from the wound surface [180]. Keratin is a novel fibrous protein that forms outer coverings of the body, such as wool, hair, and nails. Recently, keratin has been attractive in skin wound repair and regeneration for its outstanding biocompatibility and biodegradability [180,181]. An advanced PU/keratin/AgNP nanofibrous mat has been successfully developed for wound dressings. Results from a histological examination indicated that these biocomposite mats remarkably promoted wound healing, in comparison with conventional gauze sponge dressing [182]. Considering their excellent antibacterial properties, biocompatibility, and very mild inflammatory responses, PU/keratin/AgNP mats are promising to be utilized as a wound-dressing material for skin reparation.

Hypertrophic scarring (HS) is another challenging problem that often occurs following severe surgical incision, which belongs to a dermal fibroproliferative disorder [183,184]. HS is normally characterized by neovascularization, excessive deposition of fibroblast-derived ECM proteins, and persistent inflammation [185]. It was once reported that inducing apoptosis of human hypertrophic scar fibroblasts selectively inhibited HS growth [186]. G-Rg3, a saponin extracted from Red Panax ginseng, is found to be able to reduce the generation of new blood capillaries by inhibiting the expression of vascular endothelial growth factor [185,187], which further prevents HS formation. G-Rg3/PLLA electrospun fibrous membranes have been designed using hexafluoroisopropanol (HFIP)/DCM as the co-solvent in a one-step process (Fig. 12). This membrane was used to suppress the hypertrophic scar formation *in vivo* by covering full-thickness skin excisions [165]. The fabrication process allowed successful incorporation of the G-Rg3 within the fibrous membranes in an amorphous state. The electrospun fibrous G-Rg3/PLLA dressings exhibited a gradual release profile for more than 30 days and meanwhile was able to minimize HS formation by decreasing the hSFs proliferation, dermis layer thickness, and a number of collagen fibers [188].

2.3.2. Anti-adhesion membranes

Post-surgery tissue adhesion often occurs after plastic surgery and repair operations of abdomen, pelvis, and tendon [189]. It not only complicates a secondary surgery, but also causes several post-surgical problems, including functional obstruction, chronic pain, and female infertility [190,191]. Electrospun mats can be employed as a physical barrier and a drug carrier simultaneously, therefore, numerous investigators have focused on using electrospun fibrous membranes to prevent postoperative adhesion [192,193]. A bilayer electrospun fibrous membrane that composed by a core of hyaluronic acid (HA) and a shell of PCL has been investigated the anti-adhesion efficacy in a rat cecum abrasion model [194]. It was found that the bi-layer system exhibited excellent tensile strength, hydrophilicity, and flexibility. More importantly, the bilayer fibrous membrane-treated animals showed a lower adhesion score than the pure PCL membrane-treated animals [194]. This suggested that the bilayer membrane efficiently prevented the adhesion formation *in vivo* in the abdominal cavity. By analysis, the outer PCL layer played the anti-adhesion role through preventing the intra-abdominal adhesion from surrounding tissue, and at the same time, such inner HA/PCL layer efficiently decreased adhesion formation by modulating fibrinolysis.

In many surgeries, antibiotics have been employed for infection prevention and alleviating adhesion formation. While, antibiotics are limited in inhibiting the fibrin connection with nearby normal tissues, and the physical barriers might bring the postoperative infection [195]. Silver is famous with its strong antibacterial activity and physical–chemical properties. PLLA fibrous membrane loaded with both ibuprofen and low concentrations of Ag nanoparticles has been reported recently, which is highly effective at infection prevention and adhesion inhibition, especially compared with other single systems previously described [193]. Similarly, silver nanoparticles-loaded electrospun HA/PCL membranes also exhibit great potential in preventing bacterial infection after tendon surgery. This dual-functional anti-adhesion barrier is composed of emulsion electrospun nanofibers, in which the HA solution and the photo-reduced silver nitrate/PCL solution act as core and sheath, respectively. Furthermore, a rabbit flexor tendon model is employed to confirm the efficacy of HA/PCL+Ag membrane in alleviating peritendinous adhesion and infection [196].

The poor gas permeability of traditional anti-adhesion devices is another main reason resulting in a very high risk of the infection and inflammation to occur. In our recent work, the atorvastatin (ATV)-loaded thermogel plus porous PLA film was prepared to prevent peritoneal adhesion, where PLA film was used to prevent the fibrin bridge-connections, and ATV was released to achieve the anti-inflammatory effect. The high porosities of PLA film and thermogel increased the gas permeability and anti-inflammatory responses synergistically. The *in vivo* results fully verified that such porous PLA film with ATV-loaded thermogel had great potential for a wide range of clinical applications due to its excellent anti-adhesion and anti-inflammation capacity [197].

An ideal anti-adhesion membrane should also contain growth factors that can improve the efficiency of tissue healing. Basic fibroblast growth factor (bFGF) is a representative bioactive agent that can positively affect tendon reparation [198] by stimulating cellular differentiation, angiogenesis, and matrix synthesis [199]. As shown in Fig. 13, to secure the stability of bFGF dextran glassy nanoparticles (DGNs) encapsulated with bFGF were electrospun into a PLLA copolymer fiber. The bioactivity retention of bFGF was verified according to cell proliferation and tendon healing rates. The barrier effect of the electrospun membrane to prevent peritendinous adhe-

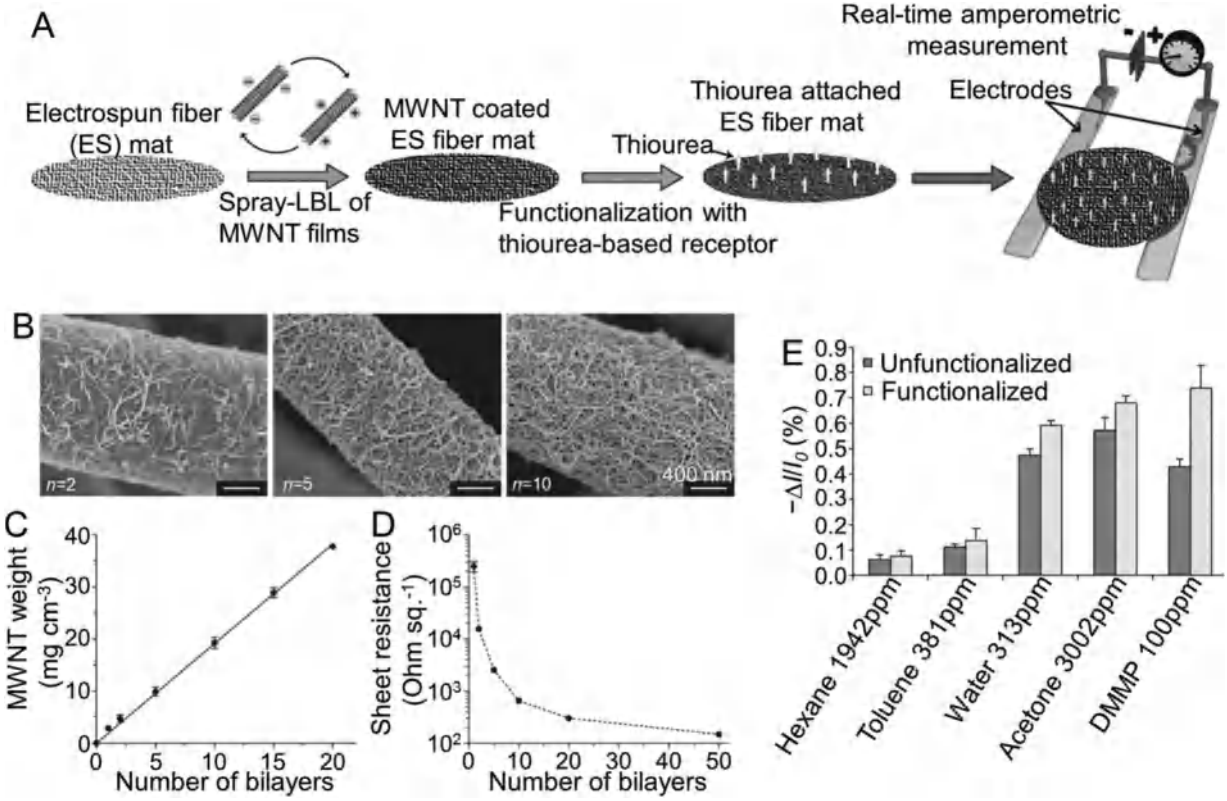

Fig. 14. Preparation and characterizations of MWNT films and their sensing response to different analytes. (A) Schematic representation of fabrication steps of a chemiresistive sensor based on MWNT-film coated electrospun fiber mat. (B) SEM images of ES fibers coated with MWNT films, where *n* indicates the number of bilayers (2, 5, and 10, respectively) in $(MWNT\text{-}COO^{-}/MWNT\text{-}NH_3^{+})_n$ films. (C) Correlation of cumulative weight to layer pair number of MWNT films. The straight line is a linear fit. (D) Sheet resistance of the MWNT/ES fiber electrodes. (E) Average sensing response of unfunctionalized and thiourea-functionalized MWNT/ES fiber electrodes to different analytes. The concentration of each analyte represented 1% of its equilibrium vapor concentration at room temperature except DMMP, which was used at ~6% of its equilibrium vapor concentration at room temperature. [214], Copyright 2013. Reproduced with permission from John Wiley & Sons Inc.

sion was also evaluated for clinical concerns [200]. As seen through *in vivo* experiments, such bFGF/DGNs-loaded PLLA fibrous membrane completely secured the biological activity of bFGF, release bFGF sustainably, and enhanced intrinsic tendon-healing ability, which promoted tendon healing and realized adhesion-prevention at the meantime.

Currently, the prevention of peritoneal adhesion based on integrating pharmaceutical therapy and physical isolation in one platform is still challenging. First, the poor hydrophilicity and the low bioadhesion ability of normal polymer anti-adhesion membranes decrease the healing efficacies. Second, the obviously different release behaviors of various drugs limit their synergistic effects. In the context, a kind of highly bioadhesive polymer membrane with core – sheath structure has been designed, where an integrated effect of physical isolation and pharmaceutical treatment synergistically prevent the peritoneal adhesion. Specifically, diclofenac sodium (DS) and10-hydroxycamptothecin (HCPT) were first used to form the core and sheath of nanofiber, respectively. Afterward, ultraviolet-ozone (UVO) treatment was conducted for improving hydrophilicity and bioadhesion. Due to the core – sheath structure, both drugs presented sustained release profiles, for the possessing the ideal cytostatic and anti-inflammatory effects, high anti-adhesion capacity, and great potential in clinical applications [201].

2.4. Others

In addition to the above-mentioned biomedical applications, electrospun polymer nanofibers have been steadily extended into other fields in recent years, including sensors [202,203], reinforcement [204], sound absorption [205], filtration systems [206], and electrodialysis separation [207]. A kind ultralight electrospun fiber/spongy composite structure has been reported recently, which has a density as low as 2.7 mg/cm^3 and a corresponding porosity of 99.6%. It is prepared *per* the following five steps, that is electrospinning, UV crosslinking, mechanical cutting, suspending the cut fibers in liquid dispersion, and finally freeze-drying [208]. Interestingly, such ultralight highly-porous scaffold with extremely low specific surface area and density also shows a surprisingly-reversible bendability and compressibility, and no structural destruction is observed, providing a great potential for the preparation of biomimetic polymer-based sponges. There is a broad spectrum of applications for these multifunctional materials including efficient filters, insulators, electrodes, catalysts, and shape-responsive materials, which will be briefly introduced in this section.

2.4.1. Sensors

Fluorescent polymer nanofibers are promising candidates in the applications of nano-optoelectronics, nano-photonics, light-emitting diodes, and chemical sensors, due to their flexibility, charge transportability, and compatibility [209]. Doping small fluorophores onto low-cost polymers is an alternative route to produce cost-effective and high-performance optical devices. A highly-sensitive sensor has been synthesized recently for nitro-compounds. The sensing composite nanofibrous film exhibited high quenching efficiency and immediate response toward 2,4-dinitrotoluene (DNT) vapor, which were ascribed to an improved MePyCz exciton migration in PEG [210]. Similarly, an optical-chemical sensor has been obtained by electrospinning

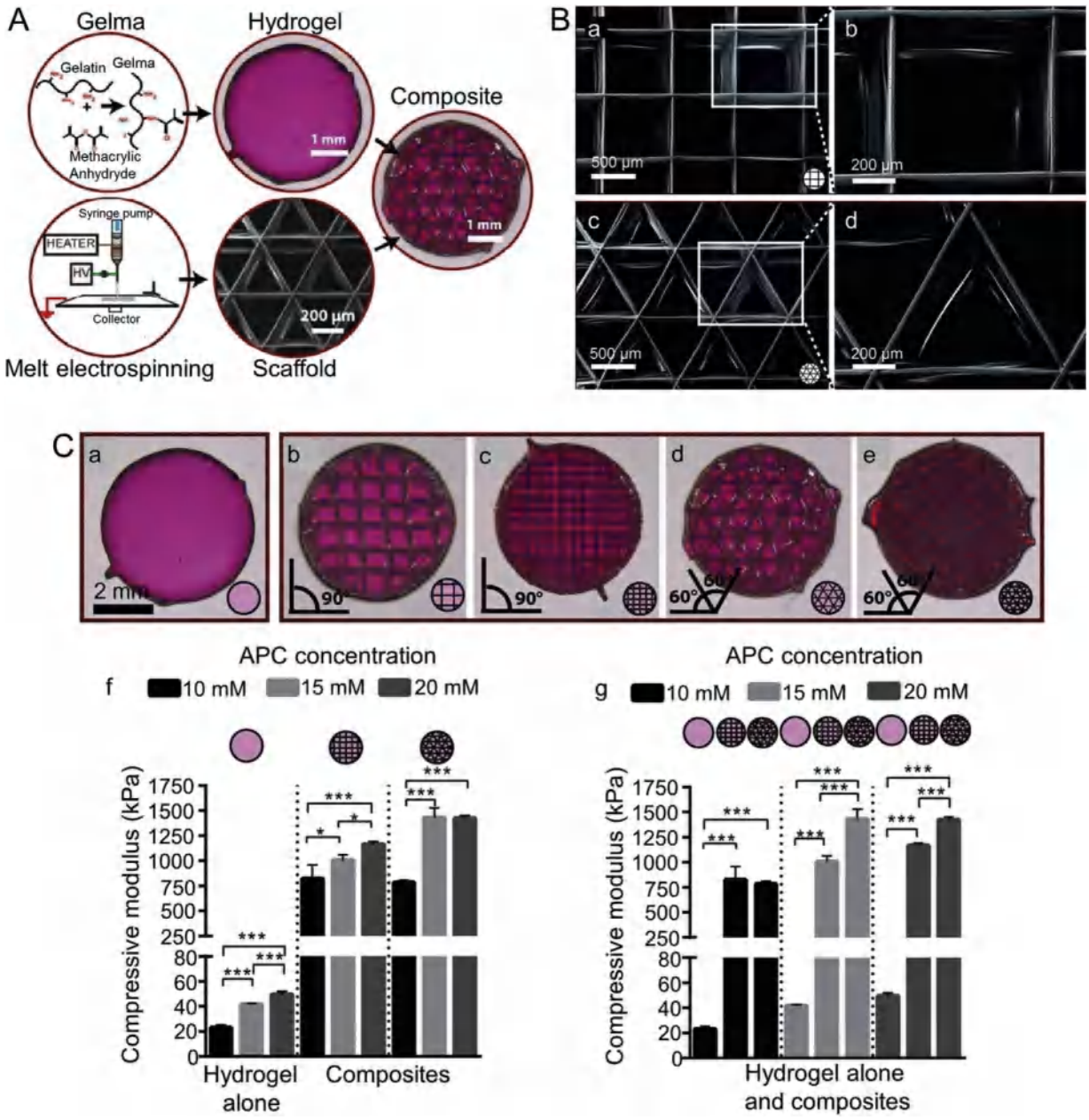

Fig. 15. Preparation and properties of the hydrogel-scaffold composite. (A) Illustration of preparation of hydrogel–scaffold composite. (B) SEM images of melt-electrospun fibrous constructs produced for hydrogel reinforcement with (a) 0–90° lay-down (LD) pattern and 800 μm line spacing (LS) and (b) magnified portion of the highlighted inset, (c) 0–60–120° lay-down pattern and 800 μm LS and (d) magnified portion of the highlighted inset. (C) Stereomicroscopy images (constructs stained with red dye) of (a) 10% gelatin methacrylamide (GelMA)/0.5% hyaluronic acid – methacrylamide (HAMA) hydrogel alone (b–e) and fibre-reinforced hydrogel samples having (b) 0–90° LD pattern and 800 μm fibre spacing (FS), (c) 0–90° LD and 400 μm FD, (d) 0–60–120° LD and 800 μm FD, (e) 0–60–120° LD and 400 μm FD fibrous constructs. The icons showed a schematic representation of the type of reinforcement used for each construct. (f) Effect of hydrogel matrix properties on compressive Young's modulus of fiber-reinforced 10% Gelma hydrogels polymerized with 10, 15, or 20 mM ammonium persulfate (APS) in comparison to the hydrogel alone group. (g) Effect of architecture of reinforcement (0–90° and 0–60–120° LD with 400 μm FD) on compressive Young's modulus of fiber-reinforced 10% GelMa hydrogels with different APS concentrations in comparison to that of hydrogel alone group. All tests were conducted at 0.01 mm/s strain rate (n = 5; *P < 0.05, ***P < 0.001). [218], Copyright 2015. Reproduced with permission from Elsevier Ltd (For interpretation of the references to colour in this figure legend, the reader is referred to the web version of this article).

PAA – poly(pyrene methanol) (PAA – PM) followed by thermally crosslinking with PU latex mixture solutions. However, owing to the random fiber orientation as well as a small bearable strain, some applications of such nonwoven mats are extremely limited, like the cutting-edge flexible electronic devices [211,212]. To this end, a patterned PANI/PVDF nanofibrous membrane with ideal electrical and physical – mechanical properties has been fabricated *via* a cost-effective strategy of electrospinning and *in situ* polymerization. Due to such well-organized structure, nanofibrous PANI/PVDF strain sensor can measure and withstand a strain of 2.6 times higher than other common nonwoven sensors. Furthermore, the strain sensor can also be used to detect finger motion in a fast and repeatable response. These interesting features endow the patterned nanofibrous membranes a promising application of in the field of stretchable electronic devices [213].

Compared to conventional film sensors, electrospun films generally show higher sensitivity and response to DNT and metal ions, such as Fe^{3+} and Hg^{2+}. This significant enhancement of sensitivity is ascribed to the high specific surface area of the porous structure [202]. Introduction of conductive materials into textiles

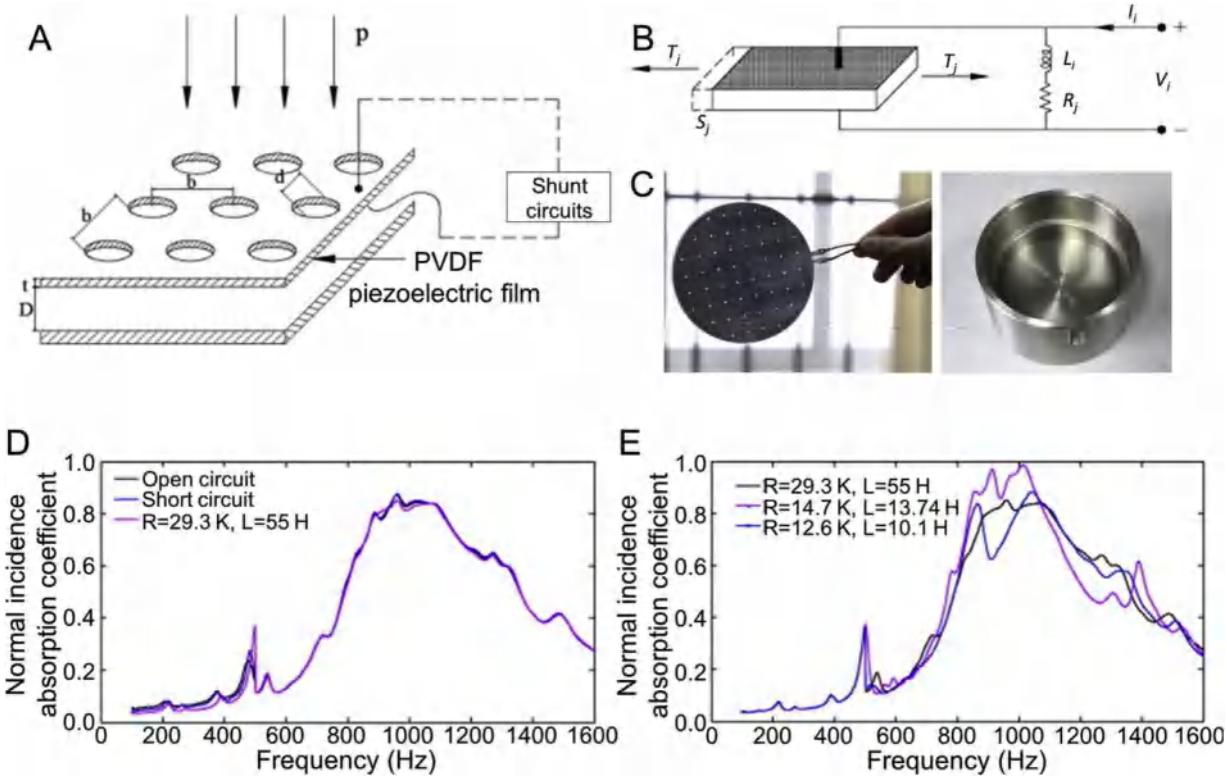

Fig. 16. Preparation of PVDF films based micro-perforated panel absorber (MPPA) and evaluation of its absorption properties. (A) Schematic of proposed PVDF-MPPA structure. (B) A resonant shunted piezoelectric structure assumed the force in the j_{th} direction and electric field in the i_{th} direction. (C) Photos of perforated PVDF piezoelectric film (left) and customized cavity (right). (D) Absorption performance of PVDF-MPPA in an open circuit (black line), in a short circuit (blue line), and in a resonant circuit (pink line). (E) Absorption performance of PVDF-MPPA with different resonant circuits: the first resonant circuits parameters (black line), the second set (pink line), the third set (blue line). [233], Copyright 2015. Reproduced with permission from Elsevier Ltd (For interpretation of the references to colour in this figure legend, the reader is referred to the web version of this article).

further develops the smart devices and wearable electronics, for instance, the real-time detecting and monitoring chemicals in the environment for security. It was reported that the vacuum-assisted LbL-assembly process enabled conformal coatings of functionalized MWCNTs on electrospun fiber mats [214]. Afterward, a covalent-attachment of the thiourea-based receptor to the amine groups on the MWCNTs films was conducted to strengthen the dimethyl methylphosphonate (DMMP) sensing response, simulating the sarin nerve agent (as shown in Fig. 14). In summary, it is an easily-scalable strategy to generate intelligent devices and wearable electronics based on flexible CNT-based sensors.

2.4.2. Reinforcement

Electrospun micro/nanofibers are regarded as promising candidates for composite reinforcement. The large specific surface area of the electrospun fibers facilitates interfacial adhesion between fillers and matrices, and electrospun fibers are generally continuous with few fiber ends [215], where the stress concentration is hard to occur. With regard to the epoxy and rubber matrix, incorporation of electrospun nanofibers substantially improves their mechanical properties [216]. Additionally, some latest studies reinforced the thermoplastic matrices by employing the same method. After incorporating with low content of nylon-6,6 (PA-6,6) nanofibers, significant improvements in tensile strength, modulus, and toughness were presented, which was ascribed to the increased crystallinity and during the hot-compaction the impregnation of high-density polyethylene (HDPE) melt [217]. Fig. 15 illustrated the reinforcement of hydrogels by introducing some defined melt electrospinning writing (MEW) fiber architectures, where a drastic increase in the mechanical performance at high strain rates was achieved [218]. Tensile modulus and failure properties of these fiber-reinforced composites were closely determined by the fiber network pattern [219]. Similarly, compression, tensile, and bending strength of the electrospun nanofiber/aerogel composites were dramatically enhanced 32, 24, and 3-fold, respectively, in comparison with the pure aerogel. Electrospinning belongs to a facile method to prepare aerogel composites with high strength and excellent thermal insulation [220].

Regarding the fiber-reinforced polymer composites, after integrating strong fibers and polymer matrix into one entity, these materials will present a combination of desirable properties, which is unable to be acquired in any single materials [221]. However, conventional fiber-reinforced polymer materials generally yield non-transparent composite films, which are extremely limited in many optical applications of windows, canopies, and electronic devices [2,222,223]. Nanoscale fibersn solve this problem perfectly because the nanomaterial size is less than the wavelength of visible light which will significantly reduce the loss of light [224]. It was once reported that an optically-transparent composite film which was reinforced by 50 nm-size bacterial cellulose nanofiber, had a light transmittance as high as 80% even though the fiber content was 70 wt% [225,226]. Additionally, utilizing randomly-oriented nanofibers becomes another attractive choice to acquire an improved mechanical strength and maintain the desired light transmittance at the same time. In short, these studies will lay a solid foundation toward preparing high-performance polymer composites for various industrial applications.

2.4.3. Sound absorption

Noise pollution is one prevalent nuisance in urban settings and has significant negative effects on human health. Generally, conventional acoustic foams have the ability to absorb univer-

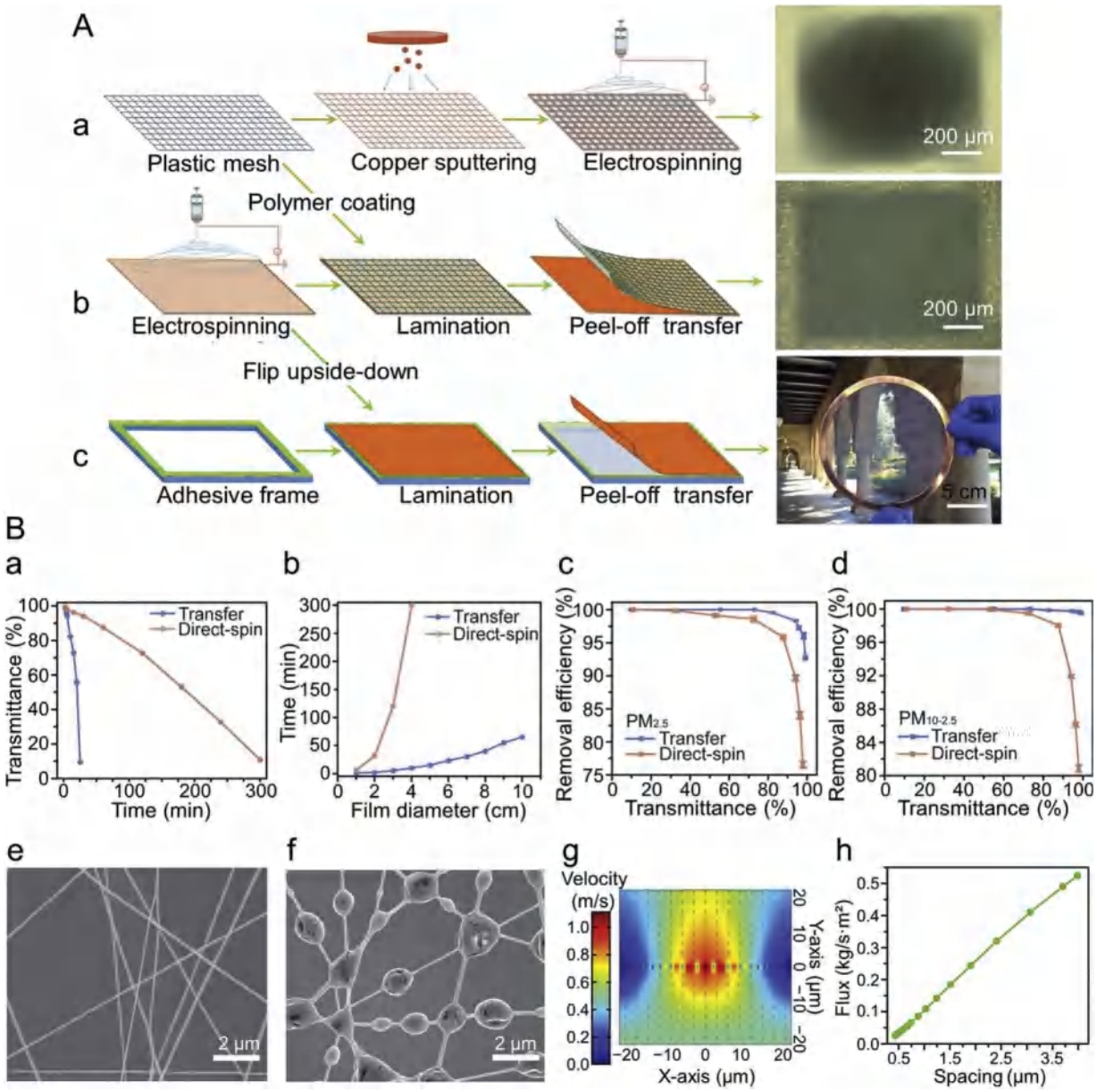

Fig. 17. Preparation and evaluation of electrospun nanofiber film for high-efficiency transparent air filter. (A) Preparation of air filter based on electrospinning method. (a) Schematic showed the fabrication of transparent air filter by direct-spinning on a conductive mesh, and image of corresponding filter. (b) Schematic showed the fabrication of transparent air filter by transferring electrospun nanofiber film onto a plastic mesh and image of corresponding filter. (c) Schematic showed the transfer of freestanding electrospun nanofiber film and photograph of corresponding film. (B) (a) Transmittance of filters of same size (25 cm^2) fabricated by transfer method and direct-spin method at different electrospinning time. (b) Time required to obtain circular freestanding nanofiber films of 70% transmittance at different diameters through two methods. (c) $PM_{2.5}$ removal efficiencies of transparent filters from two methods at different transmittances (PM, particulate matter). (d) $PM_{10-2.5}$ removal efficiencies of transparent filters from two methods at different transmittances. (e, f) SEM images of nylon-6 (PA-6) nanofibers before and after filtration. Scale bars in e and f are 2 μm. (g) Flow velocity field in the vicinity of an inhomogeneous nanofiber filter. Black spots represent for nanofibers with diameter of 100 nm. The air flow (0.2 m/s) comes from the bottom, and the top boundary is the outlet (1 atm). The spacing between nanofibers is sparse at the central and dense at the edge. (h) Flux at different spacing between nanofibers. Large spacing results in high flux and therefore high penetration of PM. [248], Copyright 2016. Reproduced with permission from the American Chemical Society.

sal sound at the high-frequency region. While, noise at middle- and low-frequency always bring more harm to the human body, urging the development of various sound-absorbing materials. Owing to the excellent viscoelasticity, high specific surface area, easy processing properties, and continuous porous structure, electrospun fiber-based polymer materials is promising in the field of sound absorption, where the noise absorption efficiency is expected to rise exponentially due to a drastic increase in the interaction sites between air molecules and fiber surface [227]. As Ma et al. once demonstrated, electrospun fibers have good acoustical damping performance in both low and medium frequency range (100–2500 Hz), making them promising candidates as the environment-friendly material for reducing noise [228]. In addition, it was indicated that with increasing the membrane thickness [229,230], the back cavity, as well as the surface density of nanofiber layers, the first resonance-absorption frequency of nanofibrous membranes shifted to a lower frequency [231]. Meanwhile, the flow resistivity increased with a decrease in fiber diameter. Due to the high flow resistivity and low stiffness of fiber, laminates comprised of the thinnest silica fiber showed the highest sound absorption as well as sample vibration.

More recently, a sound-absorption material has been proposed based on the electrospun PVDF/CNTs or PVDF/graphene composite membranes. As we all know, these composites always exhibit superior piezoelectric properties compared to some conventional electrospun polymers [232]. As a piezoelectric composite material of PVDF/CNTs is subjected to stress, an electrical potential or voltage proportional to the force magnitude is generated, making the material optimal for converting mechanical energy to electric property. Fig. 16 showed a piezoelectric audio transducer, which converted sound energy into electric voltage and voltage into sound pressure in turn [233]. As a result, piezoelectric materials well reduced noise and were employed in sound-absorbing and energy acquisition. By this concept, CNTs or graphene were considered to be introduced and then coelectrospun with PVDF to improve the membrane piezoelectric properties. By comprehensively examining the effect of CNTs or graphene on the piezoelectric properties of composite nanofiber membranes, it was found that adding CNTs or graphene drastically improved the piezoelectricity through interfacial polarization, which were efficient in converting sound energy at low-frequency region [234,235]. In conclusion, the electrospun PVDF/CNT or PVDF/graphene nonwoven has excellent potential as sound absorber due to its favorable absorption performance in low-frequency regions.

2.4.4. Filtration

The electrospun nanoweb for liquid separation and particulate removal has gained increasing appeal as its large surface-to-volume ratio facilitates the filtration efficiency by providing enough particle-capture sites [236,237]. The fiber size distribution can be precisely controlled by tip-to-collector distance, solution concentration, and feeding rate [238]. It was once reported that more excellent fibers and higher filtering efficiency were generated when using a longer tip-to-collector distance, a lower polymer concentration, as well as a slower feeding rate [239]. However, widespread applications of the electrospun nanofiber membranes (ENMs) are largely hindered for lacking mechanical integrity and the poor hydrophilicity. Because of the low mechanical strength and chemical instability, electrospun membranes are challenging for the pressure-driven liquid filtration. As a result, increasing fiber – fiber interactions and reinforcing the mechanical properties of electrospun fibers *via* nanoparticles are promising routes to address the issue [240–242].

A gentle chemical-modification approach has been proposed in recent days, which is capable of both increasing wettability of a nanofiber mat and binding fibers together for an increased strength [243]. Such chemical modification involves a hydrophilic polymer named polydopamine (PDA). After depositing the PDA onto PAN and polysulfone (PSu) ENMs, the junction points throughout the nonwoven are significantly increased. Moreover, to provide flexibility of the carbon nanofiber (CNF) mats, tetraethoxyorthosilicate is also added to the PAN precursor solution. Consequently, the acquired membranes are mechanically-strong enough to withstand pressure- or vacuum-caused filtration. It was once reported that electrospun membranes could efficiently reject diverse nanoparticles (Ag, Au, and TiO_2) with variable diameters (10–100 nm) from aqueous solutions [244]. Similarly, water filtration membranes can be prepared by coating chitin nanocrystals onto the random electrospun cellulose acetate (CA) mats. In detail, the chitin nanocrystals realize a self-assembling on the CA fiber surface *via* hydrogen bonding, and finally form the webbed-structures, so as to guarantying superior mechanical properties [245]. Such coated-membranes exhibit high hydrophilicity and improved resistance to fouling. All these works open up more mainstream and efficient applications for separation technology, such as water purification prior to reverse osmosis or the pre-filters to minimize fouling.

In addition to the liquid separation, another serious environmental issue is the particulate-matter pollution. Considering the mixture of solid and liquid droplets poses a considerable threat to public health, a new type of filter technology is urgently required [246]. Previously, individuals have made transparent filters by electrospinning polymer nanofibers directly onto a conductive mesh [247]. However, a highly-nonuniform electric field distribution is presented across the entire surface of the conductive mesh, thus resulting in a nonuniform deposition of polymer nanofibers as well as a low efficiency of air filtration [247]. Following this, a new fabrication process for making uniformly-distributed polymer nanofibers has been developed. As shown in Fig. 17, this high throughput method is fast transferring electrospun film from a roughed metal foil to a mesh substrate, instead of metallic mesh. Afterward, the nanofibrous polymer mats are peeled off from the foil and transferred onto mesh [248]. Compared with the direct electrospinning, such transfer method possesses 10-times faster production speed and higher filtration efficiency while under the same transmittance. This is caused by the uniformity of the transferred nanofiber film. With these advantages, it is reasonable to predict that the transparent air filter with enhanced filtration performance can be widely-utilized as commercial products.

3. Summary and outlooks

This review covered recent advances and the diverse biomedical applications of fabricating fibrous matrices *via* electrospinning processes, including pharmaceutical repositories, tissue engineering scaffolds, wound healing, sensors, reinforcement, sound absorption, and filtration. Compared to other nanofiber fabrication, electrospinning is superior in preparing ordered or complex fibrous assemblies, depending on several innovative techniques, such as rotating collector, coaxial electrospinning, post-processing of as-spun fibers, multilayer electrospinning, and surface functionalization with biological molecules. Much progress have been realized in the design and modification of electrospun fibers during the past two decades. Nevertheless, there are still considerable challenges ahead that need to be addressed.

Firstly, production of the electrospun fibers at the industrial level is always restricted by the poor consistency and low efficiency. With the aim of facilitating a transition from laboratory to industry, a few approaches based on modification of the electrospinning apparatus have been developed. For example, incorporation of multi-spinneret systems during the electrospinning process is able to achieve commercially feasible scale compared with a single needle [249]. Meantime, different geometries for the multiple spinnerets further open the possibility of fabricating fibers with various structures and multi-functionalities by employing different materials. Unfortunately, variation in the electric field generally forms because the jets are placed close to each another and then causes undesirable changes on nanofiber morphology [250]. In addition, free surface electrospinning has been proposed recently to spin large volumes of polymer solution without clogging, while morphology and smoothness of these resultant fibers have limited reproduction ability [251,252].

Secondly, a precise control of average fiber diameter (below 100 nm) and its distribution within a wide range remains a technological bottleneck to achieve, which is currently relied on regulating some interrelated variables, including the spinneret design, electric field intensity, solution concentration, flow rate, and collection distance [253,254]. However, through these approaches to control fiber diameter is extremely limited. For instance, the diameter of most electrospun fibers produced from solution is varied with the concentration due to the solvent removal, while the limited change

of spinnable solution concentration results in finiteness of fiber diameter changes [255].

Last but not least, for electronics, photonics, drug delivery, and tissue engineering, the random morphology of fibrous mats may restrict the potential developments of electrospun fibers. Although there are several set-ups designed like rotating drum collectors have been widely accepted to achieve fiber alignment, it is still not able to develop highly-aligned membrane with a substantial thickness. This complication is presented because of the electrostatic repulsion between deposited and coming fibers [256]. It was reported that the ultrasonication post-treatment or hydration of crosslinking was able to increase the overall thickness of nanofiber sheets from 0.20 to maximum 1.25 mm due to the formation of loosening structure, while at the cost of weakening mechanical strength and molecular weight [257,258].

Due to these limitations as summarized, practical applications of polymer micro/nanofibers are relatively confined thus far. Therefore, further development in optimizing the industrial-scale production and clinical performance of electrospun matrices will be crucial. With ongoing interdisciplinary research involving chemists, biologists, engineers, and clinicians, applying electrospun polymer biomaterials toward real-world biomedical applications are foreseen to become commercially viable.

Acknowledgments

This article was financially supported by the National Key Research and Development Program of China (Grant No. 2016YFC1100701), the National Natural Science Foundation of China (Grant Nos. 51873207, 51873218, 51673190, 51603204, 51673187, and 51520105004), and the Science and Technology Development Program of Jilin Province (Grant Nos. 20160204015SF, 20160204018SF, and 20170101102JC).

References

[1] Wang Z, Crandall C, Sahadevan R, Menkhaus TJ, Fong H. Microfiltration performance of electrospun nanofiber membranes with varied fiber diameters and different membrane porosities and thicknesses. Polymer 2017;114:64–72.
[2] Agarwal S, Wendorff JH, Greiner A. Use of electrospinning technique for biomedical applications. Polymer 2008;49:5603–21.
[3] Pham QP, Sharma U, Mikos AG. Electrospinning of polymeric nanofibers for tissue engineering applications: A review. Tissue Eng 2006;12:1197–211.
[4] Liang D, Hsiao BS, Chu B. Functional electrospun nanofibrous scaffolds for biomedical applications. Adv Drug Deliv Rev 2007;59:1392–412.
[5] Filatov Y, Budyka A, Kirichenko V. Electrospinning of micro- and nanofibers: Fundamentals in separation and filtration processes. Redding CT: Begell House Inc; 2007. p. 488.
[6] Mitchell GR, Ahn KH, Davis FJ. The potential of electrospinning in rapid manufacturing processes: The fundamentals of electrospinning, key process parameters, materials and potential application in rapid manufacturing are presented in this paper. Virtual Phys Prototyp 2011;6:63–77.
[7] Wang A, Liu Z, Hu M, Wang C, Zhang X, Shi B, et al. Piezoelectric nanofibrous scaffolds as *in vivo* energy harvesters for modifying fibroblast alignment and proliferation in wound healing. Nano Energy 2018;43:63–71.
[8] Liao Y, Zhang L, Gao Y, Zhu ZT, Fong H. Preparation, characterization, and encapsulation/release studies of a composite nanofiber mat electrospun from an emulsion containing poly(lactic-*co*-glycolic acid). Polymer 2008;49:5294–9.
[9] Park JH, Lee HW, Chae DK, Oh W, Yun JD, Deng Y, et al. Electrospinning and characterization of poly(vinyl alcohol)/chitosan oligosaccharide/clay nanocomposite nanofibers in aqueous solutions. Colloid Polym Sci 2009;287:943–50.
[10] Xu X, Zhuang X, Chen X, Wang X, Yang L, Jing X. Preparation of core-sheath composite nanofibers by emulsion electrospinning. Macromol Rapid Commun 2006;27:1637–42.
[11] Wei M, Kang B, Sung C, Mead J. Core-sheath structure in electrospun nanofibers from polymer blends. Macromol Mater Eng 2006;291:1307–14.
[12] Li D, Xia Y. Direct fabrication of composite and ceramic hollow nanofibers by electrospinning. Nano Lett 2004;4:933–8.
[13] Ren B, Fan M, Liu Q, Wang J, Song D, Bai X. Hollow NiO nanofibers modified by citric acid and the performances as supercapacitor electrode. Electrochim Acta 2013;92:197–204.
[14] Gupta P, Wilkes GL. Some investigations on the fiber formation by utilizing a side-by-side bicomponent electrospinning approach. Polymer 2003;44:6353–9.
[15] Horst M, Madduri S, Milleret V, Sulser T, Gobet R, Eberli D. A bilayered hybrid microfibrous PLGA–Acellular matrix scaffold for hollow organ tissue engineering. Biomaterials 2013;34:1537–45.
[16] Gu BK, Shin MK, Sohn KW, Kim SI, Kim SJ, Kim SK, et al. Direct fabrication of twisted nanofibers by electrospinning. Appl Phys Lett 2007;90:1–3, 263902.
[17] Canejo JP, Borges JP, Godinho MH, Brogueira P, Teixeira PIC, Terentjev EM. Helical twisting of electrospun liquid crystalline cellulose micro- and nanofibers. Adv Mater 2008;20:4821–5.
[18] Ji LW, Medford AJ, Zhang XW. Porous carbon nanofibers loaded with manganese oxide particles: Formation mechanism and electrochemical performance as energy-storage materials. J Mater Chem 2009;19:5593–601.
[19] Dayal P, Liu J, Kumar S, Kyu T. Experimental and theoretical investigations of porous structure formation in electrospun fibers. Macromolecules 2007;40:7689–94.
[20] Lin YP, Lin SY, Lee YC, Chen-Yang YW. High surface area electrospun prickle-like hierarchical anatase TiO_2 nanofibers for dye-sensitized solar cell photoanodes. J Mater Chem A Mater Energy Sustain 2013;1:9875–84.
[21] Sabba D, Mathews N, Chua J, Pramana SS, Mulmudi HK, Wang Q, et al. High-surface-area, interconnected, nanofibrillar TiO_2 structures as photoanodes in dye-sensitized solar cells. Scr Mater 2013;68:487–90.
[22] Yoshimoto H, Shin YM, Terai H, Vacanti JP. A biodegradable nanofiber scaffold by electrospinning and its potential for bone tissue engineering. Biomaterials 2003;24:2077–82.
[23] Smith LA, Ma PX. Nano-fibrous scaffolds for tissue engineering. Colloids Surf B 2004;39:125–31.
[24] Pedicini A, Farris RJ. Mechanical behavior of electrospun polyurethane. Polymer 2003;44:6857–62.
[25] Liu G, Gu Z, Hong Y, Cheng L, Li C. Electrospun starch nanofibers: Recent advances, challenges, and strategies for potential pharmaceutical applications. J Control Release 2017;252:95–107.
[26] Kim HS, Yoo HS. MMPs-responsive release of DNA from electrospun nanofibrous matrix for local gene therapy: *In vitro* and *in vivo* evaluation. J Control Release 2010;145:264–71.
[27] Duque Sanchez L, Brack N, Postma A, Pigram PJ, Meagher L. Surface modification of electrospun fibres for biomedical applications: A focus on radical polymerization methods. Biomaterials 2016;106:24–45.
[28] Hu Q, Sun W, Lu Y, Bomba HN, Ye Y, Jiang T, et al. Tumor microenvironment-mediated construction and deconstruction of extracellular drug-delivery depots. Nano Lett 2016;16:1118–26.
[29] Jiang T, Mo R, Bellotti A, Zhou J, Gu Z. Gel–liposome-mediated co-delivery of anticancer membrane-associated proteins and small-molecule drugs for enhanced therapeutic efficacy. Adv Funct Mater 2014;24:2295–304.
[30] Yu DG Wang X, Li XY, Chian W, Li Y, Liao YZ. Electrospun biphasic drug release polyvinylpyrrolidone/ethyl cellulose core/sheath nanofibers. Acta Biomater 2013;9:5665–72.
[31] Yang T, Yang H, Zhen SJ, Huang CZ. Hydrogen-bond-mediated *in situ* fabrication of AgNPs/Agar/PAN electrospun nanofibers as reproducible SERS substrates. ACS Appl Mater Interfaces 2015;7:1586–94.
[32] Yu H, Yang P, Jia Y, Zhang Y, Ye Q, Zeng S. Regulation of biphasic drug release behavior by graphene oxide in polyvinyl pyrrolidone/poly(ε-caprolactone) core/sheath nanofiber mats. Colloids Surf B 2016;146:63–9.
[33] Rodriguez K, Renneckar S, Gatenholm P. Biomimetic calcium phosphate crystal mineralization on electrospun cellulose-based scaffolds. ACS Appl Mater Interfaces 2011;3:681–9.
[34] Li L, Zhou G, Wang Y, Yang G, Ding S, Zhou S. Controlled dual delivery of BMP-2 and dexamethasone by nanoparticle-embedded electrospun nanofibers for the efficient repair of critical-sized rat calvarial defect. Biomaterials 2015;37:218–29.
[35] Xue J, He M, Liu H, Niu Y, Crawford A, Coates PD, et al. Drug loaded homogeneous electrospun PCL/gelatin hybrid nanofiber structures for anti-infective tissue regeneration membranes. Biomaterials 2014;35:9395–405.
[36] Zeng J, Yang L, Liang Q, Zhang X, Guan H, Xu X, et al. Influence of the drug compatibility with polymer solution on the release kinetics of electrospun fiber formulation. J Control Release 2005;105:43–51.
[37] Zeng J, Xu X, Chen X, Liang Q, Bian X, Yang L, et al. Biodegradable electrospun fibers for drug delivery. J Control Release 2003;92:227–31.
[38] Cui W, Li X, Zhu X, Yu G, Zhou S, Weng J. Investigation of drug release and matrix degradation of electrospun poly(DL-lactide) fibers with paracetanol inoculation. Biomacromolecules 2006;7:1623–9.
[39] Wang SD, Zhang SZ, Liu H, Zhang YZ. Controlled release of antibiotics encapsulated in the electrospinning polylactide nanofibrous scaffold and their antibacterial and biocompatible properties. Mater Res Express 2014;1:1–17, 025406.
[40] Jiang J, Xie J, Ma B, Bartlett DE, Xu A, Wang CH. Mussel-inspired protein-mediated surface functionalization of electrospun nanofibers for pH-responsive drug delivery. Acta Biomater 2014;10:1324–32.
[41] Loscertales IG, Barrero A, Guerrero I, Cortijo R, Marquez M, Ganan-Calvo AM. Micro/nano encapsulation *via* electrified coaxial liquid jets. Science 2002;295:1695–8.
[42] Saraf A, Baggett LS, Raphael RM, Kasper FK, Mikos AG. Regulated non-viral gene delivery from coaxial electrospun fiber mesh scaffolds. J Control Release 2010;143:95–103.

[43] Jiang T, Sun W, Zhu Q, Burns NA, Khan SA, Mo R, et al. Furin-mediated sequential delivery of anticancer cytokine and small-molecule drug shuttled by graphene. Adv Mater 2015;27:1021–8.
[44] Li J, Xu W, Li D, Liu T, Zhang YS, Ding J, et al. Locally deployable nanofiber patch for sequential drug delivery in treatment of primary and advanced orthotopic hepatomas. ACS Nano 2018;12:6685–99.
[45] Kang MS, Kim JH, Singh RK, Jang JH, Kim HW. Therapeutic-designed electrospun bone scaffolds: Mesoporous bioactive nanocarriers in hollow fiber composites to sequentially deliver dual growth factors. Acta Biomater 2015;16:103–16.
[46] Gelain F, Unsworth LD, Zhang S. Slow and sustained release of active cytokines from self-assembling peptide scaffolds. J Control Release 2010;145:231–9.
[47] Bago JR, Pegna GJ, Okolie O, Mohiti-Asli M, Loboa EG, Hingtgen SD. Electrospun nanofibrous scaffolds increase the efficacy of stem cell-mediated therapy of surgically resected glioblastoma. Biomaterials 2016;90:116–25.
[48] Ke P, Jiao XN, Ge XH, Xiao WM, Yu B. From macro to micro: Structural biomimetic materials by electrospinning. RSC Adv 2014;4:39704–24.
[49] Luu YK, Kim K, Hsiao BS, Chu B, Hadjiargyrou M. Development of a nanostructured DNA delivery scaffold *via* electrospinning of PLGA and PLA-PEG block copolymers. J Control Release 2003;89:341–53.
[50] Kobsa S, Kristofik NJ, Sawyer AJ, Bothwell ALM, Kyriakides TR, Saltzman WM. An electrospun scaffold integrating nucleic acid delivery for treatment of full-thickness wounds. Biomaterials 2013;34:3891–901.
[51] Benoit DSW, Boutin ME. Controlling mesenchymal stem cell gene expression using polymer-mediated delivery of siRNA. Biomacromolecules 2012;13:3841–9.
[52] Lee SJ, Oh SH, Liu J, Soker S, Atala A, Yoo JJ. The use of thermal treatments to enhance the mechanical properties of electrospun poly(ε-caprolactone) scaffolds. Biomaterials 2008;29:1422–30.
[53] Tucking KS, Grutzner V, Unger RE, Schonherr H. Dual enzyme-responsive capsules of hyaluronic acid-*block*-poly(lactic acid) for sensing bacterial enzymes. Macromol Rapid Commun 2015;36:1248–54.
[54] Azuma Y, Zschoche R, Tinzl M, Hilvert D. Quantitative packaging of active enzymes into a protein cage. Angew Chem Int Ed 2016;55:1531–4.
[55] Bäcker M, Rakowski D, Poghossian A, Biselli M, Wagner P, Schöning MJ. Chip-based amperometric enzyme sensor system for monitoring of bioprocesses by flow-injection analysis. J Biotechnol 2013;163:371–6.
[56] Wong DE, Dai M, Talbert JN, Nugen SR, Goddard JM. Biocatalytic polymer nanofibers for stabilization and delivery of enzymes. J Mol Catal B Enzym 2014;110:16–22.
[57] Xie JB, Hsieh YL. Ultra-high surface fibrous membranes from electrospinning of natural proteins: Casein and lipase enzyme. J Mater Sci 2003;38:2125–33.
[58] Ji X, Wang P, Su Z, Ma G, Zhang S. Enabling multi-enzyme biocatalysis using coaxial-electrospun hollow nanofibers: Redesign of artificial cells. J Mater Chem B 2014;2:181–90.
[59] Zeng J, Aigner A, Czubayko F, Kissel T, Wendorff JH, Greiner A. Poly(vinyl alcohol) nanofibers by electrospinning as a protein delivery system and the retardation of enzyme release by additional polymer coatings. Biomacromolecules 2005;6:1484–8.
[60] Herricks TE, Kim SH, Kim J, Li D, Kwak JH, Grate JW, et al. Direct fabrication of enzyme-carrying polymer nanofibers by electrospinning. J Mater Chem A 2005;15:3241–5.
[61] Murase SK, Lv LP, Kaltbeitzel A, Landfester K, del Valle LJ, Katsarava R, et al. Amino acid-based poly(ester amide) nanofibers for tailored enzymatic degradation prepared by miniemulsion-electrospinning. RSC Adv 2015;5:55006–14.
[62] Lu Y, Aimetti AA, Langer R, Gu Z. Bioresponsive materials. Nat Rev Mater 2017;2:1–17, 16075.
[63] Zhang J, Zheng T, Alarçin E, Byambaa B, Guan X, Ding J, et al. Porous electrospun fibers with self-sealing functionality: An enabling strategy for trapping biomacromolecules. Small 2017;13:1–15, 1701949.
[64] Boffito M, Sartori S, Ciardelli G. Polymeric scaffolds for cardiac tissue engineering: Requirements and fabrication technologies. Polym Int 2014;63:2–11.
[65] Guilak F, Butler DL, Goldstein SA, Baaijens FPT. Biomechanics and mechanobiology in functional tissue engineering. J Biomech 2014;47:1933–40.
[66] Orth P, Zurakowski D, Alini M, Cucchiarini M, Madry H. Reduction of sample size requirements by bilateral versus unilateral research designs in animal models for cartilage tissue engineering. Tissue Eng Part C Methods 2013;19:885–91.
[67] Levengood SL, Zhang M. Chitosan-based scaffolds for bone tissue engineering. J Mater Chem B Mater Biol Med 2014;2:3161–84.
[68] Cheng TY, Chen MH, Chang WH, Huang MY, Wang TW. Neural stem cells encapsulated in a functionalized self-assembling peptide hydrogel for brain tissue engineering. Biomaterials 2013;34:2005–16.
[69] Akbarzadeh R, Yousefi AM. Effects of processing parameters in thermally induced phase separation technique on porous architecture of scaffolds for bone tissue engineering. J Biomed Mater Res B 2014;102:1304–15.
[70] Dhand C, Ong ST, Dwivedi N, Diaz SM, Venugopal JR, Navaneethan B, et al. Bio-inspired *in situ* crosslinking and mineralization of electrospun collagen scaffolds for bone tissue engineering. Biomaterials 2016;104:323–38.
[71] Agarwal S, Greiner A, Wendorff JH. Functional materials by electrospinning of polymers. Prog Polym Sci 2013;38:963–91.
[72] Wang L, Wu Y, Guo B, Ma PX. Nanofiber yarn/hydrogel core–shell scaffolds mimicking native skeletal muscle tissue for guiding 3D myoblast alignment, elongation, and differentiation. ACS Nano 2015;9:9167–79.
[73] Phipps MC, Clem WC, Grunda JM, Clines GA, Bellis SL. Increasing the pore sizes of bone-mimetic electrospun scaffolds comprised of polycaprolactone, collagen I and hydroxyapatite to enhance cell infiltration. Biomaterials 2012;33:524–34.
[74] Reboredo JW, Weigel T, Steinert A, Rackwitz L, Rudert M, Walles H. Investigation of migration and differentiation of human mesenchymal stem cells on five-layered collagenous electrospun scaffold mimicking native cartilage structure. Adv Healthcare Mater 2016;5:2191–8.
[75] Nosar MN, Salehi M, Ghorbani S, Beiranvand SP, Goodarzi A, Azami M. Characterization of wet-electrospun cellulose acetate based 3-dimensional scaffolds for skin tissue engineering applications: influence of cellulose acetate concentration. Cellulose 2016;23:3239–48.
[76] Rayatpisheh S, Heath DE, Shakouri A, Rujitanaroj PO, Chew SY, Chan-Park MB. Combining cell sheet technology and electrospun scaffolding for engineered tubular, aligned, and contractile blood vessels. Biomaterials 2014;35:2713–9.
[77] Baiguera S, Del Gaudio C, Lucatelli E, Kuevda E, Boieri M, Mazzanti B, et al. Electrospun gelatin scaffolds incorporating rat decellularized brain extracellular matrix for neural tissue engineering. Biomaterials 2014;35:1205–14.
[78] Wade RJ, Bassin EJ, Rodell CB, Burdick JA. Protease-degradable electrospun fibrous hydrogels. Nat Commun 2015;6:1–10, 6639.
[79] Wickham A, Sjölander D, Bergström G, Wang E, Rajendran V, Hildesjö C, et al. Near-infrared emitting and pro-angiogenic electrospun conjugated polymer scaffold for optical biomaterial tracking. Adv Funct Mater 2015;25:4274–81.
[80] Fishman JM, Tyraskis A, Maghsoudlou P, Urbani L, Totonelli G, Birchall MA, et al. Skeletal muscle tissue engineering: Which cell to use? Tissue Eng Part B Rev 2013;19:503–15.
[81] Ten Broek RW, Grefte S. Von den Hoff JW. Regulatory factors and cell populations involved in skeletal muscle regeneration. J Cell Physiol 2010;224:7–16.
[82] Lee CH, Lim YC, Farson DF, Powell HM, Lannutti JJ. Vascular wall engineering *via* femtosecond laser ablation: Scaffolds with self-containing smooth muscle cell populations. Ann Biomed Eng 2011;39:3031–41.
[83] McKeon-Fischer KD, Freeman JW. Characterization of electrospun poly(L-lactide) and gold nanoparticle composite scaffolds for skeletal muscle tissue engineering. J Regener Med Tissue Eng 2011;5:560–8.
[84] He M, Callanan A. Comparison of methods for whole-organ decellularization in tissue engineering of bioartificial organs. Tissue Eng Part B Rev 2013;19:194–208.
[85] Saxena AK, Marler J, Benvenuto M, Willital GH, Vacanti JP. Skeletal muscle tissue engineering using isolated myoblasts on synthetic biodegradable polymers: Preliminary studies. Tissue Eng 1999;5:525–31.
[86] Riboldi SA, Sampaolesi M, Neuenschwander P, Cossu G, Mantero S. Electrospun degradable polyesterurethane membranes: Potential scaffolds for skeletal muscle tissue engineering. Biomaterials 2005;26:4606–15.
[87] Martin JT, Milby AH, Ikuta K, Poudel S, Pfeifer CG, Elliott DM, et al. A radiopaque electrospun scaffold for engineering fibrous musculoskeletal tissues: Scaffold characterization and *in vivo* applications. Acta Biomater 2015;26:97–104.
[88] Chen MC, Sun YC, Chen YH. Electrically conductive nanofibers with highly oriented structures and their potential application in skeletal muscle tissue engineering. Acta Biomater 2013;9:5562–72.
[89] Tonazzini I, Jacchetti E, Meucci S, Beltram F, Cecchini M. Schwann cell contact guidance *versus* boundary interaction in functional wound healing along nano and microstructured membranes. Adv Healthcar Mater 2015;4:1849–60.
[90] Yang K, Park E, Lee JS, Kim IS, Hong K, Park KI, et al. Biodegradable nanotopography combined with neurotrophic signals enhances contact guidance and neuronal differentiation of human neural stem cells. Macromol Biosci 2015;15:1348–56.
[91] San Choi J, Lee SJ, Christ GJ, Atala A, Yoo JJ. The influence of electrospun aligned poly(ε-caprolactone)/collagen nanofiber meshes on the formation of self-aligned skeletal muscle myotubes. Biomaterials 2008;29:2899–906.
[92] Xiong GM, Yuan S, Wang JK, Do AT, Tan NS, Yeo KS, et al. Imparting electroactivity to polycaprolactone fibers with heparin-doped polypyrrole: Modulation of hemocompatibility and inflammatory responses. Acta Biomater 2015;23:240–9.
[93] Hosseinzadeh S, Mahmoudifard M, Mohamadyar-Toupkanlou F, Dodel M, Hajarizadeh A, Adabi M, et al. The nanofibrous PAN-PANi scaffold as an efficient substrate for skeletal muscle differentiation using satellite cells. Bioprocess Biosyst Eng 2016;39:1163–72.
[94] Lima MD, Hussain MW, Spinks GM, Naficy S, Hagenasr D, Bykova JS, et al. Efficient, absorption-powered artificial muscles based on carbon nanotube hybrid yarns. Small 2015;11:3113–8.
[95] Han J, Ding J, Wang Z, Yan S, Zhuang X, Chen X, et al. The synthesis, deprotection and properties of poly(γ-benzyl-L-glutamate). Sci China Chem 2013;56:729–38.
[96] Knoblauch M, Noll GA, Muller T, Prufer D, Schneider-Huther I, Scharner D, et al. ATP-independent contractile proteins from plants. Nat Mater 2003;2:600–3.
[97] Krishen K. Space applications for ionic polymer-metal composite sensors, actuators, and artificial muscles. Acta Astronaut 2009;64:1160–6.

[98] McKeon-Fischer KD, Flagg DH, Freeman JW. Coaxial electrospun poly(ε-caprolactone), multiwalled carbon nanotubes, and polyacrylic acid/polyvinyl alcohol scaffold for skeletal muscle tissue engineering. J Biomed Mater Res A 2011;99A:493–9.
[99] Giannoudis PV, Dinopoulos H, Tsiridis E. Bone substitutes: An update. Injury 2005;36. S20-S7.
[100] Zhang Y, Venugopal JR, El-Turki A, Ramakrishna S, Su B, Lim CT. Electrospun biomimetic nanocomposite nanofibers of hydroxyapatite/chitosan for bone tissue engineering. Biomaterials 2008;29:4314–22.
[101] Song X, Ling F, Ma L, Yang C, Chen X. Electrospun hydroxyapatite grafted poly(L-lactide)/poly(lactic-*co*-glycolic acid) nanofibers for guided bone regeneration membrane. Compos Sci Technol 2013;79:8–14.
[102] Meng ZX, Wang YS, Ma C, Zheng W, Li L, Zheng YF. Electrospinning of PLGA/gelatin randomly-oriented and aligned nanofibers as potential scaffold in tissue engineering. Mater Sci Eng C 2010;30:1204–10.
[103] Zhang J, Liu H, Ding JX, Zhuang XL, Chen XS, Li ZM. Annealing regulates the performance of an electrospun poly(ε-caprolactone) membrane to accommodate tissue engineering. RSC Adv 2015;5:32604–8.
[104] Yao Q, Cosme JG, Xu T, Miszuk JM, Picciani PH, Fong H, et al. Three dimensional electrospun PCL/PLA blend nanofibrous scaffolds with significantly improved stem cells osteogenic differentiation and cranial bone formation. Biomaterials 2017;115:115–27.
[105] Yang X, Shah JD, Wang H. Nanofiber enabled layer-by-layer approach toward three-dimensional tissue formation. Tissue Eng Part A 2009;15:945–56.
[106] Li X, Xie J, Yuan X, Xia Y. Coating electrospun poly(ε-caprolactone) fibers with gelatin and calcium phosphate and their use as biomimetic scaffolds for bone tissue engineering. Langmuir 2008;24:14145–50.
[107] Chiu LH, Lai WFT, Chang SF, Wong CC, Fan CY, Fang CL, et al. The effect of type II collagen on MSC osteogenic differentiation and bone defect repair. Biomaterials 2014;35:2680–91.
[108] Liao SS, Cui FZ, Zhang W, Feng QL. Hierarchically biomimetic bone scaffold materials: Nano-HA/collagen/PLA composite. J Biomed Mater Res B 2004;69B:158–65.
[109] Yang F, Wolke JGC, Jansen JA. Biomimetic calcium phosphate coating on electrospun poly(ε-caprolactone) scaffolds for bone tissue engineering. Chem Eng J 2008;137:154–61.
[110] Yoo HS, Kim TG, Park TG. Surface-functionalized electrospun nanofibers for tissue engineering and drug delivery. Adv Drug Deliv Rev 2009;61:1033–42.
[111] Dinarvand P, Seyedjafari E, Shafiee A, Jandaghi AB, Doostmohammadi A, Fathi MH, et al. New approach to bone tissue engineering: Simultaneous application of hydroxyapatite and bioactive glass coated on a poly(L-lactic acid) scaffold. ACS Appl Mater Interfaces 2011;3:4518–24.
[112] Mi HY, Palumbo S, Jing X, Turng LS, Li WJ, Peng XF. Thermoplastic polyurethane/hydroxyapatite electrospun scaffolds for bone tissue engineering: Effects of polymer properties and particle size. J Biomed Mater Res B 2014;102:1434–44.
[113] Ji W, Yang F, Ma J, Bouma MJ, Boerman OC, Chen Z, et al. Incorporation of stromal cell-derived factor-1α in PCL/gelatin electrospun membranes for guided bone regeneration. Biomaterials 2013;34:735–45.
[114] Niece KL, Hartgerink JD, Donners JJM, Stupp SI. Self-assembly combining two bioactive peptide-amphiphile molecules into nanofibers by electrostatic attraction. J Am Chem Soc 2003;125:7146–7.
[115] Wu K, Zhang X, Yang W, Liu X, Jiao Y, Zhou C. Influence of layer-by-layer assembled electrospun poly(L-lactic acid) nanofiber mats on, the bioactivity of endothelial cells. Appl Surf Sci 2016;390:838–46.
[116] Leong MF, Chian KS, Mhaisalkar PS, Ong WF, Ratner BD. Effect of electrospun poly(D,L-lactide) fibrous scaffold with nanoporous surface on attachment of porcine esophageal epithelial cells and protein adsorption. J Biomed Mater Res A 2009;89A:1040–8.
[117] Li C, Vepari C, Jin HJ, Kim HJ, Kaplan DL. Electrospun silk-BMP-2 scaffolds for bone tissue engineering. Biomaterials 2006;27:3115–24.
[118] Zhang Y, Xiao C, Li M, Chen J, Ding J, He C, et al. Co-delivery of 10-hydroxycamptothecin with doxorubicin conjugated prodrugs for enhanced anticancer efficacy. Macromol Biosci 2013;13:584–94.
[119] Moutos FT, Freed LE, Guilak F. A biomimetic three-dimensional woven composite scaffold for functional tissue engineering of cartilage. Nat Mater 2007;6:162–7.
[120] Li WJ, Tuli R, Okafor C, Derfoul A, Danielson KG, Hall DJ, et al. A three-dimensional nanofibrous scaffold for cartilage tissue engineering using human mesenchymal stem cells. Biomaterials 2005;26:599–609.
[121] Xue J, Feng B, Zheng R, Lu Y, Zhou G, Liu W, et al. Engineering ear-shaped cartilage using electrospun fibrous membranes of gelatin/polycaprolactone. Biomaterials 2013;34:2624–31.
[122] Zhang Y, Yang F, Liu K, Shen H, Zhu Y, Zhang W, et al. The impact of PLGA scaffold orientation on *in vitro* cartilage regeneration. Biomaterials 2012;33:2926–35.
[123] Man Z, Yin L, Shao Z, Zhang X, Hu X, Zhu J, et al. The effects of co-delivery of BMSC-affinity peptide and rhTGF-β1 from coaxial electrospun scaffolds on chondrogenic differentiation. Biomaterials 2014;35:5250–60.
[124] Alves da Silva ML, Martins A, Costa-Pinto AR, Costa P, Faria S, Gomes M, et al. Cartilage tissue engineering using electrospun PCL nanofiber meshes and MSCs. Biomacromolecules 2010;11:3228–36.
[125] Subramanian A, Vu D, Larsen GF, Lin HY. Preparation and evaluation of the electrospun chitosan/PEO fibers for potential applications in cartilage tissue engineering. J Biomater Sci Polym Ed 2005;16:861–73.
[126] Albanna MZ, Bou-Akl TH, Blowytsky O, Walters III HL, Matthew HWT. Chitosan fibers with improved biological and mechanical properties for tissue engineering applications. J Mech Behav Biomed Mater 2013;20:217–26.
[127] Kim DH, Heo SJ, Shin JW, Mun CW, Park KM, Park KD, et al. Preparation of thermosensitive gelatin-Pluronic copolymer for cartilage tissue engineering. Macromol Res 2010;18:387–91.
[128] Chen JP, Su CH. Surface modification of electrospun PLLA nanofibers by plasma treatment and cationized gelatin immobilization for cartilage tissue engineering. Acta Biomater 2011;7:234–43.
[129] Simson JA, Strehin IA, Lu Q, Uy MO, Elisseeff JH. An adhesive bone marrow scaffold and bone morphogenetic-2 protein carrier for cartilage tissue engineering. Biomacromolecules 2013;14:637–43.
[130] Shi D, Xu X, Ye Y, Song K, Cheng Y, Di J, et al. Photo-cross-linked scaffold with kartogenin-encapsulated nanoparticles for cartilage regeneration. ACS Nano 2016;10:1292–9.
[131] Wang X, Wenk E, Zhang X, Meinel L, Vunjak-Novakovic G, Kaplan DL. Growth factor gradients *via* microsphere delivery in biopolymer scaffolds for osteochondral tissue engineering. J Control Release 2009;134:81–90.
[132] Kim SH, Kim SH, Jung Y. TGF-β3 encapsulated PLCL scaffold by a supercritical CO_2-HFIP co-solvent system for cartilage tissue engineering. J Control Release 2015;206:101–7.
[133] Albro MB, Nims RJ, Durney KM, Cigan AD, Shim JJ, Vunjak-Novakovic G, et al. Heterogeneous engineered cartilage growth results from gradients of media-supplemented active TGF-β and is ameliorated by the alternative supplementation of latent TGF-β. Biomaterials 2016;77:173–85.
[134] MacNeil S. Progress and opportunities for tissue-engineered skin. Nature 2007;445:874–80.
[135] Kumbar SG, Nair LS, Bhattacharyya S, Laurencin CT. Polymeric nanofibers as novel carriers for the delivery of therapeutic molecules. J Nanosci Nanotechnol 2006;6:2591–607.
[136] Wu C, Chen T, Xin Y, Zhang Z, Ren Z, Lei J, et al. Nanofibrous asymmetric membranes self-organized from chemically heterogeneous electrospun mats for skin tissue engineering. Biomed Mater 2016;11:1–12, 035019.
[137] Gautam S, Chou CF, Dinda AK, Potdar PD, Mishra NC. Surface modification of nanofibrous polycaprolactone/gelatin composite scaffold by collagen type I grafting for skin tissue engineering. Mater Sci Eng C 2014;34:402–9.
[138] Liu NH, Pan JF, Miao YE, Liu TX, Xu F, Sun H. Electrospinning of poly(ε-caprolactone-*co*-lactide)/Pluronic blended scaffolds for skin tissue engineering. J Mater Sci 2014;49:7253–62.
[139] Choi JK, Jang JH, Jang WH, Kim J, Bae IH, Bae J, et al. The effect of epidermal growth factor (EGF) conjugated with low-molecular-weight protamine (LMWP) on wound healing of the skin. Biomaterials 2012;33:8579–90.
[140] Norouzi M, Shabani I, Atyabi F, Soleimani M. EGF-loaded nanofibrous scaffold for skin tissue engineering applications. Fibers Polym 2015;16:782–7.
[141] Kumbar SG, Nukavarapu SP, James R, Nair LS, Laurencin CT. Electrospun poly(lactic acid-*co*-glycolic acid) scaffolds for skin tissue engineering. Biomaterials 2008;29:4100–7.
[142] Zhu X, Cui W, Li X, Jin Y. Electrospun fibrous mats with high porosity as potential scaffolds for skin tissue engineering. Biomacromolecules 2008;9:1795–801.
[143] Liu Y, Lu J, Li H, Wei J, Li X. Engineering blood vessels through micropatterned co-culture of vascular endothelial and smooth muscle cells on bilayered electrospun fibrous mats with pDNA inoculation. Acta Biomater 2015;11:114–25.
[144] Stefani I, Cooper-White JJ. Development of an in-process UV-crosslinked, electrospun PCL/aPLA-*co*-TMC composite polymer for tubular tissue engineering applications. Acta Biomater 2016;36:231–40.
[145] Abebayehu D, Spence A, Sell S, Bowlin G, Ryan J. Characterizing bone marrow-derived mast cell interaction with electrospun bioresorbable vascular grafts. J Immunol 2014;192(56):19–56, 19.
[146] Wang Z, Cui Y, Wang J, Yang X, Wu Y, Wang K, et al. The effect of thick fibers and large pores of electrospun poly(ε-caprolactone) vascular grafts on macrophage polarization and arterial regeneration. Biomaterials 2014;35:5700–10.
[147] Sung HJ, Meredith C, Johnson C, Galis ZS. The effect of scaffold degradation rate on three-dimensional cell growth and angiogenesis. Biomaterials 2004;25:5735–42.
[148] Williams C, Xie AW, Yamato M, Okano T, Wong JY. Stacking of aligned cell sheets for layer-by-layer control of complex tissue structure. Biomaterials 2011;32:5625–32.
[149] Wang ZX, Liu SQ, Guidoin R, Kodama M. Polyurethane vascular grafts with thorough porosity: Does an internal or an external membrane wrapping improve their *in vivo* blood compatibility and biofunctionality? Artif Cells Blood Substit Immobil Biotechnol 2004;32:463–84.
[150] Deng X, Guidoin R. Alternative blood conduits: Assessment of whether the porosity of synthetic prostheses is the key to long-term biofunctionality. Med Biol Eng Comput 2000;38:219–25.
[151] Zheng W, Wang Z, Song L, Zhao Q, Zhang J, Li D, et al. Endothelialization and patency of RGD-functionalized vascular grafts in a rabbit carotid artery model. Biomaterials 2012;33:2880–91.
[152] Guan J, Sacks MS, Beckman EJ, Wagner WR. Biodegradable poly(ether ester urethane) urea elastomers based on poly(ether ester) triblock copolymers and putrescine: Synthesis, characterization and cytocompatibility. Biomaterials 2004;25:85–96.

[153] Jeong SI, Kim SY, Cho SK, Chong MS, Kim KS, Kim H, et al. Tissue-engineered vascular grafts composed of marine collagen and PLGA fibers using pulsatile perfusion bioreactors. Biomaterials 2007;28:1115–22.
[154] Caves JM, Kumar VA, Martinez AW, Kim J, Ripberger CM, Haller CA, et al. The use of microfiber composites of elastin-like protein matrix reinforced with synthetic collagen in the design of vascular grafts. Biomaterials 2010;31:7175–82.
[155] Ren X, Feng Y, Guo J, Wang H, Li Q, Yang J, et al. Surface modification and endothelialization of biomaterials as potential scaffolds for vascular tissue engineering applications. Chem Soc Rev 2015;44:5680–742.
[156] Masaeli E, Morshed M, Nasr-Esfahani MH, Sadri S, Hilderink J, van Apeldoorn A, et al. Fabrication, characterization and cellular compatibility of poly(hydroxy alkanoate) composite nanofibrous scaffolds for nerve tissue engineering. PLoS ONE 2013;8:1–13, e57157.
[157] Guan S, Zhang XL, Lin XM, Liu TQ, Ma XH, Cui ZF. Chitosan/gelatin porous scaffolds containing hyaluronic acid and heparan sulfate for neural tissue engineering. J Biomater Sci Polym Ed 2013;24:999–1014.
[158] Yang F, Murugan R, Wang S, Ramakrishna S. Electrospinning of nano/micro scale poly(L-lactic acid) aligned fibers and their potential in neural tissue engineering. Biomaterials 2005;26:2603–10.
[159] Domingos M, Intranuovo F, Gloria A, Gristina R, Ambrosio L, Bártolo PJ, et al. Improved osteoblast cell affinity on plasma-modified 3D extruded PCL scaffolds. Acta Biomater 2013;9:5997–6005.
[160] Oh SH, Lee JH. Hydrophilization of synthetic biodegradable polymer scaffolds for improved cell/tissue compatibility. Biomed Mater 2013;8:1–16, 014101.
[161] Nickels JD, Schmidt CE. Surface modification of the conducting polymer, polypyrrole, *via* affinity peptide. J Biomed Mater Res A 2013;101:1464–71.
[162] Ghasemi-Mobarakeh L, Prabhakaran MP, Morshed M, Nasr-Esfahani MH, Ramakrishna S. Electrospun poly(ε-caprolactone)/gelatin nanofibrous scaffolds for nerve tissue engineering. Biomaterials 2008;29:4532–9.
[163] Shi Z, Gao H, Feng J, Ding B, Cao X, Kuga S, et al. *In situ* synthesis of robust conductive cellulose/polypyrrole composite aerogels and their potential application in nerve regeneration. Angew Chem Int Ed 2014;53:5380–4.
[164] Thunberg J, Kalogeropoulos T, Kuzmenko V, Hägg D, Johannesson S, Westman G, et al. *In situ* synthesis of conductive polypyrrole on electrospun cellulose nanofibers: Scaffold for neural tissue engineering. Cellulose 2015;22:1459–67.
[165] Cui W, Cheng L, Hu C, Li H, Zhang Y, Chang J. Electrospun poly(L-lactide) fiber with ginsenoside Rg3 for inhibiting scar hyperplasia of skin. PLoS ONE 2013;8:1–12, e68771.
[166] Yi R. The Skin(ny) on regenerating the largest organ to save a patient's life. Cell Stem Cell 2018;22:14–5.
[167] Ensrud KE, Blackwell TL, Cawthon PM, Bauer DC, Fink HA, Schousboe JT, et al. Degree of trauma differs for major osteoporotic fracture events in older men versus older women. J Bone Miner Res 2016;31:204–7.
[168] Abdel-Sayed P, Kaeppeli A, Siriwardena T, Darbre T, Perron K, Jafari P, et al. Anti-microbial dendrimers against multidrug-resistant P. Aeruginosa enhance the angiogenic effect of biological burn-wound bandages. Sci Rep 2016;6:1–10, 22020.
[169] Augustine R, Dominic EA, Reju I, Kaimal B, Kalarikkal N, Thomas S. Electrospun poly(ε-caprolactone)-based skin substitutes: *In vivo* evaluation of wound healing and the mechanism of cell proliferation. J Biomed Mater Res B 2015;103:1445–54.
[170] Lowe A, Bills J, Verma R, Lavery L, Davis K, Balkus Jr KJ. Electrospun nitric oxide releasing bandage with enhanced wound healing. Acta Biomater 2015;13:121–30.
[171] Dong RH, Jia YX, Qin CC, Zhan L, Yan X, Cui L, et al. *In situ* deposition of a personalized nanofibrous dressing *via* a handy electrospinning device for skin wound care. Nanoscale 2016;8:3482–8.
[172] Ansari MA, Khan HM, Khan AA, Cameotra SS, Pal R. Antibiofilm efficacy of silver nanoparticles against biofilm of extended spectrum β-lactamase isolates of Escherichia coli and Klebsiella pneumoniae. Appl Nanosci 2014;4:859–68.
[173] Arockia John Paul J, Karunai Selvi B, Karmegam N. Biosynthesis of silver nanoparticles from Premna serratifolia L. Leaf and its anticancer activity in CCl_4-induced hepato-cancerous Swiss albino mice. Appl Nanosci 2015;5:937–44.
[174] Gaddala B, Nataru S. Synthesis, characterization and evaluation of silver nanoparticles through leaves of Abrus precatorius L.: An important medicinal plant. Appl Nanosci 2015;5:99–104.
[175] Augustine R, Kalarikkal N, Thomas S. Electrospun PCL membranes incorporated with biosynthesized silver nanoparticles as antibacterial wound dressings. Appl Nanosci 2016;6:337–44.
[176] Levy SB, Marshall B. Antibacterial resistance worldwide: Causes, challenges and responses. Nat Med 2004;10:122–9.
[177] Li W, Dong K, Ren J, Qu X. A β-lactamase-imprinted responsive hydrogel for the treatment of antibiotic-resistant bacteria. Angew Chem Int Ed 2016;55:8049–53.
[178] Wang Z, Dong K, Liu Z, Zhang Y, Chen Z, Sun H, et al. Activation of biologically relevant levels of reactive oxygen species by Au/g-C_3N_4 hybrid nanozyme for bacteria killing and wound disinfection. Biomaterials 2017;113:145–57.
[179] Yang X, Yang J, Wang L, Ran B, Jia Y, Zhang L, et al. Pharmaceutical intermediate-modified gold nanoparticles: Against multidrug-resistant bacteria and wound-healing application *via* an electrospun scaffold. ACS Nano 2017;11:5737–45.
[180] Unnithan AR, Gnanasekaran G, Sathishkumar Y, Lee YS, Kim CS. Electrospun antibacterial polyurethane-cellulose acetate-zein composite mats for wound dressing. Carbohydr Polym 2014;102:884–92.
[181] Xu S, Sang L, Zhang Y, Wang X, Li X. Biological evaluation of human hair keratin scaffolds for skin wound repair and regeneration. Mater Sci Eng C 2013;33:648–55.
[182] Wang Y, Li P, Xiang P, Lu J, Yuan J, Shen J. Electrospun polyurethane/keratin/AgNP biocomposite mats for biocompatible and antibacterial wound dressings. J Mater Chem B 2016;4:635–48.
[183] Hassan S, Reynolds G, Clarkson J, Brooks P. Challenging the dogma: Relationship between time to healing and formation of hypertrophic scars after burn injuries. J Burn Care Res 2014;35, e118-e24.
[184] Zhu Z, Ding J, Shankowsky HA, Tredget EE. The molecular mechanism of hypertrophic scar. J Cell Commun Signal 2013;7:239–52.
[185] Honardoust D, Kwan P, Momtazi M, Ding J, Tredget EE. Novel methods for the investigation of human hypertrophic scarring and other dermal fibrosis. In: Gourdie RG, Myers TA, editors. Wound repair Regen. Totowa NJ: Humana Press; 2013. p. 203–31.
[186] Li P, He QY, Luo CQ. Overexpression of miR-200b inhibits the cell proliferation and promotes apoptosis of human hypertrophic scar fibroblasts in vitro. J Dermatol 2014;41:903–11.
[187] Sun X, Cheng L, Zhu W, Hu C, Jin R, Sun B, et al. Use of ginsenoside Rg3-loaded electrospun PLGA fibrous membranes as wound cover induces healing and inhibits hypertrophic scar formation of the skin. Colloids Surf B 2014;115:61–70.
[188] Cheng L, Sun X, Zhao X, Wang L, Yu J, Pan G, et al. Surface biofunctional drug-loaded electrospun fibrous scaffolds for comprehensive repairing hypertrophic scars. Biomaterials 2016;83:169–81.
[189] Li J, Feng X, Liu B, Yu Y, Sun L, Liu T, et al. Polymer materials for prevention of postoperative adhesion. Acta Biomater 2017;61:21–40.
[190] Hoare T, Yeo Y, Bellas E, Bruggeman JP, Kohane DS. Prevention of peritoneal adhesions using polymeric rheological blends. Acta Biomater 2014;10:1187–93.
[191] Fu SZ, Li Z, Fan JM, Meng XH, Shi K, Qu Y, et al. Biodegradable and thermosensitive monomethoxy poly(ethylene glycol)-poly(lactic acid) hydrogel as a barrier for prevention of post-operative abdominal adhesion. J Biomed Nanotechnol 2014;10:427–35.
[192] Jiang S, Zhao X, Chen S, Pan G, Song J, He N, et al. Down-regulating ERK1/2 and SMAD2/3 phosphorylation by physical barrier of celecoxib-loaded electrospun fibrous membranes prevents tendon adhesions. Biomaterials 2014;35:9920–9.
[193] Chen S, Wang G, Wu T, Zhao X, Liu S, Li G, et al. Silver nanoparticles/ibuprofen-loaded poly(L-lactide) fibrous membrane: Anti-infection and anti-adhesion effects. Int J Mol Sci 2014;15:14014–25.
[194] Jiang S, Wang W, Yan H, Fan C. Prevention of intra-abdominal adhesion by bi-layer electrospun membrane. Int J Mol Sci 2013;14:11861–70.
[195] Yang DJ, Chen F, Xiong ZC, Xiong CD, Wang YZ. Tissue anti-adhesion potential of biodegradable PELA electrospun membranes. Acta Biomater 2009;5:2467–74.
[196] Chen CH, Chen SH, Shalumon KT, Chen JP. Dual functional core-sheath electrospun hyaluronic acid/polycaprolactone nanofibrous membranes embedded with silver nanoparticles for prevention of peritendinous adhesion. Acta Biomater 2015;26:225–35.
[197] Li J, Feng X, Shi J, Liu T, Ding J. Porous polylactide film plus atorvastatin-loaded thermogel as an efficient device for peritoneal adhesion prevention. ACS Omega 2018;3:2715–23.
[198] Zhao S, Zhao J, Dong S, Huangfu X, Li B, Yang H, et al. Biological augmentation of rotator cuff repair using bFGF-loaded electrospun poly(lactide-*co*-glycolide) fibrous membranes. Int J Nanomed 2014;9:2373–85.
[199] Sun X, Cheng L, Zhao J, Jin R, Sun B, Shi Y, et al. bFGF-grafted electrospun fibrous scaffolds *via* polydopamine for skin wound healing. J Mater Chem B 2014;2:3636–45.
[200] Liu S, Qin M, Hu C, Wu F, Cui W, Jin T, et al. Tendon healing and anti-adhesion properties of electrospun fibrous membranes containing bFGF loaded nanoparticles. Biomaterials 2013;34:4690–701.
[201] Li J, Xu W, Chen J, Li D, Zhang K, Liu T, et al. Highly bioadhesive polymer membrane continuously releases cytostatic and anti-inflammatory drugs for peritoneal adhesion prevention. ACS Biomater Sci Eng 2018;4:2026–36.
[202] Wang X, Drew C, Lee SH, Senecal KJ, Kumar J, Samuelson LA. Electrospun nanofibrous membranes for highly sensitive optical sensors. Nano Lett 2002;2:1273–5.
[203] Ding B, Wang M, Yu J, Sun G. Gas sensors based on electrospun nanofibers. Sensors 2009;9:1609–24.
[204] Wang G, Yu D, Kelkar AD, Zhang L. Electrospun nanofiber: Emerging reinforcing filler in polymer matrix composite materials. Prog Polym Sci 2017;75:73–107.
[205] Mohrova J, Kalinova K. Different structures of PVA nanofibrous membrane for sound absorption application. J Nanomater 2012;2012:1–4, 643043.
[206] Mansouri J, Harrisson S, Chen V. Strategies for controlling biofouling in membrane filtration systems: Challenges and opportunities. J Mater Chem 2010;20:4567–86.
[207] Shen C, Wycisk R, Pintauro PN. High performance electrospun bipolar membrane with a 3D junction. Energy Environ Sci 2017;10:1435–42.

[208] Duan G, Jiang S, Jérôme V, Wendorff JH, Fathi A, Uhm J, et al. Ultralight, soft polymer sponges by self-assembly of short electrospun fibers in colloidal dispersions. Adv Funct Mater 2015;25:2850–6.
[209] Zhang Y, Kim JJ, Chen D, Tuller HL, Rutledge GC. Electrospun polyaniline fibers as highly sensitive room temperature chemiresistive sensors for ammonia and nitrogen dioxide gases. Adv Funct Mater 2014;24:4005–14.
[210] Xue W, Zhang Y, Duan J, Liu D, Ma Y, Shi N, et al. A highly sensitive fluorescent sensor based on small molecules doped in electrospun nanofibers: Detection of explosives as well as color modulation. J Mater Chem C 2015;3:8193–9.
[211] Liu N, Fang G, Wan J, Zhou H, Long H, Zhao X. Electrospun PEDOT:PSS–PVA nanofiber based ultrahigh-strain sensors with controllable electrical conductivity. J Mater Chem 2011;21:18962–6.
[212] Sun B, Long YZ, Liu SL, Huang YY, Ma J, Zhang HD, et al. Fabrication of curled conducting polymer microfibrous arrays *via* a novel electrospinning method for stretchable strain sensors. Nanoscale 2013;5:7041–5.
[213] Yu GF Yan X, Yu M, Jia MY, Pan W, He XX, et al. Patterned, highly stretchable and conductive nanofibrous PANI/PVDF strain sensors based on electrospinning and *in situ* polymerization. Nanoscale 2016;8:2944–50.
[214] Saetia K, Schnorr JM, Mannarino MM, Kim SY, Rutledge GC, Swager TM, et al. Spray-layer-by-layer carbon nanotube/electrospun fiber electrodes for flexible chemiresistive sensor applications. Adv Funct Mater 2014;24:492–502.
[215] Zhang Y, Xiao C, Li M, Ding J, Yang C, Zhuang X, et al. Co-delivery of doxorubicin and paclitaxel with linear-dendritic block copolymer for enhanced anti-cancer efficacy. Sci China Chem 2014;57:624–32.
[216] Bergshoef MM, Vancso GJ. Transparent nanocomposites with ultrathin, electrospun nylon-4,6 fiber reinforcement. Adv Mater 1999;11:1362–5.
[217] Lu B, Zheng G, Dai K, Liu C, Chen J, Shen C. Enhanced mechanical properties of polyethylene composites with low content of electrospun nylon-66 nanofibers. Mater Lett 2015;140:131–4.
[218] Bas O, De-Juan-Pardo EM, Chhaya MP, Wunner FM, Jeon JE, Klein TJ, et al. Enhancing structural integrity of hydrogels by using highly organised melt electrospun fibre constructs. Eur Polym J 2015;72:451–63.
[219] Strange DGT, Tonsomboon K, Oyen ML. Mechanical behaviour of electrospun fibre-reinforced hydrogels. J Mater Sci 2014;25:681–90.
[220] Chen Q, Chen Y, Wu H, Zhou X. Preparation and characterisation of aerogel composites reinforced with electrospun nanofibre. Mater Res Innovations 2015;19(S2):185–9.
[221] Yang M, Cao K, Yeom B, Thouless M, Waas A, Arruda EM, et al. Aramid nanofiber-reinforced transparent nanocomposites. J Compos Mater 2015;49:1873–9.
[222] Tang C, Wu M, Wu Y, Liu H. Effects of fiber surface chemistry and size on the structure and properties of poly(vinyl alcohol) composite films reinforced with electrospun fibers. Compos Part A 2011;42:1100–9.
[223] Ifuku S, Morooka S, Morimoto M, Saimoto H. Acetylation of chitin nanofibers and their transparent nanocomposite films. Biomacromolecules 2010;11:1326–30.
[224] Mitragotri S, Anderson DG, Chen X, Chow EK, Ho D, Kabanov AV, et al. Accelerating the translation of nanomaterials in biomedicine. ACS Nano 2015;9:6644–54.
[225] Cai J, Chen J, Zhang Q, Lei M, He J, Xiao A, et al. Well-aligned cellulose nanofiber-reinforced polyvinyl alcohol composite film: Mechanical and optical properties. Carbohydr Polym 2016;140:238–45.
[226] Yano H, Sugiyama J, Nakagaito AN, Nogi M, Matsuura T, Hikita M, et al. Optically transparent composites reinforced with networks of bacterial nanofibers. Adv Mater 2005;17:153–5.
[227] Rabbi A, Bahrambeygi H, Shoushtari AM, Nasouri K. Incorporation of nanofiber layers in nonwoven materials for improving their acoustic properties. J Eng Fiber Fabr 2013;8:36–41.
[228] Liu H, Wang D, Zhao N, Ma J, Gong J, Yang S, et al. Application of electrospinning fibres on sound absorption in low and medium frequency range. Mater Res Innovations 2014;18:888–91.
[229] Gao B, Zuo L, Zuo B. Sound absorption properties of spiral vane electrospun PVA/nano particle nanofiber membrane and non-woven composite material. Fibers Polym 2016;17:1090–6.
[230] Xiang HF, Tan SX, Yu XL, Long YH, Zhang XL, Zhao N, et al. Sound absorption behavior of electrospun polyacrylonitrile nanofibrous membranes. Chin J Polym Sci 2011;29:650–7.
[231] Rabbi A, Bahrambeygi H, Nasouri K, Shoushtari AM, Babaei MR. Manufacturing of PAN or PU nanofiber layers/PET nonwoven composite as highly effective sound absorbers. Adv Polym Technol 2014;33:1–8, 21425.
[232] Ahn Y, Lim JY, Hong SM, Lee J, Ha J, Choi HJ, et al. Enhanced piezoelectric properties of electrospun poly(vinylidene fluoride)/multiwalled carbon nanotube composites due to high β-phase formation in poly(vinylidene fluoride). J Phys Chem C 2013;117:11791–9.
[233] Duan XH, Wang HQ, Li ZB, Zhu LK, Chen R, Kong DY, et al. Sound absorption of a flexible micro-perforated panel absorber based on PVDF piezoelectric film. Appl Acoust 2015;88:84–9.
[234] Wu CM, Chou MH. Polymorphism, piezoelectricity and sound absorption of electrospun PVDF membranes with and without carbon nanotubes. Compos Sci Technol 2016;127:127–33.
[235] Wu CM, Chou MH. Sound absorption of electrospun polyvinylidene fluoride/graphene membranes. Eur Polym J 2016;82:35–45.
[236] Gopal R, Kaur S, Ma Z, Chan C, Ramakrishna S, Matsuura T. Electrospun nanofibrous filtration membrane. J Membr Sci 2006;281:581–6.
[237] An AK, Guo J, Lee EJ, Jeong S, Zhao Y, Wang Z, et al. PDMS/PVDF hybrid electrospun membrane with superhydrophobic property and drop impact dynamics for dyeing wastewater treatment using membrane distillation. J Membr Sci 2017;525:57–67.
[238] Liu Y, Park M, Ding B, Kim J, El-Newehy M, Al-Deyab SS, et al. Facile electrospun polyacrylonitrile/poly(acrylic acid) nanofibrous membranes for high efficiency particulate air filtration. Fibers Polym 2015;16:629–33.
[239] Zhang S, Shim WS, Kim J. Design of ultra-fine nonwovens *via* electrospinning of nylon 6: spinning parameters and filtration efficiency. Mater Des 2009;30:3659–66.
[240] Sen R, Zhao B, Perea D, Itkis ME, Hu H, Love J, et al. Preparation of single-walled carbon nanotube reinforced polystyrene and polyurethane nanofibers and membranes by electrospinning. Nano Lett 2004;4:459–64.
[241] Xiang C, Joo YL, Frey MW. Nanocomposite fibers electrospun from poly(lactic acid)/cellulose nanocrystals. J Biobased Mater Bioenergy 2009;3:147–55.
[242] Wang X, Zhang K, Zhu M, Hsiao BS, Chu B. Enhanced mechanical performance of self-bundled electrospun fiber yarns *via* post-treatments. Macromol Rapid Commun 2008;29:826–31.
[243] Huang L, Arena JT, Manickam SS, Jiang X, Willis BG, McCutcheon JR. Improved mechanical properties and hydrophilicity of electrospun nanofiber membranes for filtration applications by dopamine modification. J Membr Sci 2014;460:241–9.
[244] Faccini M, Borja G, Boerrigter M, Martín DM, Crespiera SM, Vázquez-Campos S, et al. Electrospun carbon nanofiber membranes for filtration of nanoparticles from water. J Nanomater 2015;2015:1–9, 247471.
[245] Goetz LA, Jalvo B, Rosal R, Mathew AP. Superhydrophilic anti-fouling electrospun cellulose acetate membranes coated with chitin nanocrystals for water filtration. J Membr Sci 2016;510:238–48.
[246] Nel A. Air pollution-related illness: Effects of particles. Science 2005;308:804–6.
[247] Liu C, Hsu PC, Lee HW, Ye M, Zheng G, Liu N, et al. Transparent air filter for high-efficiency PM2.5 capture. Nat Commun 2015;6:1–9, 6205.
[248] Xu J, Liu C, Hsu PC, Liu K, Zhang R, Liu Y, et al. Roll-to-roll transfer of electrospun nanofiber film for high-efficiency transparent air filter. Nano Lett 2016;16:1270–5.
[249] Persano L, Camposeo A, Tekmen C, Pisignano D. Industrial upscaling of electrospinning and applications of polymer nanofibers: A review. Macromol Mater Eng 2013;298:504–20.
[250] Tijing LD, Woo YC, Yao M, Ren J, Shon HK. 1.16 electrospinning for membrane fabrication: Strategies and applications. In: Drioli E, Giorno L, Fontananova E, editors. Comprehensive membrane science and engineering 2 Ed vol 1 London. Elsevier Ltd; 2017. p. 418–44.
[251] Brettmann BK, Tsang S, Forward KM, Rutledge GC, Myerson AS, Trout BL. Free surface electrospinning of fibers containing microparticles. Langmuir 2012;28:9714–21.
[252] Bazbouz MB, Liang H, Tronci G. A UV-cured nanofibrous membrane of vinylbenzylated gelatin-poly(ε-caprolactone) dimethacrylate co-network by scalable free surface electrospinning. Mater Sci Eng C 2018;91:541–55.
[253] Luo CJ, Stoyanov SD, Stride E, Pelan E, Edirisinghe M. Electrospinning versus fibre production methods: From specifics to technological convergence. Chem Soc Rev 2012;41:4708–35.
[254] Huan S, Liu G, Han G, Cheng W, Fu Z, Wu Q, et al. Effect of experimental parameters on morphological, mechanical and hydrophobic properties of electrospun polystyrene fibers. Materials 2015;8:2718–34.
[255] Deitzel JM, Kleinmeyer J, Harris D, Tan NB. The effect of processing variables on the morphology of electrospun nanofibers and textiles. Polymer 2001;42:261–72.
[256] Teo WE, Ramakrishna S. A review on electrospinning design and nanofibre assemblies. Nanotechnology 2006;17:R89–106.
[257] Lee JB, Jeong SI, Bae MS, Yang DH, Heo DN, Kim CH, et al. Highly porous electrospun nanofibers enhanced by ultrasonication for improved cellular infiltration. Tissue Eng Part A 2011;17:2695–702.
[258] Shields KJ, Beckman MJ, Bowlin GL, Wayne JS. Mechanical properties and cellular proliferation of electrospun collagen type II. Tissue Eng 2004;10:1510–7.
[259] Fong H, Liu W, Wang CS, Vaia RA. Generation of electrospun fibers of nylon 6 and nylon 6-montmorillonite nanocomposite. Polymer 2002;43:775–80.
[260] Jiang S, Duan G, Hou H, Greiner A, Agarwal S. Novel layer-by-layer procedure for making nylon-6 nanofiber reinforced high strength, tough, and transparent thermoplastic polyurethane composites. ACS Appl Mater Interfaces 2012;4:4366–72.
[261] Jiang S, Greiner A, Agarwal S. Short nylon-6 nanofiber reinforced transparent and high modulus thermoplastic polymeric composites. Compos Sci Technol 2013;87:164–9.
[262] Wang C, Jheng JH, Chiu FC. Electrospun nylon-4,6 nanofibers: Solution rheology and Brill transition. Colloid Polym Sci 2013;291:2337–44.
[263] Guan X, Zheng G, Dai K, Liu C, Yan X, Shen C, et al. Carbon nanotubes-adsorbed electrospun PA66 nanofiber bundles with improved conductivity and robust flexibility. ACS Appl Mater Interfaces 2016;8:14150–9.
[264] Shrestha BK, Mousa HM, Tiwari AP, Ko SW, Park CH, Kim CS. Development of polyamide-6,6/chitosan electrospun hybrid nanofibrous scaffolds for tissue engineering application. Carbohydr Polym 2016;148:107–14.
[265] Zhang S, Liu H, Yu J, Luo W, Ding B. Microwave structured polyamide-6 nanofiber/net membrane with embedded poly(m-phenylene

isophthalamide) staple fibers for effective ultrafine particle filtration. J Mater Chem A 2016;4:6149–57.
[266] Wang X, Lee SH, Drew C, Senecal KJ, Kumar J, Samuelson LA. Highly sensitive optical sensors using electrospun polymeric nanofibrous membranes. Mater Res Soc Symp Proc 2011;708:1–6. BB10.44.
[267] Boas M, Gradys A, Vasilyev G, Burman M, Zussman E. Electrospinning polyelectrolyte complexes: pH-responsive fibers. Soft Matter 2015;11:1739–47.
[268] Morozov V, Morozova T, Kallenbach N. Atomic force microscopy of structures produced by electrospraying polymer solutions. Int J Mass Spectrom 1998;178:143–59.
[269] Desai K, Kit K. Effect of spinning temperature and blend ratios on electrospun chitosan/poly(acrylamide) blends fibers. Polymer 2008;49:4046–50.
[270] Patel S, Hota G. Adsorptive removal of malachite green dye by functionalized electrospun PAN nanofibers membrane. Fibers Polym 2014;15:2272–82.
[271] Wang Y, Serrano S, Santiago-Aviles JJ. Conductivity measurement of electrospun PAN-based carbon nanofiber. J Mater Sci Lett 2002;21:1055–7.
[272] Selloum D, Chaaya AA, Bechelany M, Rouessac V, Miele P, Tingry S. A highly efficient gold/electrospun PAN fiber material for improved laccase biocathodes for biofuel cell applications. J Mater Chem A 2014;2:2794–800.
[273] Khan WS, Asmatulu R, Ahmed I, Ravigururajan TS. Thermal conductivities of electrospun PAN and PVP nanocomposite fibers incorporated with MWCNTs and NiZn ferrite nanoparticles. Int J Therm Sci 2013;71:74–9.
[274] Uh K, Kim T, Lee CW, Kim JM. A precursor approach to electrospun polyaniline nanofibers for gas sensors. Macromol Mater Eng 2016;301:1320–6.
[275] Simotwo SK, DelRe C, Kalra V. Supercapacitor electrodes based on high-purity electrospun polyaniline and polyaniline-carbon nanotube nanofibers. ACS Appl Mater Interfaces 2016;8:21261–9.
[276] Macagnano A, Perri V, Zampetti E, Bearzotti A, De Cesare F. Humidity effects on a novel eco-friendly chemosensor based on electrospun PANi/PHB nanofibres. Sens Actuators B 2016;232:16–27.
[277] Shokry H, Vanamo U, Wiltschka O, Niinimaki J, Lerche M, Levon K, et al. Mesoporous silica particle-PLA-PANI hybrid scaffolds for cell-directed intracellular drug delivery and tissue vascularization. Nanoscale 2015;7:14434–43.
[278] Anandhan S, Ponprapakaran K, Senthil T, George G. Parametric study of manufacturing ultrafine polybenzimidazole fibers by electrospinning. Int J Plast Technol 2012;16:101–16.
[279] Kim JS, Reneker DH. Mechanical properties of composites using ultrafine electrospun fibers. Polym Compos 1999;20:124–31.
[280] Li HY, Liu YL. Polyelectrolyte composite membranes of polybenzimidazole and crosslinked polybenzimidazole-polybenzoxazine electrospun nanofibers for proton exchange membrane fuel cells. J Mater Chem A 2013;1:1171–8.
[281] Datsyuk V, Trotsenko S, Reich S. Carbon-nanotube–polymer nanofibers with high thermal conductivity. Carbon 2013;52:605–8.
[282] Tsai PP, Schreuder-Gibson H, Gibson P. Different electrostatic methods for making electret filters. J Electrostat 2002;54:333–41.
[283] Li Q, Xu Y, Wei H, Wang X. An electrospun polycarbonate nanofibrous membrane for high efficiency particulate matter filtration. RSC Adv 2016;6:65275–81.
[284] Si J, Cui Z, Wang Q, Liu Q, Liu C. Biomimetic composite scaffolds based on mineralization of hydroxyapatite on electrospun poly(varepsilon-caprolactone)/nanocellulose fibers. Carbohydr Polym 2016;143:270–8.
[285] Croisier F, Duwez AS, Jerome C, Leonard AF, van der Werf KO, Dijkstra PJ, et al. Mechanical testing of electrospun PCL fibers. Acta Biomater 2012;8:218–24.
[286] Cho SJ, Jung SM, Kang M, Shin HS, Youk JH. Preparation of hydrophilic PCL nanofiber scaffolds *via* electrospinning of PCL/PVP-*b*-PCL block copolymers for enhanced cell biocompatibility. Polymer 2015;69:95–102.
[287] Xia Q, Liu Z, Wang C, Zhang Z, Xu S, Han CC. A biodegradable trilayered barrier membrane composed of sponge and electrospun layers: Hemostasis and antiadhesion. Biomacromolecules 2015;16:3083–92.
[288] Jiang W, Li L, Zhang D, Huang S, Jing Z, Wu Y, et al. Incorporation of aligned PCL-PEG nanofibers into porous chitosan scaffolds improved the orientation of collagen fibers in regenerated periodontium. Acta Biomater 2015;25:240–52.
[289] Badami AS, Kreke MR, Thompson MS, Riffle JS, Goldstein AS. Effect of fiber diameter on spreading, proliferation, and differentiation of osteoblastic cells on electrospun poly(lactic acid) substrates. Biomaterials 2006;27:596–606.
[290] Kim J, Lee TS. Full-color emissive poly(ethylene oxide) electrospun nanofibers containing a single hyperbranched conjugated polymer for large-scale, flexible light-emitting sheets. Macromol Rapid Commun 2016;37:303–10.
[291] Korehei R, Kadla JF. Encapsulation of T4 bacteriophage in electrospun poly(ethylene oxide)/cellulose diacetate fibers. Carbohydr Polym 2014;100:150–7.
[292] Megelski S, Stephens JS, Chase DB, Rabolt JF. Micro- and nanostructured surface morphology on electrospun polymer fibers. Macromolecules 2002;35:8456–66.
[293] Flanagan KE, Tien LW, Elia R, Wu J, Kaplan D. Development of a sutureless dural substitute from Bombyx mori silk fibroin. J Biomed Mater Res B 2015;103:485–94.
[294] Choi SS, Lee SG, Joo CW, Im SS, Kim SH. Formation of interfiber bonding in electrospun poly(etherimide) nanofiber web. J Mater Sci 2004;39:1511–3.
[295] Lee HJ, Lim JM, Kim HW, Jeong SH, Eom SW, Hong T, et al. Electrospun polyetherimide nanofiber mat-reinforced, permselective polyvinyl alcohol composite separator membranes: A membrane-driven step closer toward rechargeable zinc–air batteries. J Membr Sci 2016;499:526–37.
[296] Hao J, Lei G, Li Z, Wu L, Xiao Q, Wang L. A novel polyethylene terephthalate nonwoven separator based on electrospinning technique for lithium ion battery. J Membr Sci 2013;428:11–6.
[297] de Almeida KM, Almeida MM, Fingola FF, Ferraz HC. Membrane adsorber for endotoxin removal. Braz J Pharm Sci 2016;52:171–7.
[298] Sharma J, Lizu M, Stewart M, Zygula K, Lu Y, Chauhan R, et al. Multifunctional nanofibers towards active biomedical therapeutics. Polymers 2015;7:186–219.
[299] Ignatova M, Rashkov I, Manolova N. Drug-loaded electrospun materials in wound-dressing applications and in local cancer treatment. Expert Opin Drug Delivery 2013;10:469–83.
[300] Alhusein N, Blagbrough IS, De Bank PA. Electrospun matrices for localised controlled drug delivery: Release of tetracycline hydrochloride from layers of polycaprolactone and poly(ethylene-*co*-vinyl acetate). Drug Deliv. Transl Res 2012;2:477–88.
[301] Chen ZH, Foster MD, Zhou WS, Fong H, Reneker DH, Resendes R, et al. Structure of polyferrocenyldimethylsilane in electrospun nanofibers. Macromolecules 2001;34:6156–8.
[302] Bonadies I, Cimino F, Carfagna C, Pezzella A. Eumelanin 3D architectures: Electrospun PLA fiber templating for mammalian pigment microtube fabrication. Biomacromolecules 2015;16:1667–70.
[303] Kenawy ER, Bowlin GL, Mansfield K, Layman J, Simpson DG, Sanders EH, et al. Release of tetracycline hydrochloride from electrospun poly(ethylene-*co*-vinylacetate), poly(lactic acid), and a blend. J Control Release 2002;81:57–64.
[304] Liu W, Lipner J, Moran CH, Feng L, Li X, Thomopoulos S, et al. Generation of electrospun nanofibers with controllable degrees of crimping through a simple, plasticizer-based treatment. Adv Mater 2015;27:2583–8.
[305] Arrieta MP, López J, López D, Kenny JM, Peponi L. Effect of chitosan and catechin addition on the structural, thermal, mechanical and disintegration properties of plasticized electrospun PLA–PHB biocomposites. Polym Degrad Stab 2016;132:145–56.
[306] Shao S, Zhou S, Li L, Li J, Luo C, Wang J, et al. Osteoblast function on electrically conductive electrospun PLA/MWCNTs nanofibers. Biomaterials 2011;32:2821–33.
[307] Zhang Z, Liu S, Xiong H, Jing X, Xie Z, Chen X, et al. Electrospun PLA/MWCNTs composite nanofibers for combined chemo- and photothermal therapy. Acta Biomater 2015;26:115–23.
[308] Shi Q, Zhou C, Yue Y, Guo W, Wu Y, Wu Q. Mechanical properties and *in vitro* degradation of electrospun bio-nanocomposite mats from PLA and cellulose nanocrystals. Carbohydr Polym 2012;90:301–8.
[309] Wang YF, Guo HF, Ying DJ. Multilayer scaffold of electrospun PLA–PCL–collagen nanofibers as a dural substitute. J Biomed Mater Res B 2013;101:1359–66.
[310] Ru C, Wang F, Pang M, Sun L, Chen R, Sun Y. Suspended, shrinkage-free, electrospun PLGA nanofibrous scaffold for skin tissue engineering. ACS Appl Mater Interfaces 2015;7:10872–7.
[311] Stachewicz U, Qiao T, Rawlinson SCF, Almeida FV, Li WQ, Cattell M, et al. 3D imaging of cell interactions with electrospun PLGA nanofiber membranes for bone regeneration. Acta Biomater 2015;27:88–100.
[312] Razavi S, Karbasi S, Morshed M, Zarkesh Esfahani H, Golozar M, Vaezifar S. Cell attachment and proliferation of human adipose-derived stem cells on PLGA/chitosan electrospun nano-biocomposite. Cell J 2015;17:429–37.
[313] Liu Z, Zhao JH, Liu P, He JH. Tunable surface morphology of electrospun PMMA fiber using binary solvent. Appl Surf Sci 2016;364:516–21.
[314] Serafim BM, Leitolis A, Crestani S, Marcon BH, Foti L, Petzhold CL, et al. Electrospinning induced surface activation (EISA) of highly porous PMMA microfiber mats for HIV diagnosis. J Mater Chem B 2016;4:6004–11.
[315] Winter AD, Larios E, Alamgir FM, Jaye C, Fischer D, Campo EM. Near-edge X-ray absorption fine structure studies of electrospun polydimethylsiloxane/poly(methyl methacrylate)/multiwall carbon nanotube composites. Langmuir 2013;29:15822–30.
[316] Deitzel JM, Kosik W, McKnight SH, Beck Tan NC, DeSimone JM, Crette S. Electrospinning of polymer nanofibers with specific surface chemistry. Polymer 2002;43:1025–9.
[317] Andersson RL, Ström V, Gedde UW, Mallon PE, Hedenqvist MS, Olsson RT. Micromechanics of ultra-toughened electrospun PMMA/PEO fibres as revealed by in-situ tensile testing in an electron microscope. Sci Rep 2014;4:1–8, 6335.
[318] Chen W, Weng W. Ultrafine lauric–myristic acid eutectic/poly(meta-phenylene isophthalamide) form-stable phase change fibers for thermal energy storage by electrospinning. Appl Energy 2016;173:168–76.
[319] Golestaneh SI, Mosallanejad A, Karimi G, Khorram M, Khashi M. Fabrication and characterization of phase change material composite fibers with wide phase-transition temperature range by co-electrospinning method. Appl Energy 2016;182:409–17.
[320] Jing X, Mi HY, Peng J, Peng XF, Turng LS. Electrospun aligned poly(propylene carbonate) microfibers with chitosan nanofibers as tissue engineering scaffolds. Carbohydr Polym 2015;117:941–9.

[321] Syu JH, Cheng YK, Hong WY, Wang HP, Lin YC, Meng HF, et al. Electrospun fibers as a solid-state real-time zinc ion sensor with high sensitivity and cell medium compatibility. Adv Funct Mater 2013;23:1566–74.
[322] Purcell BP, Kim IL, Chuo V, Guinen T, Dorsey SM, Burdick JA. Incorporation of sulfated hyaluronic acid macromers into degradable hydrogel scaffolds for sustained molecule delivery. Biomater Sci 2014;2:693–702.
[323] Huang C, Niu H, Wu J, Ke Q, Mo X, Lin T. Needleless electrospinning of polystyrene fibers with an oriented surface line texture. J Nanomater 2012;2012:1–7, 473872.
[324] Richard-Lacroix M, Pellerin C. Partial Disentanglement in continuous polystyrene electrospun fibers. Macromolecules 2014;48:37–42.
[325] Stephens JS, Frisk S, Megelski S, Rabolt JF, Chase DB. Ŕeal timeŘaman studies of electrospun fibers. Appl Spectrosc 2001;55:1287–90.
[326] Tian L, Gu J, Lei X, Lv Z, Qiao M, Yin C, et al. Fabrication and characterization of electrospun dopants/PS composite fibers with porous and hollow-porous structures. Macromol Mater Eng 2016;301:625–35.
[327] Hong SK, Lim G, Cho SJ. Breathability enhancement of electrospun microfibrous polyurethane membranes through pore size control for outdoor sportswear fabric. Sensor Mater 2015;27:77–85.
[328] Hua D, Liu Z, Wang F, Gao B, Chen F, Zhang Q, et al. pH-responsive polyurethane (core) and cellulose acetate phthalate (shell) electrospun fibers for intravaginal drug delivery. Carbohydr Polym 2016;151:1240–4.
[329] Senador AE, Shaw MT, Mather PT. Electrospinning of polymeric nanofibers: Analysis of jet formation. Mater Res Soc Symp Proc 2011;661:1–6. KK5.9.
[330] Zhang A, Zhang Z, Shi F, Xiao C, Ding J, Zhuang X, et al. Redox-sensitive shell-crosslinked polypeptide-*block*-polysaccharide micelles for efficient intracellular anticancer drug delivery. Macromol Biosci 2013;13:1249–58.
[331] Shao C, Kim HY, Gong J, Ding B, Lee DR, Park SJ. Fiber mats of poly(vinyl alcohol)/silica composite *via* electrospinning. Mater Lett 2003;57:1579–84.
[332] Esmaeili A, Beni AA. A novel fixed-bed reactor design incorporating an electrospun PVA/chitosan nanofiber membrane. J Hazard Mater 2014;280:788–96.
[333] Celebioglu A, Aytac Z, Umu OCO, Dana A, Tekinay T, Uyar T. One-step synthesis of size-tunable Ag nanoparticles incorporated in electrospun PVA/cyclodextrin nanofibers. Carbohydr Polym 2014;99:808–16.
[334] Bognitzki M, Czado W, Frese T, Schaper A, Hellwig M, Steinhart M, et al. Nanostructured fibers *via* electrospinning. Adv Mater 2001;13:70–2.
[335] Asmatulu R, Ceylan M, Nuraje N. Study of superhydrophobic electrospun nanocomposite fibers for energy systems. Langmuir 2011;27:504–7.
[336] Lee KH, Kim HY, La YM Lee DR, Sung NH. Influence of a mixing solvent with tetrahydrofuran and *N*,*N*-dimethylformamide on electrospun poly(vinyl chloride) nonwoven mats. J Polym Sci B Polym Phys 2002;40:2259–68.
[337] Chiscan O, Dumitru I, Postolache P, Tura V, Stancu A. Electrospun PVC/Fe_3O_4 composite nanofibers for microwave absorption applications. Mater Lett 2012;68:251–4.
[338] Kenawy ER, Abdel-Fattah YR. Antimicrobial properties of modified and electrospun poly(vinyl phenol). Macromol Biosci 2002;2:261–6.
[339] Cheng D, Xie R, Tang T, Jia X, Cai Q, Yang X. Regulating micro-structure and biomineralization of electrospun PVP-based hybridized carbon nanofibers containing bioglass nanoparticles *via* aging time. RSC Adv 2016;6:3870–81.
[340] Li J, Zhang Y, Zhong X, Yang K, Meng J, Cao X. Single-crystalline nanowires of SiC synthesized by carbothermal reduction of electrospun PVP/TEOS composite fibres. Nanotechnology 2007;18:1–4, 245606.
[341] Seon Bang H, Jang S, Soo Kang Y, Won J. Dual facilitated transport of CO_2 using electrospun composite membranes containing Ionic liquid. J Membr Sci 2015;479:77–84.
[342] Wang C, Ma C, Wu Z, Liang H, Yan P, Song J, et al. Enhanced bioavailability and anticancer effect of curcumin-loaded electrospun nanofiber: *In vitro* and *in vivo* study. Nanoscale Res Lett 2015;10:1–10, 439.
[343] Baptista AC, Botas AM, Almeida APC, Nicolau AT, Falcão BP, Soares MJ, et al. Down conversion photoluminescence on PVP/Ag-nanoparticles electrospun composite fibers. Opt Mater 2015;39:278–81.
[344] Garain S, Jana S, Sinha TK, Mandal D. Design of *in situ* poled Ce^{3+}-doped electrospun PVDF/graphene composite nanofibers for fabrication of nanopressure sensor and ultrasensitive acoustic nanogenerator. ACS Appl Mater Interfaces 2016;8:4532–40.
[345] Koombhongse S, Liu W, Reneker DH. Flat polymer ribbons and other shapes by electrospinning. J Polym Sci B Polym Phys 2001;39:2598–606.
[346] Zhang G, Sun M, Liu Y, Liu H, Qu J, Li J. Ionic liquid assisted electrospun cellulose acetate fibers for aqueous removal of triclosan. Langmuir 2015;31:1820–7.
[347] Zhou Z, Peng X, Zhong L, Wu L, Cao X, Sun RC. Electrospun cellulose acetate supported Ag@AgCl composites with facet-dependent photocatalytic properties on degradation of organic dyes under visible-light irradiation. Carbohydr Polym 2016;136:322–8.
[348] Joanne P, Kitsara M, Boitard SE, Naemetalla H, Vanneaux V, Pernot M, et al. Nanofibrous clinical-grade collagen scaffolds seeded with human cardiomyocytes induces cardiac remodeling in dilated cardiomyopathy. Biomaterials 2016;80:157–68.
[349] Li X, Li M, Sun J, Zhuang Y, Shi J, Guan D, et al. Radially aligned electrospun fibers with continuous gradient of SDF1α for the guidance of neural stem cells. Small 2016;12:5009–18.
[350] Elia R, Guo J, Budijono S, Normand V, Benczedi D, Omenetto F, et al. Encapsulation of volatile compounds in silk microparticles. J Coat Technol Res 2015;12:793–9.
[351] Das S, Sharma M, Saharia D, Sarma KK, Sarma MG, Borthakur BB, et al. *In vivo* studies of silk based gold nano-composite conduits for functional peripheral nerve regeneration. Biomaterials 2015;62:66–75.
[352] Shao W, He J, Sang F, Ding B, Chen L, Cui S, et al. Coaxial electrospun aligned tussah silk fibroin nanostructured fiber scaffolds embedded with hydroxyapatite–tussah silk fibroin nanoparticles for bone tissue engineering. Mater Sci Eng C 2016;58:342–51.
[353] Lee MH, Thomas JL, Chang YC, Tsai YS, Liu BD, Lin HY. Electrochemical sensing of nuclear matrix protein 22 in urine with molecularly imprinted poly(ethylene-*co*-vinyl alcohol) coated zinc oxide nanorod arrays for clinical studies of bladder cancer diagnosis. Biosens Bioelectron 2016;79:789–95.
[354] Chen WJ, Lee MH, Thomas JL, Lu PH, Li MH, Lin HY. Microcontact imprinting of algae on poly(ethylene-*co*-vinyl alcohol) for biofuel cells. ACS Appl Mater Interfaces 2013;5:11123–8.
[355] Kenawy ER, Layman JM, Watkins JR, Bowlin GL, Matthews JA, Simpson DG, et al. Electrospinning of poly(ethylene-*co*-vinyl alcohol) fibers. Biomaterials 2003;24:907–13.
[356] Bagheriasl D, Carreau PJ, Dubois C, Riedl B. Properties of polypropylene and polypropylene/poly(ethylene-*co*-vinyl alcohol) blend/CNC nanocomposites. Compos Sci Technol 2015;117:357–63.
[357] Ramakrishna S, Fujihara K, Teo WE, Yong T, Ma Z, Ramaseshan R. Electrospun nanofibers: Solving global issues. Mater Today 2006;9:40–50.
[358] Malik R, Garg T, Goyal AK, Rath G. Polymeric nanofibers: Targeted gastro-retentive drug delivery systems. J Drug Targeting 2015;23:109–24.
[359] Lee J, Kwon H, Seo J, Shin S, Koo JH, Pang C, et al. Conductive fiber-based ultrasensitive textile pressure sensor for wearable electronics. Adv Mater 2015;27:2433–9.
[360] Abdul Khalil HPS, Davoudpour Y, Bhat AH, Rosamah E, Tahir PM. Electrospun cellulose composite nanofibers. In: Pandey JK, Takagi H, Nakagaito AN, Kim HJ, editors. Handbook of polymer nanocomposites processing, performance and application Heidelberg. Springer; 2015. p. 191–227.
[361] Topuz F, Uyar T. Electrospinning of gelatin with tunable fiber morphology from round to flat/ribbon. Mater Sci Eng C 2017;80:371–8.
[362] Ki CS, Baek DH, Gang KD, Lee KH, Um IC, Park YH. Characterization of gelatin nanofiber prepared from gelatin–formic acid solution. Polymer 2005;46:5094–102.
[363] Nadri S, Nasehi F, Barati G. Effect of parameters on the quality of core-shell fibrous scaffold for retinal differentiation of conjunctiva mesenchymal stem cells. J Biomed Mater Res A 2017;105:189–97.
[364] Sill TJ, von Recum HA. Electrospinning: Applications in drug delivery and tissue engineering. Biomaterials 2008;29:1989–2006.
[365] Bedane AH, Eić M, Farmahini-Farahani M, Xiao H. Theoretical modeling of water vapor transport in cellulose-based materials. Cellulose 2016;23:1537–52.
[366] Liu Q, Wang Y, Dai L, Yao J. Scalable fabrication of nanoporous carbon fiber films as bifunctional catalytic electrodes for flexible Zn-Air batteries. Adv Mater 2016;28:3000–6.